

**NASA
Technical
Paper
2762**

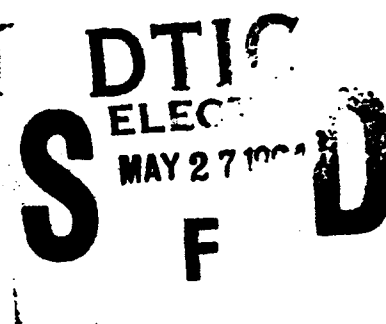
December 1987

AD-A279 721



**Planform Effects on the
Supersonic Aerodynamics
of Multibody Configurations**

**S. Naomi McMillin
and Richard M. Wood**



This document has been approved
for public release and sale; its
distribution is unlimited

94-15905



DTIC QUALITY INSPECTED 3

NASA

94 5 26 075

**NASA
Technical
Paper
2762**

1987

**Planform Effects on the
Supersonic Aerodynamics
of Multibody Configurations**

**S. Naomi McMillin
and Richard M. Wood**

*Langley Research Center
Hampton, Virginia*

Accession	
NTIS	CRP
DTIC	DA
Unannounced	
Justification	
By	
Distribution	
Availability	
Dist	Avail
A-1	3



National Aeronautics
and Space Administration

Scientific and Technical
Information Division

DTIC QUALITY INSPECTED 3

Summary

An experimental and theoretical investigation of the effects of planform on the supersonic aerodynamics of low-fineness-ratio multibody configurations has been conducted in the Langley Unitary Plan Wind Tunnel at Mach numbers of 1.60, 1.80, 2.00, and 2.16. Longitudinal and lateral-directional aerodynamic force and moment data and flow visualization photographs were obtained for three multibody configurations. In general, the data indicated that planform has a small effect on the zero-lift drag of a multibody configuration. In contrast, the longitudinal aerodynamic data obtained at lifting conditions indicated that planform has a significant effect on the lift, pitching-moment, and drag-due-to-lift characteristics of a multibody configuration. Although planform significantly affected the lateral-directional stability of the multibody configurations, the data did not uncover any unusual stability traits associated with the multibody configurations.

A comparison study was made between the planform effects observed for single-body and multibody configurations. Results from this study indicate that the multibody concept offers a mechanism for employing a low-sweep wing (such as the trapezoidal wing) with no significant increase in zero-lift drag and no decrease in high-performance characteristics at high-lift conditions. In general, the study shows that the single-body and multibody configurations experience the same planform effects for the lift, drag-due-to-lift, and lateral stability characteristics. However, planform does not appear to affect the zero-lift drag for the multibody configuration as drastically as it does for the single-body configuration. Also, in contrast to the trend found for the single-body configuration, the multibody configuration experiences increasing longitudinal stability with increasing Mach number.

Evaluation of the linear-theory prediction methods reveals a general inability of the methods to predict the characteristics of low-fineness-ratio multibody geometries. However, the methods did predict the correct trends in the lift, pitching-moment, and drag-due-to-lift characteristics with variations in Mach number and planform. The methods also predict the correct change in zero-lift drag with variations in Mach number but not that with variations in planform. Finally, the methods did predict that the change in zero-lift drag due to variations in planform is small, as was found experimentally.

Introduction

The multiple-fuselage aircraft design concept is well established in aviation history (ref. 1). Since

the beginning of powered flight, this design concept has continually resurfaced. However, all previous applications have been for subsonic designs in which the multiple-fuselage concept was primarily employed for structural or propulsion integration reasons. In reference 2, it is estimated that a 30-percent saving in structural weight could be obtained without the application of advanced engines, advanced materials, or aerodynamic benefits simply by employing two fuselages rather than the conventional single fuselage. In general, the benefits afforded by twin fuselages are an effective increase in wing aspect ratio, a reduced wing weight because of a reduced wing bending moment, and a reduced total fuselage weight when both single- and twin-fuselage geometries are configured for the same number of passengers or payload. Although this study was conducted for subsonic aircraft, the weight reduction should be independent of operating speed and could be equally applicable to supersonic as well as subsonic designs.

Recent theoretical studies of advanced supersonic aircraft concepts indicate that significant improvements in aerodynamic performance may be realized for aircraft with two fuselages rather than the traditional single fuselage. Reference 3 indicates that a twin-fuselage supersonic transport aircraft could have levels of aerodynamic performance which equal or exceed those of a single-fuselage configuration having only half the passenger capacity. Additional theoretical and experimental research (refs. 4 to 9) on the multibody concept at supersonic speeds has shown that zero-lift drag can be significantly reduced through body shaping or body positioning or both. In a linear-theory sense, the multibody concept creates an aerodynamically thinner configuration (i.e., equivalent body with a higher fineness ratio) (ref. 8) compared with a conventional single-body concept, and in a real-flow sense, pressure drag is reduced through the management of the near-field interference effects between the aircraft components.

For uncambered configurations at supersonic speeds, the zero-lift drag is a combination of inviscid (e.g., wave drag) and viscous (e.g., skin-friction drag) terms. Application of the multibody concept typically results in an increase in skin-friction drag because of the increased wetted area; however, there is a decrease in total zero-lift drag, which indicates a large decrease in zero-lift wave drag. As concluded in reference 8, the zero-lift drag reduction potential of the concept is dependent upon configuration fineness ratio. For high-fineness-ratio configurations (≈ 20), such as transports, skin friction is the dominant zero-lift drag term; however, as configuration fineness ratio is decreased (≈ 10), the wave drag begins to dominate. Figure 1 (from ref. 9) shows the results of a very

fundamental theoretical study that was conducted to determine the impact of configuration fineness ratio on the zero-lift drag reduction potential of the multi-body concept at supersonic speeds. Shown is the variation in zero-lift drag of a single-body configuration and a comparative double-body configuration with fineness ratio (l/d). The graph shows that application of the multibody concept to low-fineness-ratio geometries provides significantly greater drag reductions.

To further study the supersonic aerodynamics of low-fineness-ratio multibody configurations, an experimental and theoretical investigation was conducted to determine the effect of body cross-sectional shape (ref. 9). This study concluded that body cross-sectional shape is an important parameter in determining the zero-lift drag. The gross geometric characteristics of the model of reference 9 were based upon an existing conventional fighter aircraft design (ref. 10).

In the experimental investigation conducted on the conventional model of reference 10, it was found that changes in wing planform could significantly influence the zero-lift drag of low-fineness-ratio single-body configurations. To further study the effect of the multibody concept on the aerodynamic characteristics of low-fineness-ratio configurations, a wind-tunnel test program was conducted. Longitudinal as well as lateral and directional characteristics were measured for a series of outboard wing panels mounted on the multibody model of reference 9. All configurations were tested at Mach numbers of 1.60, 1.80, 2.00, and 2.16 in the Langley Unitary Plan Wind Tunnel. This paper reports the results of the experimental testing and supporting theoretical analysis. It also presents a comparison of the planform effects on a single-body model and a multibody model.

Symbols

The measurements and calculations of this investigation were made in U.S. Customary Units.

b	wing reference span, in.
C_A	corrected axial-force coefficient, Axial force/ qS
C_D	corrected drag coefficient, Drag/ qS
ΔC_D	incremental change in drag coefficient, $C_D - C_{D,0}$
$\Delta C_D / \Delta C_L^2$	drag-due-to-lift factor
C_{Dc}	zero-lift drag correction

$C_{D,0}$	zero-lift drag coefficient
C_L	lift coefficient, Lift/ qS
ΔC_L	incremental change in lift coefficient, $C_L - C_{L,C_{D,0}}$
$C_{L\alpha}$	curve slope at $\alpha = 0^\circ$
C_l	rolling-moment coefficient, Rolling moment/ qS
$C_{l\beta}$	lateral stability parameter, $\partial C_l / \partial \beta$, deg^{-1}
C_m	pitching-moment coefficient, Pitching moment/ $qS\bar{c}$
C_N	normal-force coefficient, Normal force/ qS
C_n	yawing-moment coefficient, Yawing moment/ qSb
$C_{n\beta}$	directional stability parameter, $\partial C_n / \partial \beta$, deg^{-1}
C_{SF}	internal duct drag coefficient, Duct drag/ qS
C_Y	side-force coefficient, Side force/ qS
\bar{c}	wing reference chord, in.
d	maximum diameter of body, in.
dC_m / dC_L	longitudinal stability parameter at $\alpha = 0^\circ$
L/D	lift-drag ratio
l	side-body or maximum configuration length, in.
M	free-stream Mach number
M_D	duct Mach number
q	free-stream dynamic pressure, lb/ft^2
R	Reynolds number, ft^{-1}
S	wing reference area, in^2
s	cross-sectional area, in^2
x	Cartesian coordinate in streamwise direction, in.
\bar{x}	streamwise location of wing reference chord, in.
α	angle of attack, deg

β = $\sqrt{M^2 - 1}$; also angle of sideslip, deg

A sweep angle, deg

Subscripts:

b base

c chamber

LE leading edge

TE trailing edge

unc uncorrected

Model components:

B strongback (balance housing, duct, and inboard wing panel)

F side body

V vertical tail

W_1 delta outboard wing panel

W_2 arrow outboard wing panel

W_3 trapezoidal outboard wing panel

Model Description

Shown in figure 2 is a three-view sketch of the multibody model with the delta outboard wing panels. Listed in table I are the geometric characteristics of the multibody model. Details of the multibody models are presented in figure 3. The balance housing was located on the lower surface of the center wing panel and was bracketed by the two flow-through ducts. The design was an attempt to limit the propagation of the interference effects from the balance housing to the free-stream flow field and model geometry. The two flow-through ducts were designed with a linear area growth ratio of 1.13 to account for the boundary layer in order to maintain supersonic flow within the duct system. Presented in figure 3(b) are lateral, longitudinal, and cross-sectional views through the balance housing and duct system. The balance housing geometry consisted of a combined cone and wedge surface with leading-edge surface slopes of 28° and 19° , respectively. These large surface slopes resulted in a significant drag penalty and a very complex and nonlinear flow field (ref. 9). Shown in figure 4 is a photograph of the balance housing and duct arrangement as it was mounted underneath the multibody models. Figures 3(c) and 3(d) contain details of the inboard wing

panel and vertical tails. Figures 3(e), 3(f), and 3(g) contain details of the delta, arrow, and trapezoidal outboard wing panels. Each side body was 30 in. long and circular in cross section. The normal area distribution of the side body is presented in table II. Photographs of each of the three test models are presented in figure 5.

In an effort to provide a reference geometry for comparison, the gross geometry characteristics of the multibody models were based upon those of a 4-percent-scale conventional fighter aircraft model reported in reference 10. This model is referred to as the single-body model throughout this report. A photograph of the single-body model with the delta wing in test section 1 of the Langley Unitary Plan Wind Tunnel (UPWT) is shown in figure 6. As shown in this figure, the single-body model consisted of a single fuselage with two side-mounted, flow-through, half-axisymmetric inlets, twin vertical tails, and a delta wing with a leading-edge-sweep angle of 65° .

The three multibody wing planforms shown in figure 3 were based on a series of wing planforms tested on the single-body models in reference 10. The single-body models varied in planform only and were part of an investigation to evaluate the planform effects on a low-fineness-ratio single-body configuration at supersonic speeds. However, the design of these wing planforms was based not only on supersonic aerodynamic efficiency but also on a preselected mission profile as discussed in reference 11. Thus the single-body planforms of reference 10 were considered to be able to accommodate all speed regimes.

Presented in figure 7 is a comparison of planforms for the three single-body models of reference 10 and the three multibody models. Listed in table III are the geometric characteristics of the reference single-body models. The geometric characteristics of the multibody models are contained in table I. The single-body and multibody models had similar areas and spans for each planform shape. The moment reference center for each single-body and multibody model was located at the $0.5\bar{c}$ location of the planform. The same inboard wing panel was used throughout the test for the multibody models. The outboard wing panel was the component which was designed to have a shape similar to the planform on the single-body models.

The single-body model fuselage was also used as a reference in designing the side bodies. Presented in figure 8 are the fuselage normal area distributions of the models. The sum of the volumes of the two side bodies on the multibody models was equal to the volume of the single fuselage on the single-body models, and the sum of the maximum cross-sectional areas of

the two side bodies was equal to the maximum cross-sectional area of the single fuselage. The two side bodies were shorter than the single fuselage. In addition, the fuselage area distribution for the multibody models did not reflect the volume associated with the balance housing and duct arrangement which, if taken into account, would result in a greater total volume and increased maximum cross-sectional area compared with the single-body models.

Test Description

The wind-tunnel test program was conducted in test section 1 of the Langley Unitary Plan Wind Tunnel (ref. 12) at Mach numbers of 1.60, 1.80, 2.00, and 2.16. The tests were conducted under the following conditions:

Mach number	Stagnation pressure, lb/ft ²	Stagnation temperature, °F	Reynolds number, per foot
1.60	1079	125	2×10^6
1.80	1154	125	2×10^6
2.00	1253	125	2×10^6
2.16	1349	125	2×10^6

The dew point was maintained sufficiently low during the force tests to prevent condensation in the tunnel. There was a maximum variation in Mach number of ± 0.03 . A more detailed description of the wind-tunnel calibrations is given in reference 12. These test conditions were similar to those used in the single-body model tests (ref. 10).

Boundary-layer transition-inducing strips of No. 60 sand grit were applied 0.2 in. aft of the leading edge of all airfoil surfaces, 1.2 in. aft of the nose region for the side bodies, and 0.2 in. aft of the inlet lip leading edges. The grit size and location were selected according to the method of reference 13 to ensure fully turbulent flow over the model and inside the inlet duct.

Balance chamber pressure and base pressure were measured throughout the test with a pressure transducer mounted externally to the wind-tunnel test section and connected by pressure tubing to a pressure probe located in the balance cavity and at the model base. Force and moment data were corrected to free-stream static pressure at the model base and chamber.

As stated in the *Model Description* section, the balance housing geometry, which consisted of a wedge surface bracketing a partially axisymmetric body of revolution, resulted in a significant zero-lift drag penalty throughout the test. Therefore a nonlinear

zero-lift drag correction derived in reference 9 was applied to the drag data obtained throughout the test. The correction used at each Mach number was as follows:

M	SC_{DC} , in ²
1.60	1.0840
1.80	.9611
2.00	.9815
2.16	.9202

The total pressure and static pressure at the exit plane of the ducts were also measured throughout the test with a pressure transducer mounted externally to the wind-tunnel test section and connected by pressure tubing to a pressure probe located at the center of the duct exit plane. These measurements were then used to correct the experimental data for internal duct friction drag. This correction is more fully discussed in appendix A.

Forces and moments were measured with a six-component electrical strain-gage balance contained within the model and connected through a supporting sting to a permanent model-actuating system in the tunnel. Shown in the table below is the error associated with the balance and the pressure transducers used in this test.

Instrumentation	Load	Coefficient
Balance:		
Normal	± 3.0 lb	± 0.00423
Axial	$\pm .3$ lb	$\pm .00042$
Side	± 1.5 lb	$\pm .00211$
Pitch	± 7.5 in-lb	$\pm .00075$
Roll	± 2.0 in-lb	$\pm .00021$
Yaw	± 5.0 in-lb	$\pm .00050$
Pressure transducer	$\pm .07$ psi	$\pm .02016$

The external flow force and moment data were obtained at angles of attack from -4° to 20° and angles of sideslip from -4° to 8° . All angles of attack were adjusted for tunnel flow misalignment and for sting and balance deflections. Schlieren flow visualization photographs were obtained for each configuration. The upper surface of each model was photographed at $M = 1.80$ and 2.16 at $\alpha = 0^\circ$, 4° , and 8° .

Discussion

An experimental and theoretical investigation of the effect of planform shape on the supersonic

aerodynamics of three low-fineness-ratio (≈ 10) multi-body configurations has been conducted. Each multi-body configuration was tested with and without vertical tails. Experimental data are discussed first in a comparison of the planform effects observed on the single body and multibody models. The final section of the paper presents theoretical analysis results directed at determining the capability of existing linear-theory methods to predict experimental data. A tabulation of the force data is contained in appendix B.

Experimental Data

Within this section of the paper, longitudinal aerodynamics, lateral-directional stability, and flow visualization data are presented. The longitudinal aerodynamics and flow visualization data are presented for the three test configurations without the vertical tails; the lateral-directional stability data are presented for the test configurations with and without the vertical tails.

Longitudinal aerodynamic characteristics. Presented in figure 9 are the effects of planform on the longitudinal aerodynamic characteristics for the three multibody configurations at $M = 1.80$. The drag data of figure 9(a) show a variation at zero lift because of changes in planform, with the trapezoidal wing having the highest zero-lift drag. It should be noted that the zero-lift drag produced by the trapezoidal wing is about 8 percent greater than that produced by the more highly swept delta wing and only slightly higher than that produced by the arrow wing. As also shown in figure 9(a), the trapezoidal wing has a lower drag coefficient at the higher lift coefficients than either of the more highly swept wings, thus indicating that it has better drag-due-to-lift characteristics.

The lift and pitching-moment characteristics are presented in figure 9(b). The lift data show a linear variation for all three configurations up to $\alpha = 8^\circ$ ($C_L = 0.2$), and the trapezoidal wing has the highest lift-curve slope of the three planform configurations. At angles of attack greater than 8° there is a slight decrease in lift-curve slope for all three configurations. This decrease in lift-curve slope corresponds with a change in the slope of the pitching-moment curve for all three configurations. These changes in the pitching-moment and lift curves may be due to near-field interference effects.

As documented in reference 9, the near-field interference effects are predominately caused by the shock structure existing between the side bodies. Presented in figure 10 are schlieren photographs showing the effect of planform on the shock structure at $M = 1.80$ and $\alpha = 0^\circ$. As would be expected, a change in the

outboard wing panel has little impact on the shock structure between the bodies. As shown in this figure, the shock structure consists of an interaction of the shocks from the nose of each side body with each other shock and the impingement of the nose shock onto the opposite side body, the inboard wing panel, and the balance housing. The near-field interference effects can be broken down into three primary contributions: effect of body on body, effect of body on inboard wing panel, and effect of body on balance housing. Presented in figure 11 are schlieren photographs showing the effects of planform, Mach number, and angle of attack on the shock structure at a sideslip angle of 0° . Photographs are presented for angles of attack of 0° , 4° , and 8° at $M = 1.80$ and 2.16 for each test configuration. The photographs for $\alpha = 0^\circ$ show that increasing the Mach number decreases the shock cone angle and produces a rearward shift in the location of the intersection of the nose shocks and thus in the location of the impingement of the body nose shock onto the side body. Increasing the angle of attack also produces a rearward shift in the shock impingement location. The rearward shift with increasing angle of attack is caused by the rotation and distortion of the shock cone emanating from the nose of the body. As angle of attack increases the bow shock from the balance housing becomes stronger and spills over onto the inboard wing panel, as indicated by the protrusion of the balancing housing bow shock at the leading edge of the unswept inboard wing panel. The occurrence of this detached bow shock condition interferes with the favorable pressure field generated by the body-nose shock system. Another effect of increasing angle of attack is that the inboard wing panel begins to block the body-nose shock from the upper surface of the configuration and diminishes the strength of the shock system over the leeward side of the inboard wing panel. A more thorough discussion of the shock system can be found in reference 9.

Presented in figure 12 are the effects of planform and Mach number on the longitudinal aerodynamic characteristics of the multibody model. The data presented on the left in figure 12(a) indicate that variations in zero-lift drag result from changes in planform, with the maximum variation being approximately 11 percent. The variation between planforms is fairly consistent over the Mach number range. The variations in drag-due-to-lift factor with Mach number, presented on the right in figure 12(a), show that the trapezoidal wing has lower (and therefore better) drag due to lift than the more highly swept wings. The drag-due-to-lift factor also increases with increasing Mach number for each configuration.

The data presented on the left in figure 12(b) show that the trapezoidal wing has the highest

lift-curve slope of the three planforms for the test Mach number range. The lift-curve slope of the trapezoidal wing also decreases more rapidly with increasing Mach number than the slope of the more highly swept wings. This effect can be related to the fact that the trapezoidal wing has a supersonic leading-edge condition ($\beta \cot \Lambda > 1$) while the more highly swept wings have a subsonic leading-edge condition ($\beta \cot \Lambda < 1$). These conditions are readily shown in the schlieren photographs of figure 10. Experimental data (ref. 14) show that for a supersonic leading edge, βC_{L_α} remains constant as $\beta \cot \Lambda$ increases; thus, C_{L_α} decreases by $1/\beta$. However, for a subsonic leading edge, since βC_{L_α} increases as $\beta \cot \Lambda$ increases, C_{L_α} does not decrease as rapidly as β (and therefore Mach number) increases for the highly swept wings.

The longitudinal stability data, presented on the right in figure 12(b), indicate that planform has a significant effect on the stability level such that the arrow wing is more longitudinally stable at all Mach numbers. This trend can be explained in the following manner. Although the moment center locations ($0.5\bar{c}$, see table I) of the delta and arrow wings are approximately equal, the aerodynamic center of the arrow wing is farther aft because of the higher sweep; therefore, the arrow wing has the more downward pitching moment, which contributes to the greater longitudinal stability. On the other hand, because of the lack of sweep of the trapezoidal wing, the moment center location is more forward than that of the delta wing and, likewise, the aerodynamic center is shifted forward by approximately the same amount. Hence, the trapezoidal and delta wings have comparable longitudinal stability. A more significant observation of these data is that the longitudinal stability level for each configuration increases slightly with increasing Mach number. This observation is thought to result from the dominating effects of the interference of the body on body and the body on inboard wing panel and is discussed more fully in a subsequent section.

Lateral-directional stability characteristics. In order to aid further configuration development of the multibody concept, other critical aerodynamic parameters need to be investigated. In this test an extensive amount of data has been obtained on the lateral-directional stability characteristics of each test configuration both with and without the twin vertical tails. Force and moment data were obtained at Mach numbers of 1.80 and 2.16 over a range of angles of sideslip at $\alpha = 0^\circ$ and 8° to ensure the linearity of the lateral-directional aerodynamic characteristics. The lateral-directional stability derivatives were then computed with data from correspond-

ing ranges of angles of attack at $\beta = 0^\circ$ and 4° . A summary of the lateral-directional stability characteristics is contained in figures 13 to 15.

Comparisons of the lateral and directional stability characteristics of each test configuration without the twin vertical tails at a Mach number of 1.80 are presented in figures 13(a) and 13(b). The lateral and directional stability characteristics show a strong dependence on planform leading-edge sweep. The lateral stability data of figure 13(a) show that all configurations exhibit a stable dihedral effect, with a change occurring in the slope of the curves at $\alpha = 8^\circ$ for the delta and trapezoidal wing configurations and at $\alpha = 4^\circ$ for the arrow wing configuration. This characteristic was discussed in reference 9 for the delta wing configuration. The delta-wing-alone configuration (no side bodies) of reference 9 exhibited a stable dihedral effect which increased with increasing angle of attack up to 12° and then leveled off to a constant value. Adding the side bodies produced a destabilizing effect up to $\alpha = 8^\circ$ and a stabilizing effect for $\alpha > 8^\circ$. As shown in figure 13(a), the stable dihedral effect of the trapezoidal wing does not increase with angle of attack as quickly as that of the highly swept wings. Therefore, for angles of attack greater than 8° the stabilizing effect of the side bodies (discussed in ref. 9) is probably more prominent for the trapezoidal wing than for the more highly swept wings. The observation of differing dihedral effects based on wing sweep can be related to the fact that the more highly swept wings have an asymmetric separated flow (vortex) occurring at the leading edge while the flow over the trapezoidal wing is characterized as attached (ref. 15). The asymmetric separated flow for the highly swept wings creates an asymmetric wing loading which is greater on the windward side than on the leeward side, as shown in the experimental and theoretical data of reference 16. This behavior results in the stable dihedral effect associated with the highly swept wings. The directional stability characteristics presented in figure 13(b) show that all three configurations are unstable. These characteristics were also discussed in reference 9 for the delta wing configuration. The delta-wing-alone configuration (no side bodies) was slightly unstable. Adding the side bodies produced a destabilizing effect. Since side force does not vary dramatically with a change in planform, the fact that the trapezoidal wing configuration is not as directionally unstable as the more highly swept wing configurations can be explained by the fact that the moment center of the trapezoidal wing configuration was located more forward than that of the highly swept wing configurations.

Comparisons of the lateral and directional stability characteristics for the three configurations with and without the vertical tails at a Mach number of 1.80 are presented in figures 14(a) and 14(b). The data of these figures show that adding the twin vertical tails increases both lateral and directional stability. The data of figure 14(a) show that angle of attack does not affect this stabilizing effect for the lateral stability characteristics. However, the directional stability data of figure 14(b) show that the vertical tails become less effective at angles of attack greater than 8° . This loss of tail effectiveness is probably caused by a blanketing effect of the tail by the body and wing wakes. These observations were documented in reference 9 for the delta wing configuration. The data of figure 14 indicate that planform does not significantly influence the effectiveness of the vertical tails.

Comparisons of the lateral and directional stability characteristics of the three configurations with vertical tails at $M = 1.80$ and 2.16 are presented in figures 15(a) and 15(b). The data clearly show a loss in lateral and directional stability for all configurations as Mach number increases from 1.80 to 2.16. The loss in lateral stability for the highly swept wings as Mach number increases for angles of attack less than 8° can be related to the fact that the flow is approaching an unseparated flow condition at the leading edge (i.e., the effective dihedral is decreasing). For angles of attack greater than 8° , the loss in lateral stability as Mach number increases is probably due to a decrease in the stabilizing effect from the side bodies because of changes in the near-field interference. The loss in directional stability is thought to be due to a loss in vertical-tail effectiveness with increasing Mach number.

Multibody Assessment

As stated in the *Model Description* section, the low-fineness-ratio single-body models of reference 10 were used as reference geometries in designing the multibody model and interchangeable outboard wing panels. However, as can be observed in figure 7, the planforms for the single-body and multibody models are too fundamentally different to conduct a one-on-one comparison between the models. Instead, a comparison between the planform effects observed on the single-body and multibody configurations was conducted in order to assess the aerodynamic performance benefits of the multibody concept as applied to low-fineness-ratio configurations.

The three single-body configurations were tested in the Langley Unitary Plan Wind Tunnel. The data of this test are recorded in reference 10. The three configurations differed in wing planform only,

as is evident in table I. Each configuration was tested with the twin vertical tails attached. Thus, in order to compare these data with the tail-off data obtained on the multibody configurations, a drag correction was applied to the single-body data. This drag correction was derived from a study of component drag buildup conducted in reference 10. The trapezoidal wing configuration data were further corrected for the zero-lift drag contribution from the horizontal tails. Therefore, a direct comparison between the single-body and multibody configurations for pitching-moment characteristics is not carried out. The pitching-moment center for each configuration was located at the $0.5\bar{c}$ location of its planform.

Presented in figure 16 are the longitudinal characteristics for the three single-body configurations at $M = 1.80$. The drag data of figure 16(a) show a variation at zero lift because of changes in planform such that the trapezoidal wing has the higher $C_{D,0}$ value. The value of $C_{D,0}$ produced by the trapezoidal wing is approximately 40 percent greater than that produced by the more highly swept delta wing. Also shown in the drag data of figure 16(a) is that at the higher lift coefficients the trapezoidal wing has a significantly lower drag coefficient than either of the more highly swept wings, thus indicating it has better drag-due-to-lift characteristics.

The lift and pitching-moment characteristics of the single-body configurations are presented in figure 16(b). The lift data show the trapezoidal wing has the higher C_{L_α} value. The pitching-moment curve of the trapezoidal wing is very different than those of the more highly swept wings. This was not the observation made on the multibody configuration data. This observation is due to the contribution to the pitching moment of the trapezoidal wing configuration horizontal tail. Thus, the trapezoidal wing configuration was not considered in the comparison of planform effects on the longitudinal stability for the single-body and multibody models.

Shown in figure 17 is the effect of planform and lift coefficient on the lift-drag ratio at $M = 1.80$ for the single-body models. Shown in figure 18 is the effect of planform and lift coefficient on L/D at $M = 1.80$ for the multibody models. The trends observed here are typical of those observed at all test Mach numbers. At $C_L = 0.1$ (a typical cruise condition), the data of figure 17 indicate that the single-body trapezoidal wing configuration has an L/D value that is 28 percent less than those of the more highly swept single-body delta wing configuration. However, the data of figure 18 indicate that for a $C_L = 0.1$, the multibody trapezoidal wing configuration has an L/D value that is only 3.5 percent less than that of the multibody delta wing

configuration. At a $C_L = 0.3$ (a typical maneuver condition), the data of figures 17 and 18 show that for both the single-body and multibody models, the trapezoidal wing has an L/D value which is 12 percent greater than that observed on the more highly swept delta wing. Thus, the multibody concept appears to allow a trapezoidal wing to be employed with very little effect on cruise performance ($C_L = 0.1$) while retaining the higher performance characteristics of the wing at maneuver conditions ($C_L = 0.3$).

Theoretically, for a flat wing, the drag-due-to-lift factor is inversely proportional to the lift-curve slope. A comparison between the measured $\Delta C_D / \Delta C_L^2$ and the computed $\Delta C_D / \Delta C_L^2$ (computed using experimental $C_{L\alpha}$) for the single-body models across the Mach number range is presented in figure 19. In figure 20, a similar comparison is made for the multibody models. The results of figure 19 indicate a good correlation in the measured and computed $\Delta C_D / \Delta C_L^2$ values for the single-body models. However, the computed values of the more highly swept wings are consistently greater than the measured values. This behavior is a typical result for highly swept wings with a subsonic leading-edge condition experiencing suction at the leading edge. It should be noted that because the trapezoidal wing has a supersonic leading-edge condition, the measured $\Delta C_D / \Delta C_L^2$ data agree more closely with the computed values, as would be expected. None of these trends occurs for the three multibody configurations, as shown in the results of figure 20. In fact, the measured and computed $\Delta C_D / \Delta C_L^2$ curves for both the delta and trapezoidal wing configurations cross in the test Mach number range. This behavior suggests the existence of near-field interference effects resulting from the complex flow field between the outboard wing panel and the other configuration components at all Mach numbers.

Presented in figure 21 are the effects of Mach number and planform on the pitching moment for the single-body models. The pitching-moment curves for the delta and trapezoidal wing configurations indicate increasing longitudinal stability with increasing angle of attack over the test Mach number range. However, the arrow wing configuration has an unstable break in the pitching-moment curve at $\alpha = 4^\circ$ which is especially pronounced at the lower Mach numbers. As shown in figure 22 (from ref. 10), this break can be attributed to a strong spanwise flow region along the wing trailing edge, which results in flow separation at the trailing edge at moderate angles of attack.

Presented in figure 23 are the effects of Mach number and planform on the pitching moment for the multibody models. The break in the pitching-

moment curve for the single-body arrow wing configuration is also present for the multibody arrow wing configuration. However, near $\alpha = 8^\circ$ a break occurs in the pitching-moment curves for all three multibody configurations. This break is probably the result of the interference effects discussed earlier. One possible explanation of the mechanism is related to the bow shock from the balance housing noted in the photographs of figure 11 for $\alpha = 8^\circ$ at both $M = 1.80$ and $M = 2.16$. This bow shock is thought to spill over onto the inboard wing panel and interfere with the shock system of the nose shocks in such a manner so as to move the aerodynamic center significantly and cause the break in the pitching-moment curves.

Presented in figure 24 is the effect of Mach number on the longitudinal stability for the highly swept wing configurations for both the single-body and multibody models. It should be noted that the longitudinal stability is computed at zero lift, and thus the above flow-field nonlinearities do not affect this parameter for Mach numbers greater than 1.60. The data on the left in figure 24 indicate that for the single-body models the longitudinal stability decreases with increasing Mach number. The opposite trend occurs on the multibody models, as observed in the data on the right in figure 24. One explanation for this observation is related to near-field interference effects. The interference of the body on body and the body on center wing panel dominate the location of the aerodynamic center at the lower angles of attack. As Mach number increases the shock system governing these interference effects becomes stronger and further dominates the location of the aerodynamic center. The apparent ability of the multibody concept to maintain a constant or increasing level of longitudinal stability with increasing Mach number could have a significant impact on future design studies.

Presented in figure 25 is the effect of planform on the lateral-directional stability characteristics for the single-body models with vertical tails on at $M = 1.80$. The lateral stability data of figure 25(a) indicate that all three configurations are stable laterally. The trapezoidal wing is the least stable of the three configurations but becomes more stable with increasing angle of attack above $\alpha = 8^\circ$. The arrow wing becomes less stable with increasing angle of attack above $\alpha = 4^\circ$. These trends with changes in angle of attack and planform also occur on the multibody configurations, as shown in figure 14(a).

The directional stability data of figure 25(b) indicate that all three single-body configurations are directionally stable at $\alpha = 0^\circ$. As angle of attack increases all three configurations decrease in

stability until eventually all three are directionally unstable. The single-body delta wing configuration does not decrease in stability as rapidly as the other configurations as angle of attack increases. The trends with changes in angle of attack and planform are not the same for the multibody configurations, as shown in figure 14(b). All three multibody configurations are significantly more stable at $\alpha = 0^\circ$ than the single-body configurations. The more highly swept wing multibody configurations have slightly increasing stability up to $\alpha = 8^\circ$, at which point the stability begins to decrease as angle of attack increases. The trapezoidal wing multibody configuration decreases steadily in stability as angle of attack increases. However, none of the multibody configurations become unstable in the angle-of-attack range tested.

Theoretical Analysis

Two linear-theory supersonic aerodynamics prediction codes were selected for the theoretical analysis. These codes were an arbitrary-geometry far-field wave-drag code (ref. 17) and the Supersonic Design and Analysis System (SDAS) code (ref. 18).

SDAS is an integrated system of linear theory and slender-body theory computer programs that has been developed for the design and analysis of supersonic configurations. Included in the system of codes are the lift analysis method of reference 19 and the skin friction code of reference 20.

The methods of references 17 and 20 were used to obtain the zero-lift drag characteristics, and the method of reference 18 was used to obtain the lift, pitching-moment, and drag-due-to-lift characteristics. Shown in figure 26 are the zero-lift drag theoretical model and the lift analysis theoretical model of the delta wing configuration.

A theoretical and experimental comparison of the effects of planform and Mach number on the longitudinal aerodynamic characteristics is presented in figure 27. The zero-lift drag data of figure 27(a) indicate that the theoretical codes do not consistently predict the correct trend with changes in planform but do predict the correct trend with Mach number. However, the theoretical codes predict that the changes in $C_{D,0}$ with respect to changes in planform are similar to those found experimentally. The observation that planform has little influence on the $C_{D,0}$ of the multibody concept can be explained from a linear-theory viewpoint. For a single-body configuration the effective aerodynamic fineness ratio, and thus the wave drag, is dictated by the wing planform, resulting in a nonsmooth area distribution. However, the effective aerodynamic fineness ratio of a multibody configuration is dictated by both the wing planform and the body which result in a much smoother area

distribution and thus lower wave drag. The drag-due-to-lift data of figure 27(a) indicate that the lift analysis method is adequate for predicting the effect of planform and Mach number.

The lift-curve-slope data of figure 27(b) show that the lift analysis method predicts the correct trend with respect to changes in planform and Mach number. On the right in figure 27(b), the longitudinal stability data indicate that theory overpredicts the stability of the configuration. However, the theory did predict the arrow wing as being the most longitudinally stable of the three configurations, as was found experimentally. These observations are consistent with previous applications of the theory.

Conclusions

An experimental and theoretical investigation of the effects of planform on the supersonic aerodynamics of low-fineness-ratio multibody configurations has been conducted in the Langley Unitary Plan Wind Tunnel at Mach numbers of 1.60, 1.80, 2.00, and 2.16. Longitudinal and lateral-directional aerodynamic force and moment data and flow visualization photographs were obtained for three multibody configurations. The zero-lift drag data showed that the trapezoidal wing has slightly higher drag than the more highly swept wings. In general, the data indicated that planform has a small effect on the zero-lift drag of a multibody configuration. In contrast, the longitudinal aerodynamics data obtained at lifting conditions indicated that planform has a significant effect on the lift, pitching-moment, and drag-due-to-lift characteristics of the multibody configurations. Specifically, the trapezoidal wing had a higher lift-curve slope and better drag-due-to-lift characteristics than the more highly swept wings. The arrow wing had the greatest longitudinal stability. The longitudinal stability for all three configurations increased slightly with increasing Mach number for Mach numbers from 1.60 to 2.00. Although planform significantly affected the lateral-directional stability of the multibody configurations, the data did not uncover any unusual stability traits associated with the multibody configurations.

A comparison study was made between the planform effects observed on single-body and multibody configurations. Results from this study indicate that the multibody concept offers a mechanism for employing a low-sweep wing such as the trapezoidal wing with no significant increase in zero-lift drag while retaining high-performance characteristics at high lift conditions. In general, the study showed that the single-body and multibody configurations experience the same planform effects for the lift, drag-due-to-lift, and lateral stability characteristics.

However, planform does not appear to affect the zero-lift drag of the multibody configurations as drastically as it does on the single-body configurations. Also, in contrast to the trend found on the single-body configurations, the multibody configurations experienced increasing longitudinal stability with increasing Mach number.

Evaluation of the linear-theory prediction methods revealed a general inability of the methods to predict the characteristics of low-fineness-ratio multibody geometries. However, the methods did predict the correct trends in the lift, pitching-moment,

and drag-due-to-lift characteristics with variations in Mach number and planform. The methods also predicted the correct change in zero-lift drag with variations in Mach number, but not with variations in planform. However, the methods did predict that the change in zero-lift drag due to variations in planform was small, as was found experimentally.

NASA Langley Research Center
Hampton, Virginia 23665-5225
October 13, 1987

Table I. Geometric Characteristics of Multibody Model Components

Strongback:	
Length, in.	13.000
Base area, in ²	0.697
Chamber area, in ²	1.863
Capture area (total), in ²	3.000
Exit area (total), in ²	3.399
Center wing panel:	
Area, in ²	104.000
Λ_{LE} , deg	0
Λ_{TE} , deg	0
Aspect ratio	0.615
Span, in.	8.000
Airfoil section	4-percent biconvex
Vertical tail (each):	
Area, in ²	28.881
Λ_{LE} , deg	37.006
Λ_{TE} , deg	0
Aspect ratio	3.745
Semispan, in.	5.200
Airfoil section	4-percent biconvex
Side body (each):	
Length, in.	30.000
Area distribution, in ²	See table II
Cross-sectional shape	Circular
Delta outboard wing panel (each):	
Area, in ²	39.170
Λ_{LE} , deg	65
Λ_{TE} , deg	0
Aspect ratio	1.600
Semispan, in.	5.596
Airfoil section	4-percent biconvex
Total delta planform:	
Area (reference), in ²	182.340
Aspect ratio	2.020
Wing reference chord, in.	11.160
\bar{x} , in.	1.841
Arrow outboard wing panel (each):	
Area, in ²	37.515
Λ_{LE} (inner), deg	70
Λ_{LE} (outer), deg	66
Λ_{TE} (inner), deg	0
Λ_{TE} (outer), deg	31.79
Aspect ratio	1.920
Semispan, in.	6.000
Airfoil section	4-percent biconvex

Table I. Concluded

Total arrow planform:	
Area (reference), in ²	179.030
Aspect ratio	2.234
Wing reference chord, in.	10.920
\bar{x} , in.	2.253
Trapezoidal outboard wing panel (each):	
Area, in ²	44.410
Λ_{LE} , deg	20
Λ_{TE} , deg	-20
Aspect ratio	2.090
Semispan, in.	6.810
Airfoil section	4-percent biconvex
Total trapezoidal planform:	
Area (reference), in ²	192.820
Aspect ratio	2.421
Wing reference chord, in.	10.160
\bar{x} , in.	1.420

Table II. Normal Area Distribution of Side Body

x/l	Area
0	0
.05	.400
.10	.800
.15	1.150
.20	1.500
.25	1.825
.30	2.110
.35	2.300
.40	2.410
.45	2.410
.50	2.350
.55	2.225
.60	2.075
.65	1.900
.70	1.700
.75	1.500
.80	1.250
.85	.975
.90	.680
.95	.350
1.00	0

Table III. Geometric Characteristics of Single-Body Model Components

Fuselage:	
Length, in.	32.200
Base area, in ²	1.118
Chamber area, in ²	2.667
Capture area, in ²	2.401
Exit area, in ²	2.074
Inlet area, in ²	1.997
Vertical tail (each):	
Area, in ²	12.211
Λ_{LE} , deg	60
Λ_{TE} , deg	30
Aspect ratio	1.100
Semispan, in.	3.664
Airfoil section	64A005
Horizontal tail (each):	
Area, in ²	24.336
Λ_{LE} , deg	45
Λ_{TE} , deg	21
Aspect ratio	3.000
Semispan, in.	4.300
Airfoil section (root chord)	5-percent biconvex
Airfoil section (tip chord)	3-percent biconvex
Delta wing:	
Area (reference), in ²	200.747
Λ_{LE} , deg	65.5
Λ_{TE} , deg	-6
Aspect ratio	1.490
Span, in.	17.270
Airfoil section	64A005
Wing reference chord, in.	14.327
\bar{x} , in.	13.626
Arrow wing:	
Area (reference), in ²	165.600
Λ_{LE} (inner), deg	70
Λ_{LE} (outer), deg	66
Λ_{TE} (inner), deg	0
Λ_{TE} (outer), deg	50
Aspect ratio	1.900
Span, in.	17.618
Airfoil section (0.30 semispan)	65A004
Airfoil section (root chord)	65A004
Wing reference chord, in.	12.340
\bar{x} , in.	14.876

Table III. Concluded

Trapezoidal wing:	
Area (reference), in ²	149.760
Leading-edge sweep, deg	20
Trailing-edge sweep, deg	-20
Aspect ratio	3.500
Span, in.	22.894
Airfoil section (root chord)	4-percent biconvex
Airfoil section (tip chord)	3-percent biconvex
Wing reference chord, in.	6.981
\bar{x} , in.	18.144

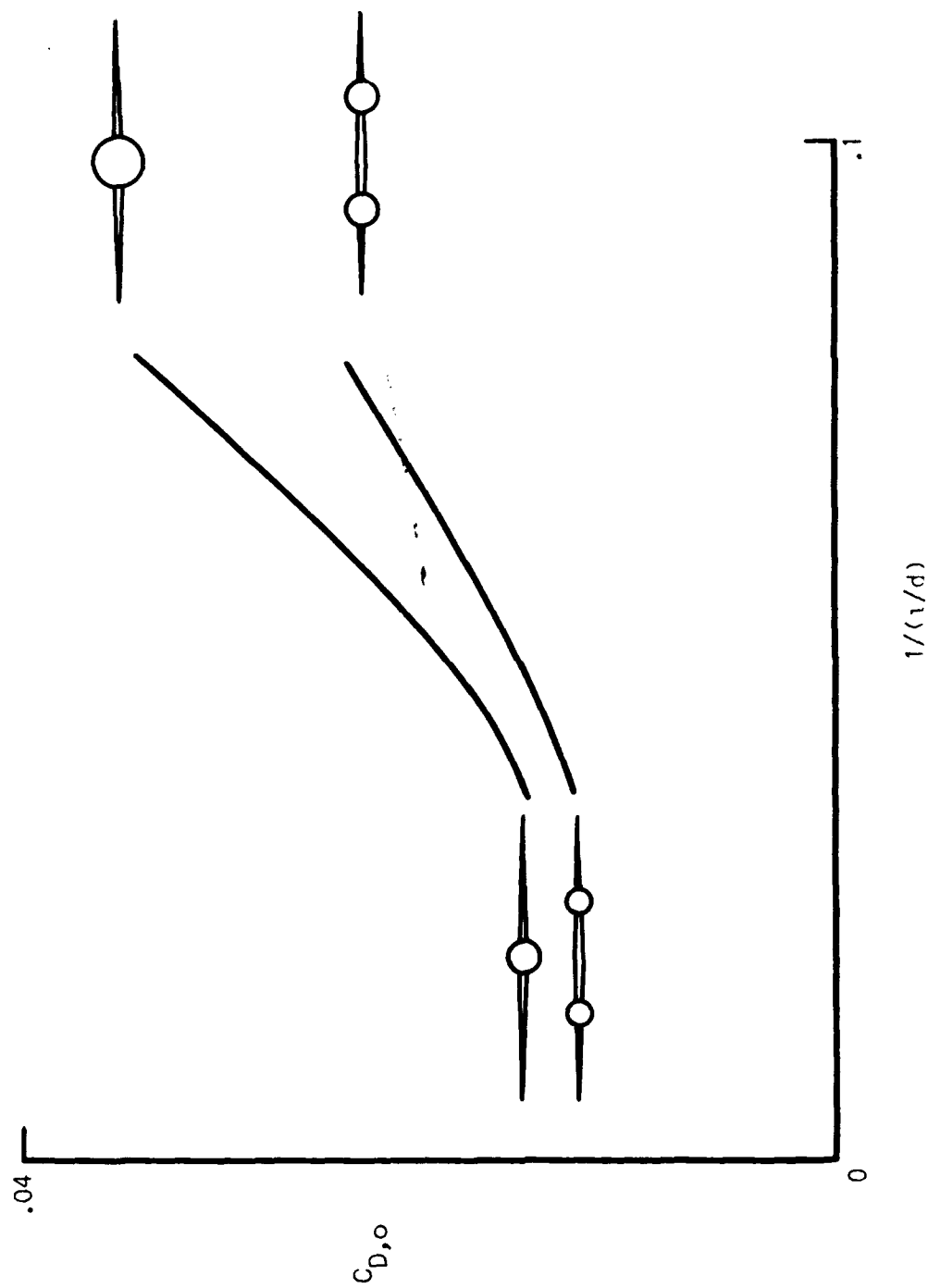
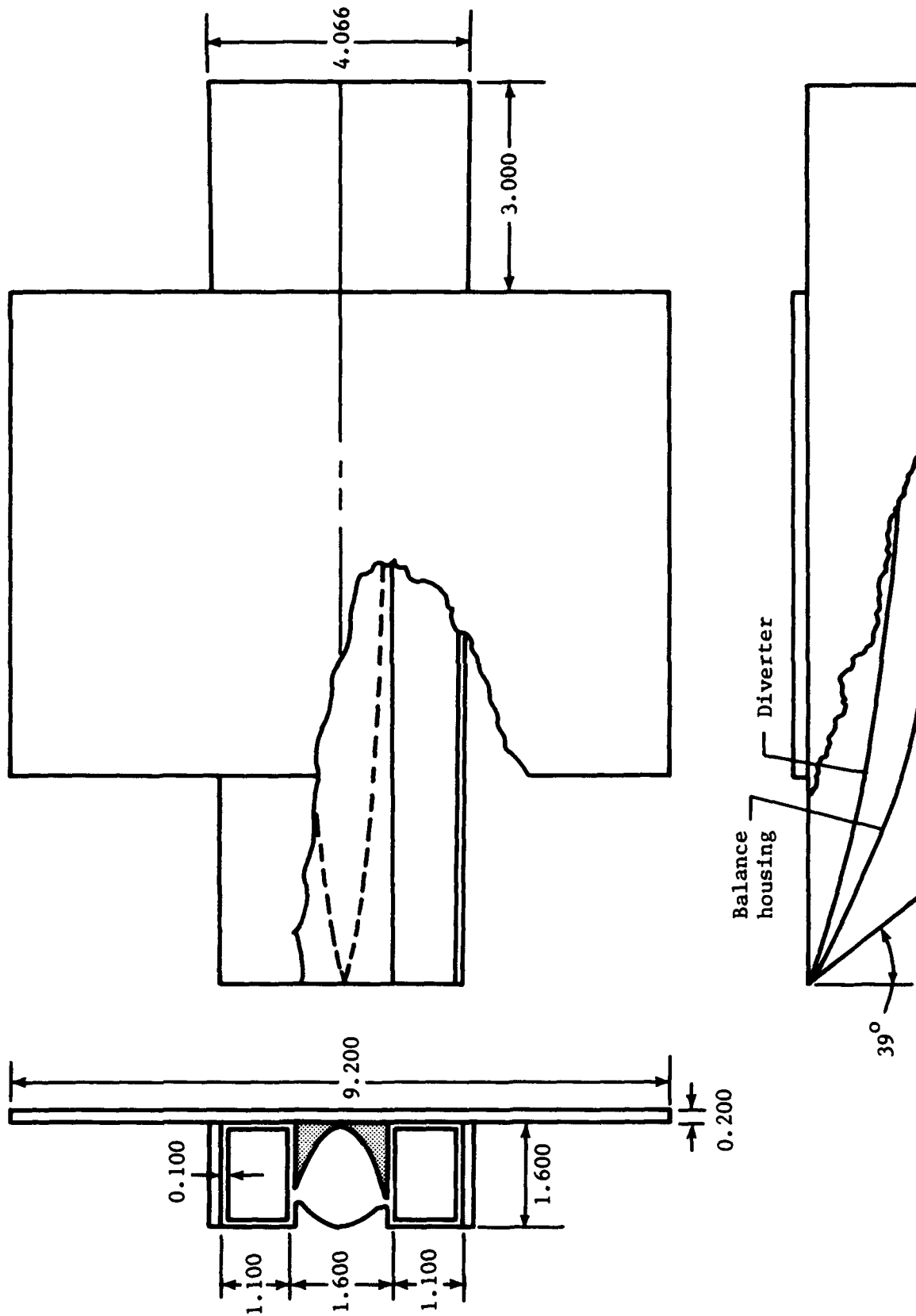
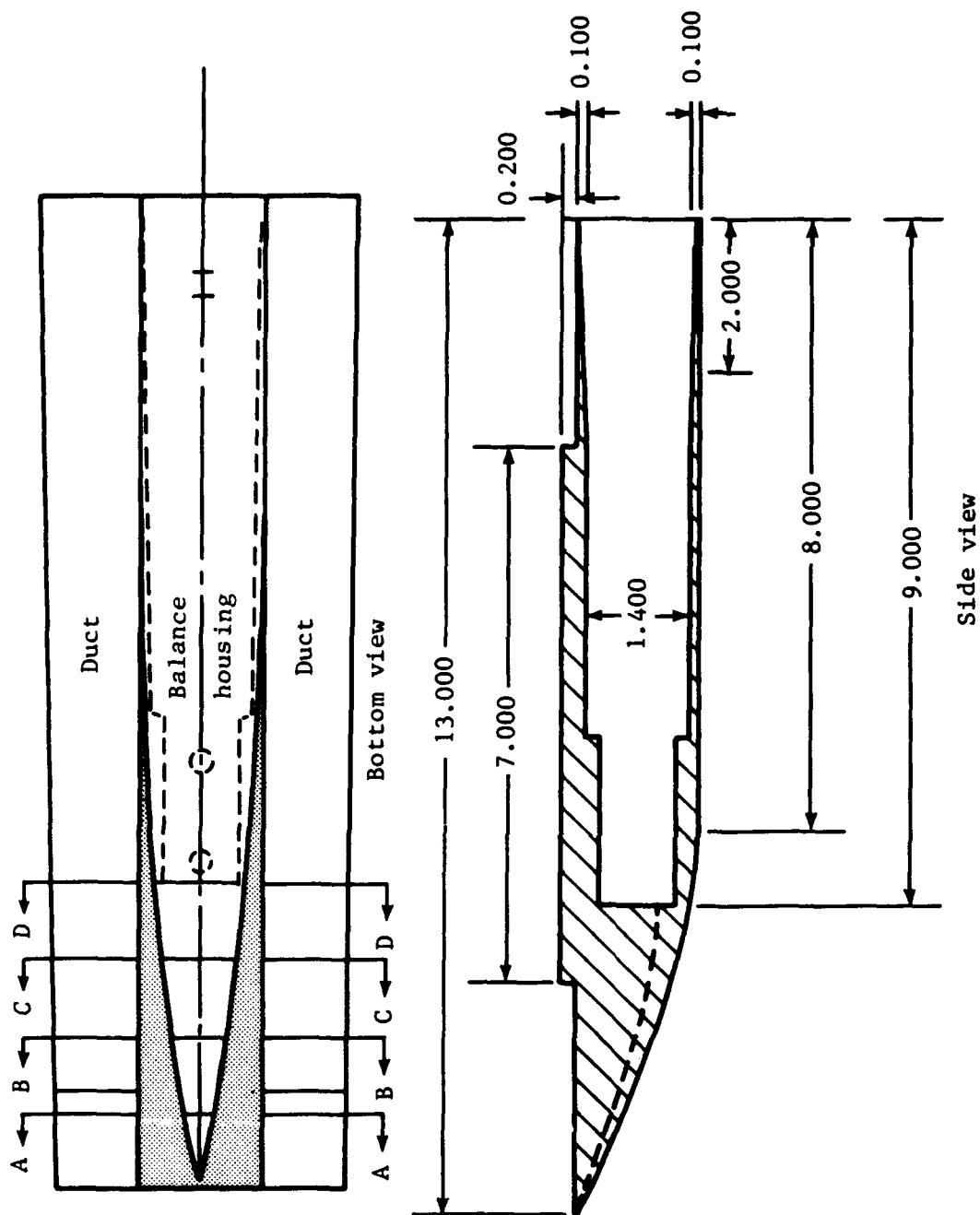
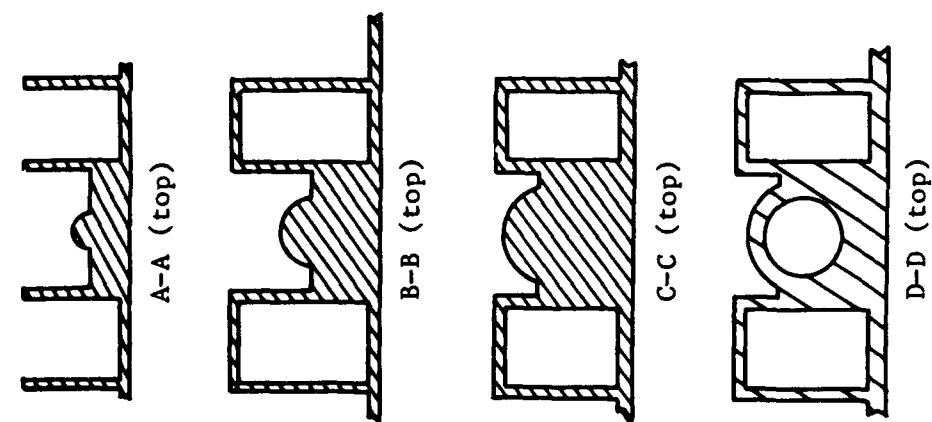


Figure 1. Effect of fineness ratio on drag reduction potential of multibody concept. (From ref. 9.)

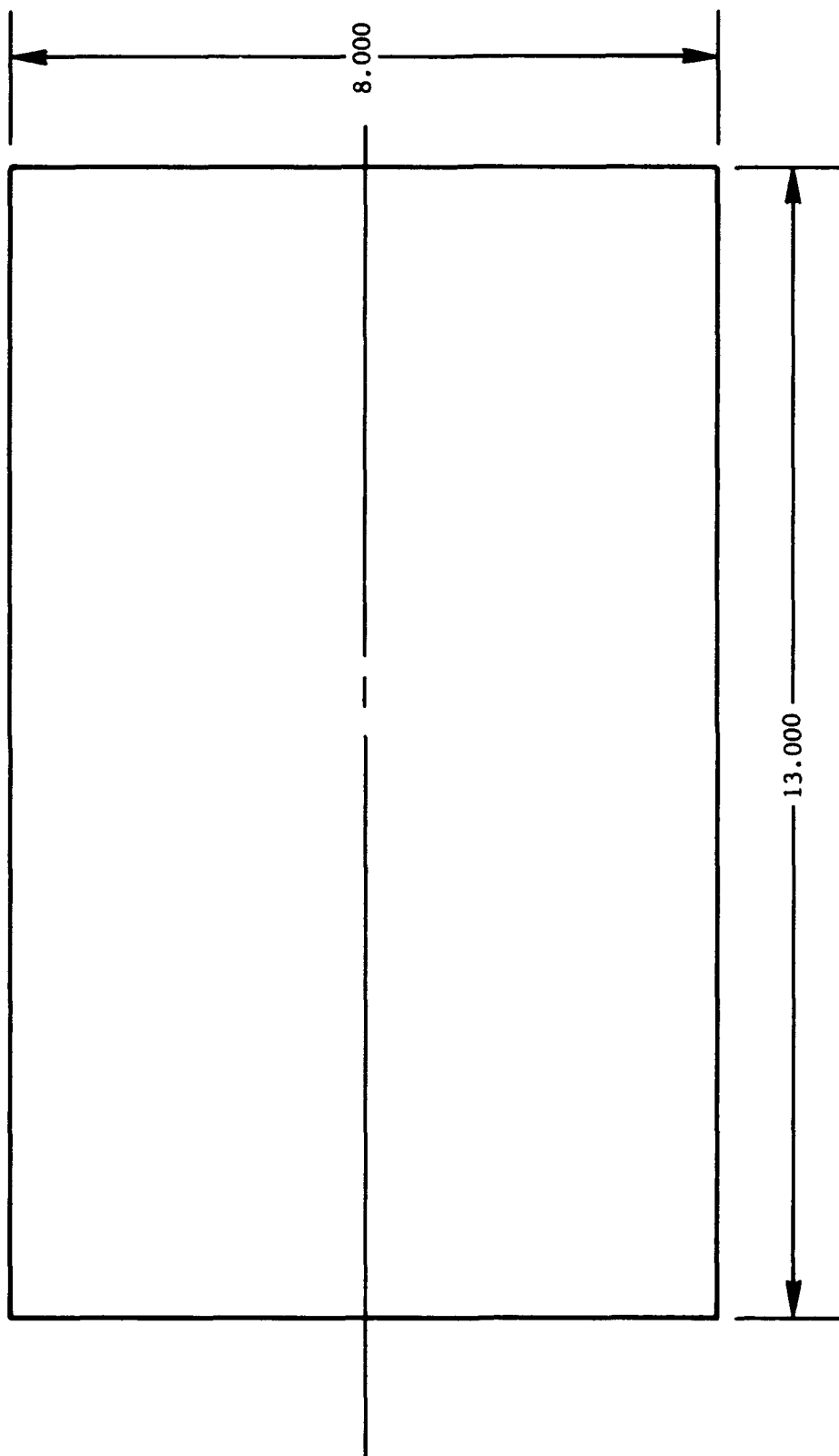


(a) Three-view sketch of balance housing and two rectangular flow-through ducts.

Figure 3. Details of multibody model. All linear dimensions are in inches.

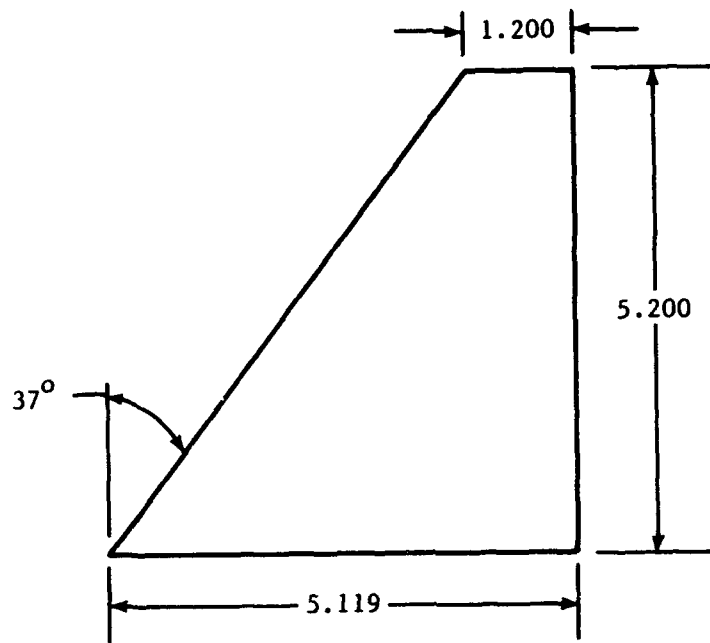


(b) Lateral, longitudinal, and cross-sectional views of balance housing and flow-through ducts.
Figure 3. Continued.



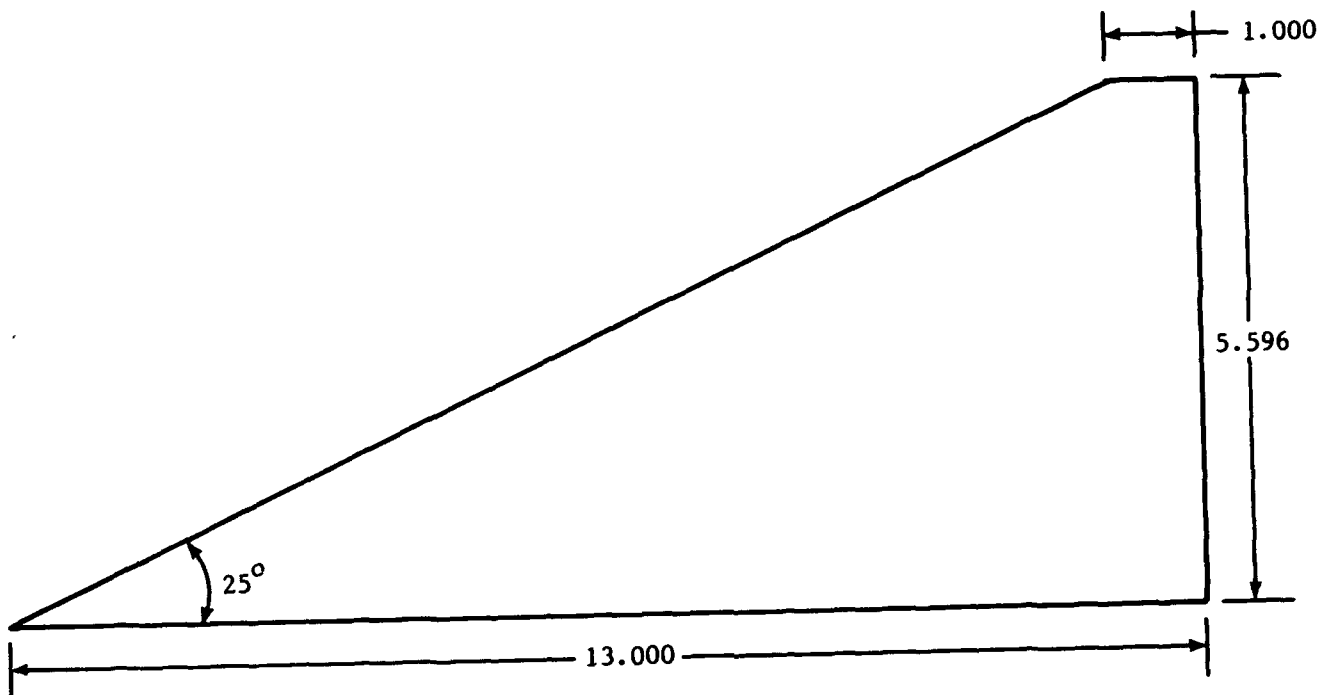
(c) Inboard wing panel.

Figure 3. Continued.



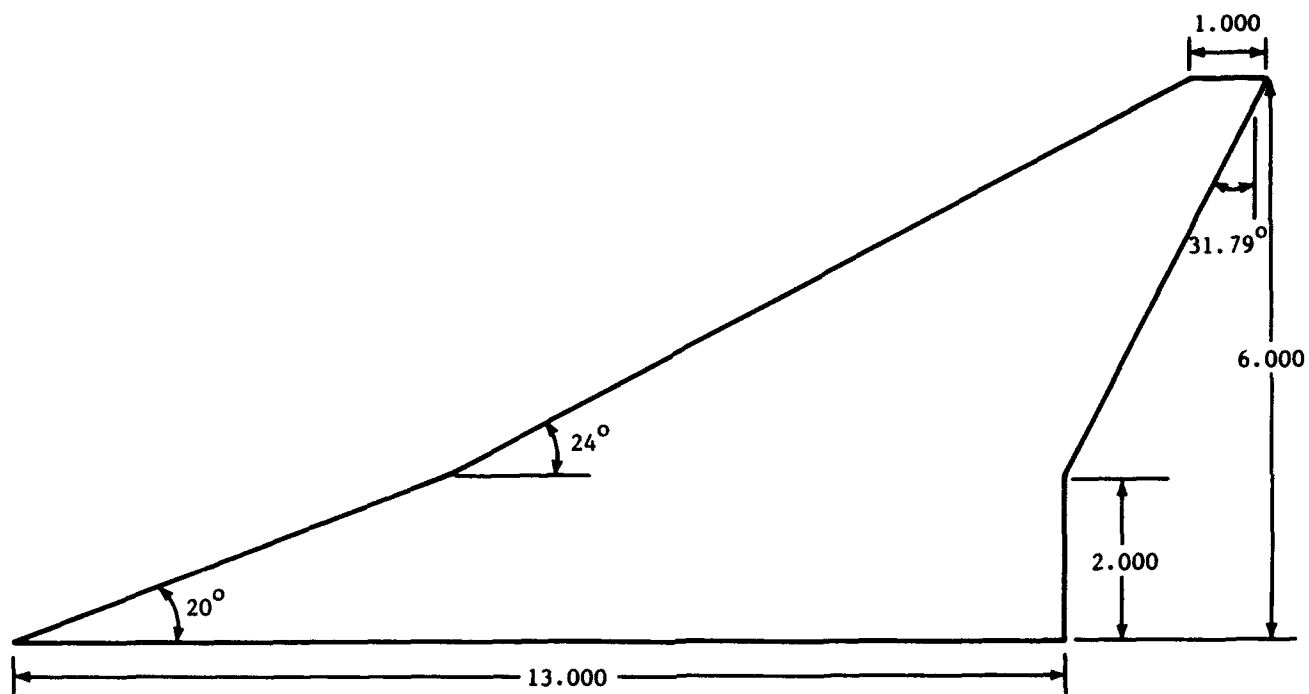
(d) Vertical tail.

Figure 3. Continued.



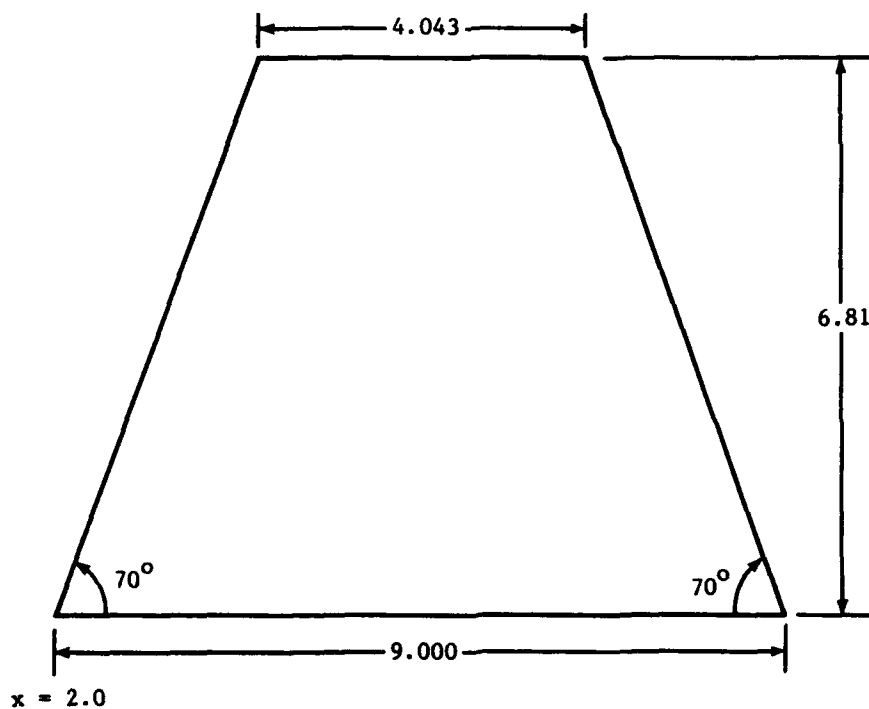
(e) Details of delta outboard wing panel.

Figure 3. Continued.



(f) Details of arrow outboard wing panel.

Figure 3. Continued.



(g) Details of trapezoidal outboard wing panel.

Figure 3. Concluded.



L-83-8,948

Figure 4. Lower view of multibody model with delta outboard wing panel.



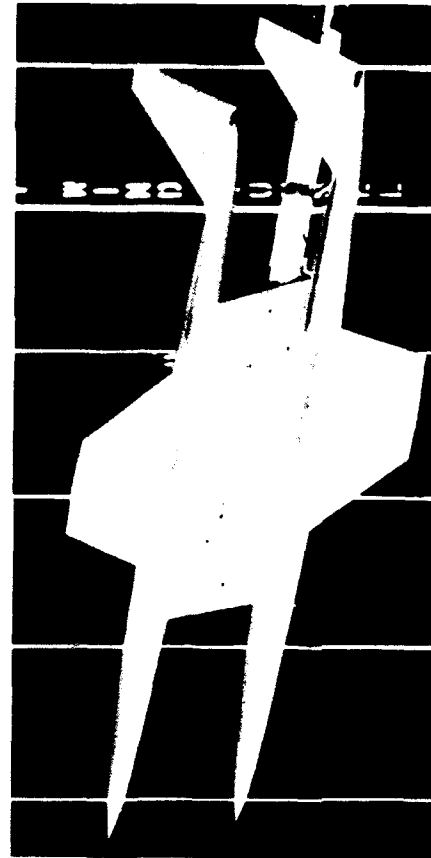
L-83-8,950

65° Delta wing



L-85-10,461

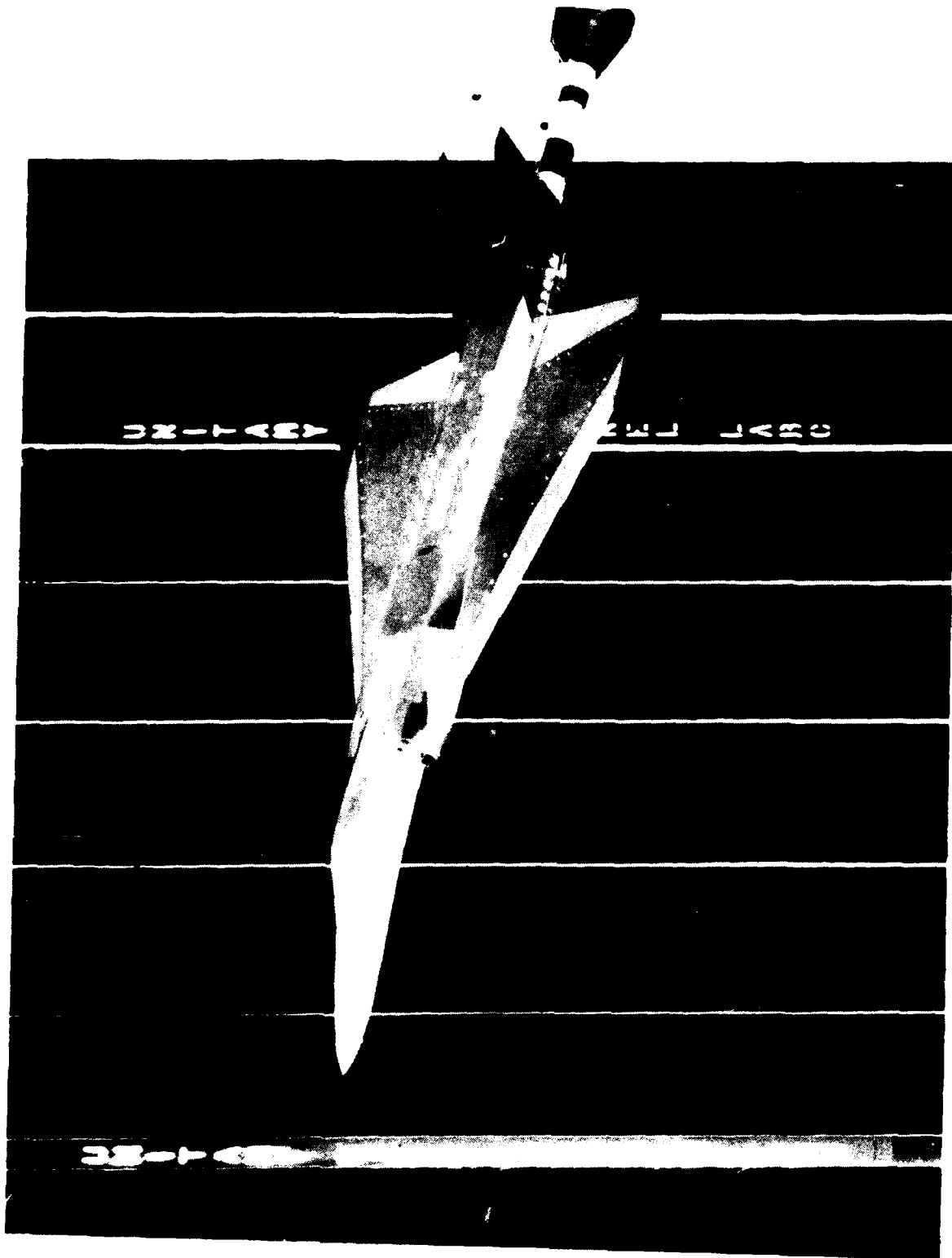
70°/66° Arrow wing



L-85-10,460

20° Trapezoidal wing

Figure 5. Multibody models.



L-82-9,809

Figure 6. Single-body model with delta wing.

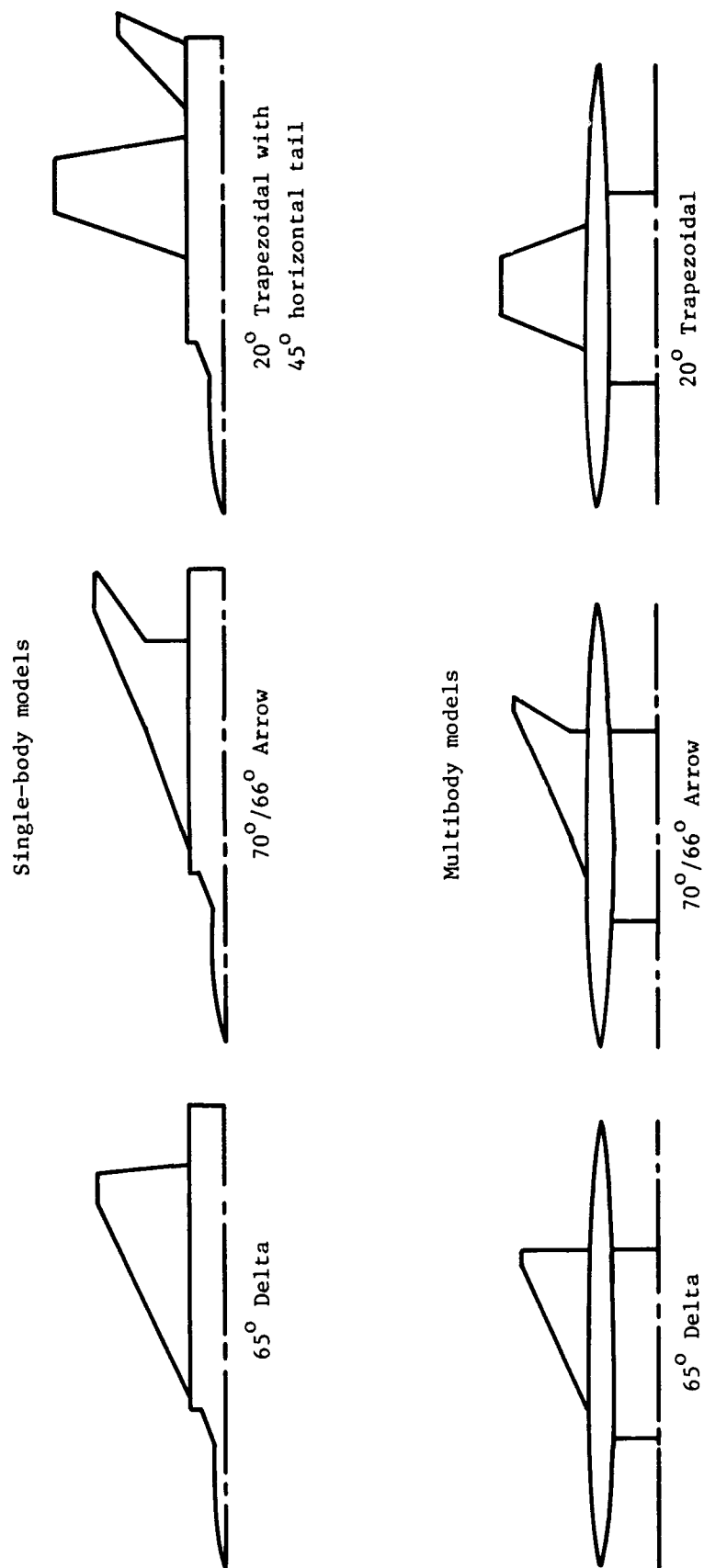


Figure 7. Comparison of planforms for single-body models and multibody models.

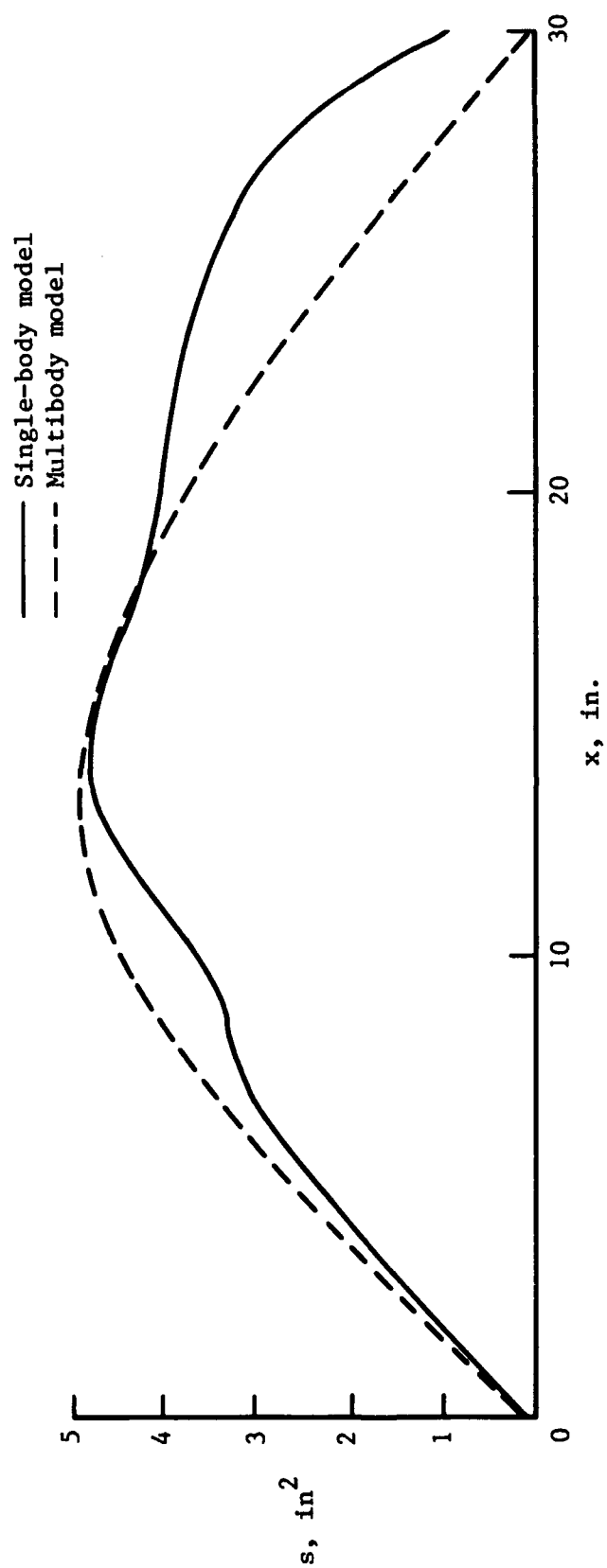
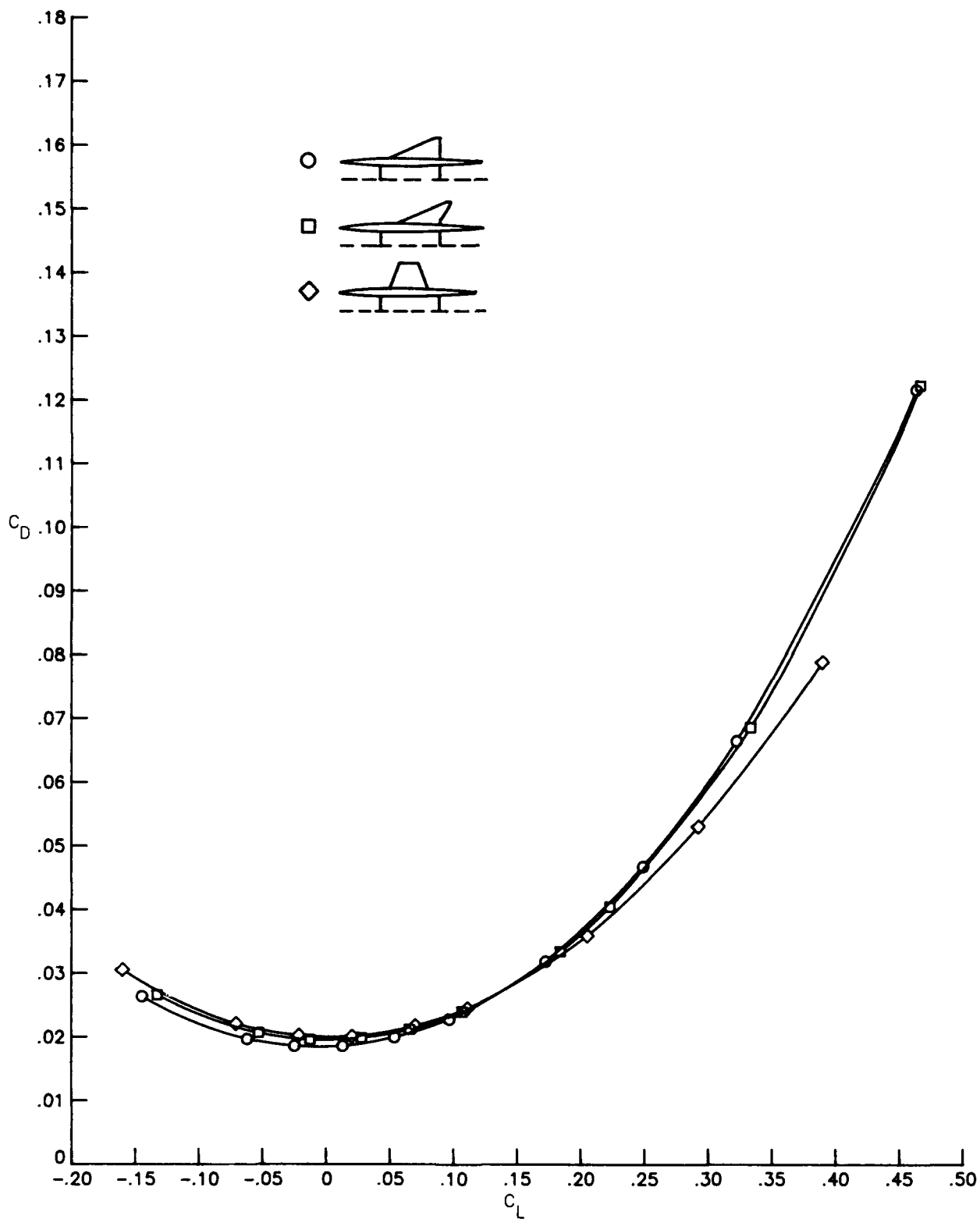
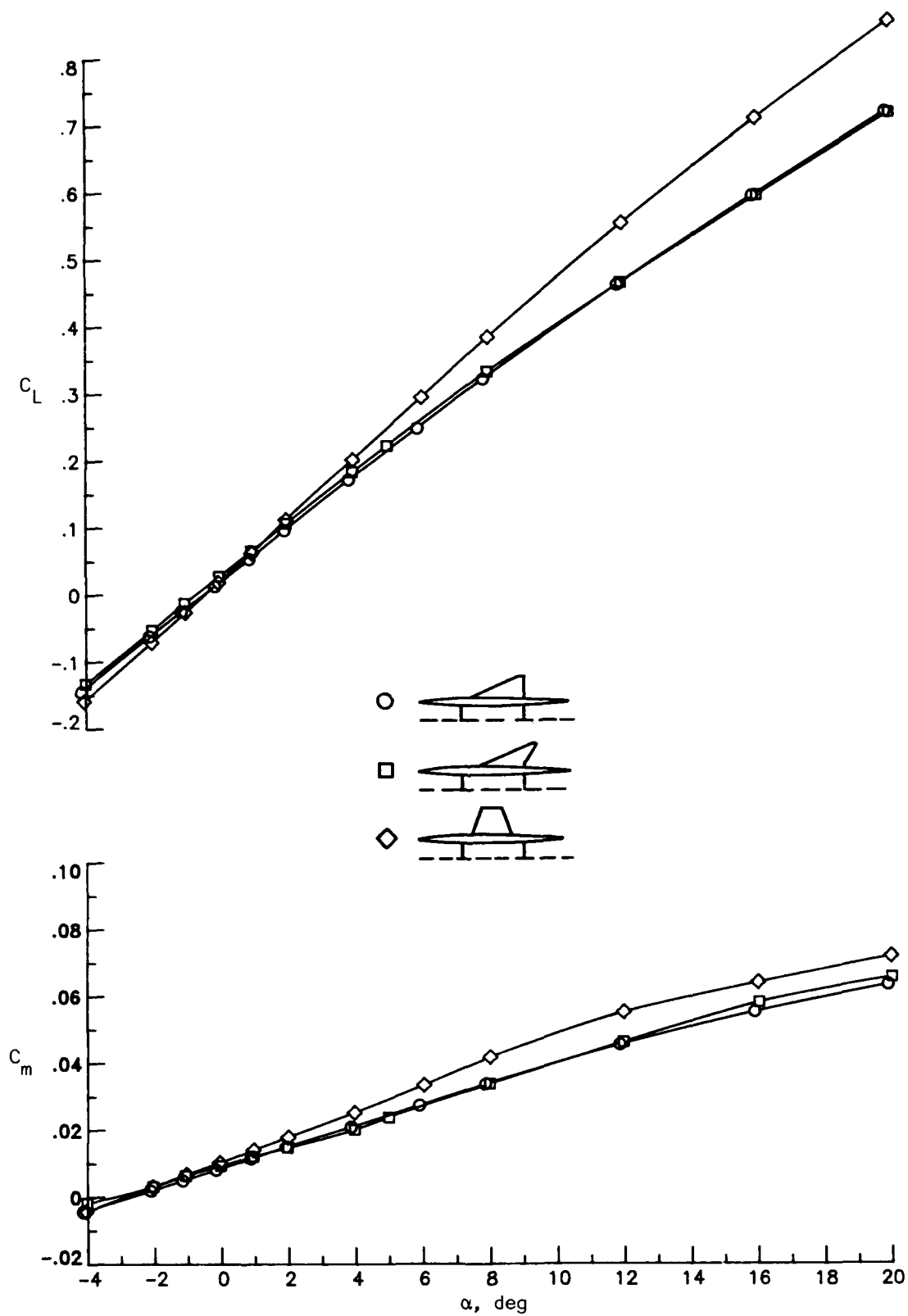


Figure 8. Comparison of fuselage-only normal area distributions for single-body and multibody models.



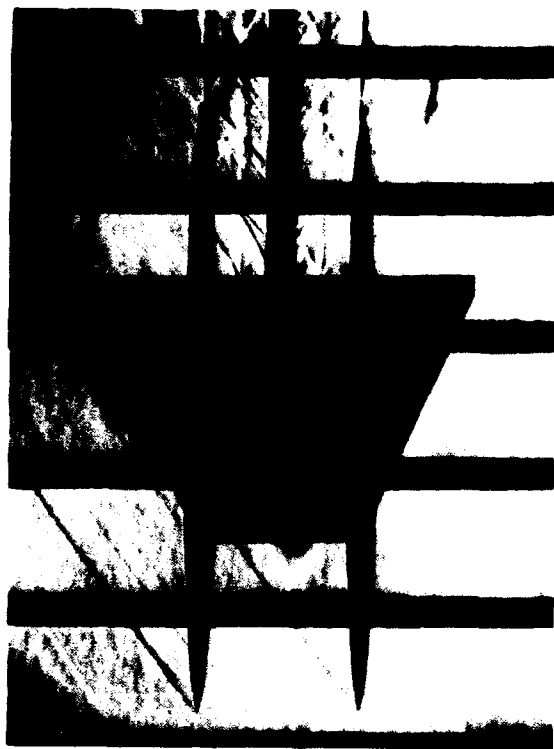
(a) Drag characteristics.

Figure 9. Effect of planform on longitudinal aerodynamic characteristics. Vertical tails off; $M = 1.80$.



(b) Lift and pitching-moment characteristics.

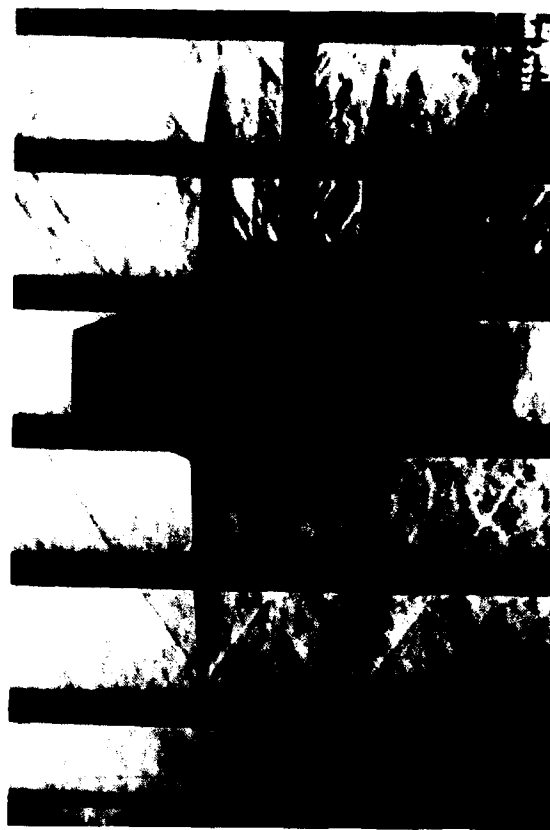
Figure 9. Concluded.



65° Delta wing

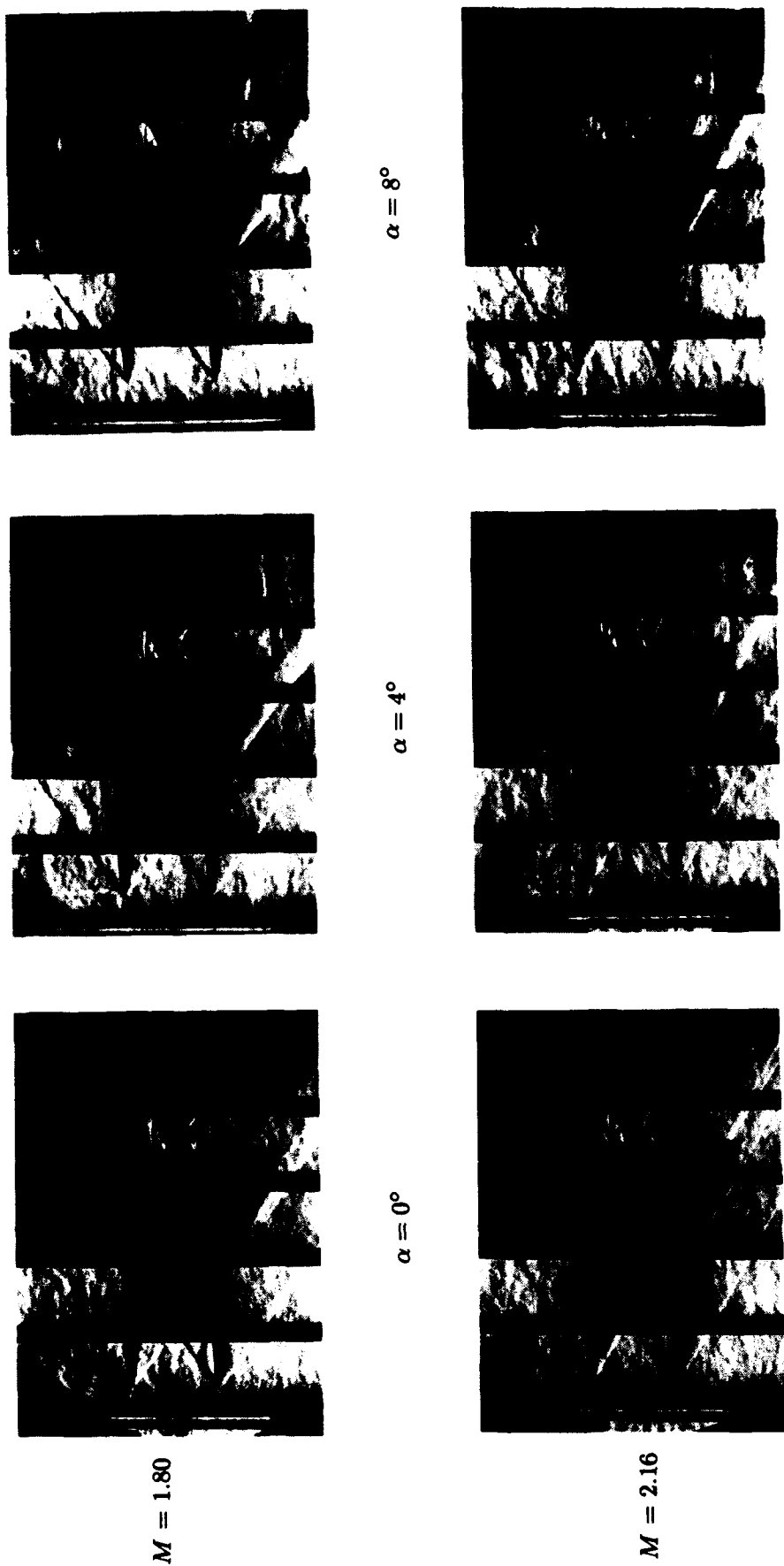


70°/66° Arrow wing



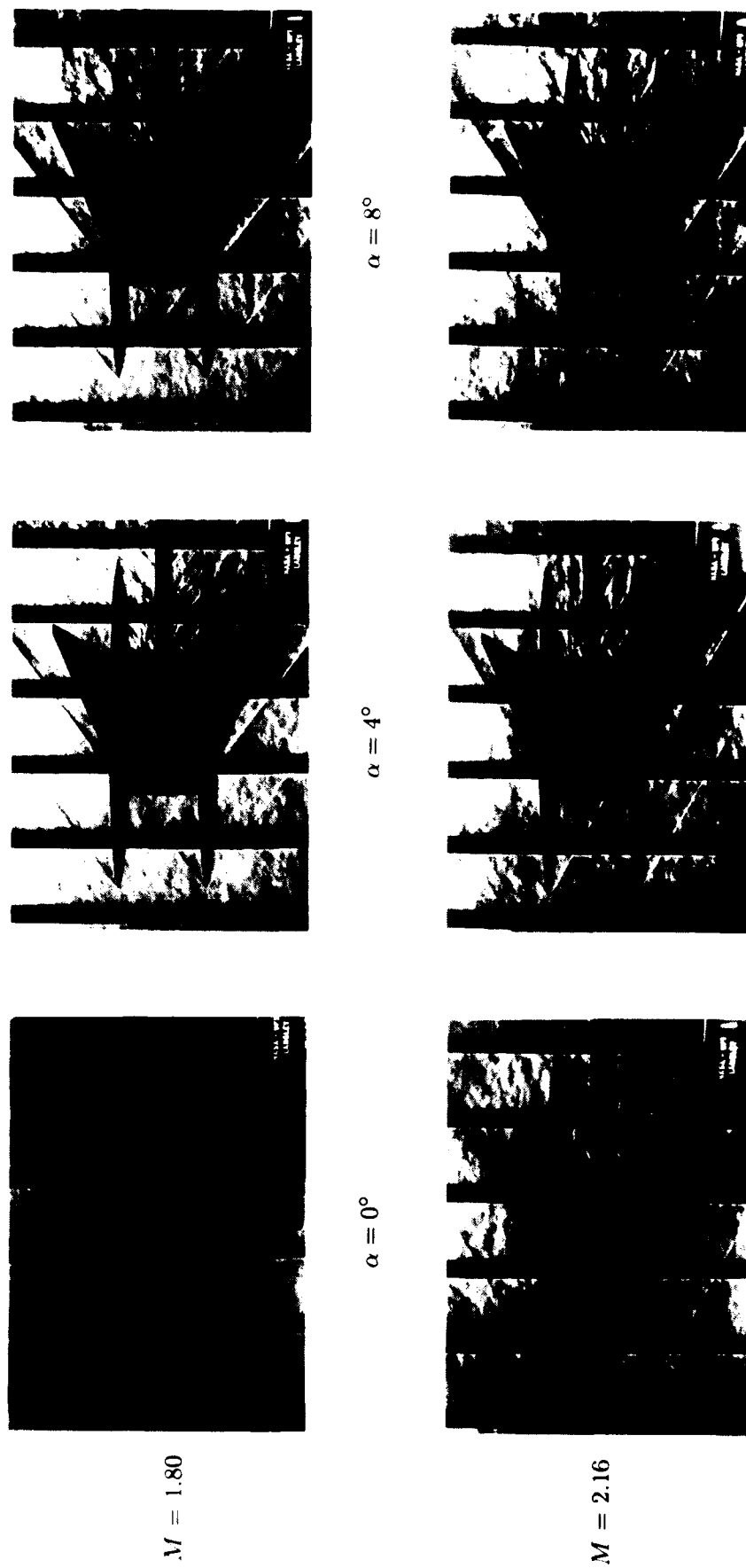
20° Trapezoidal wing

Figure 10. Schlieren photographs showing effect of planform on shock structure at $M = 1.80$ and $\alpha = 0^\circ$.



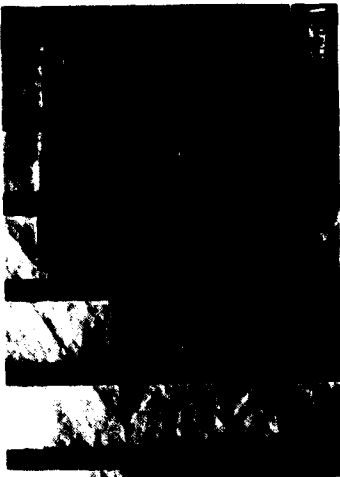
(a) Delta wing.

Figure 11. Schlieren photographs showing effects of Mach number and angle of attack for multibody models at $\beta = 0^\circ$.



(b) Arrow wing.

Figure 11. Continued.



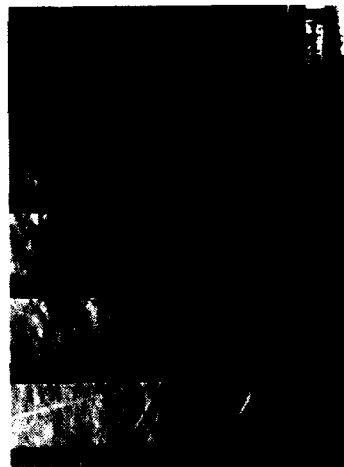
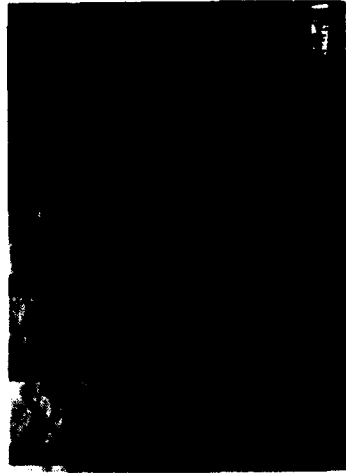
$M = 1.80$



$\alpha = 0^\circ$

$\alpha = 4^\circ$

$\alpha = 8^\circ$

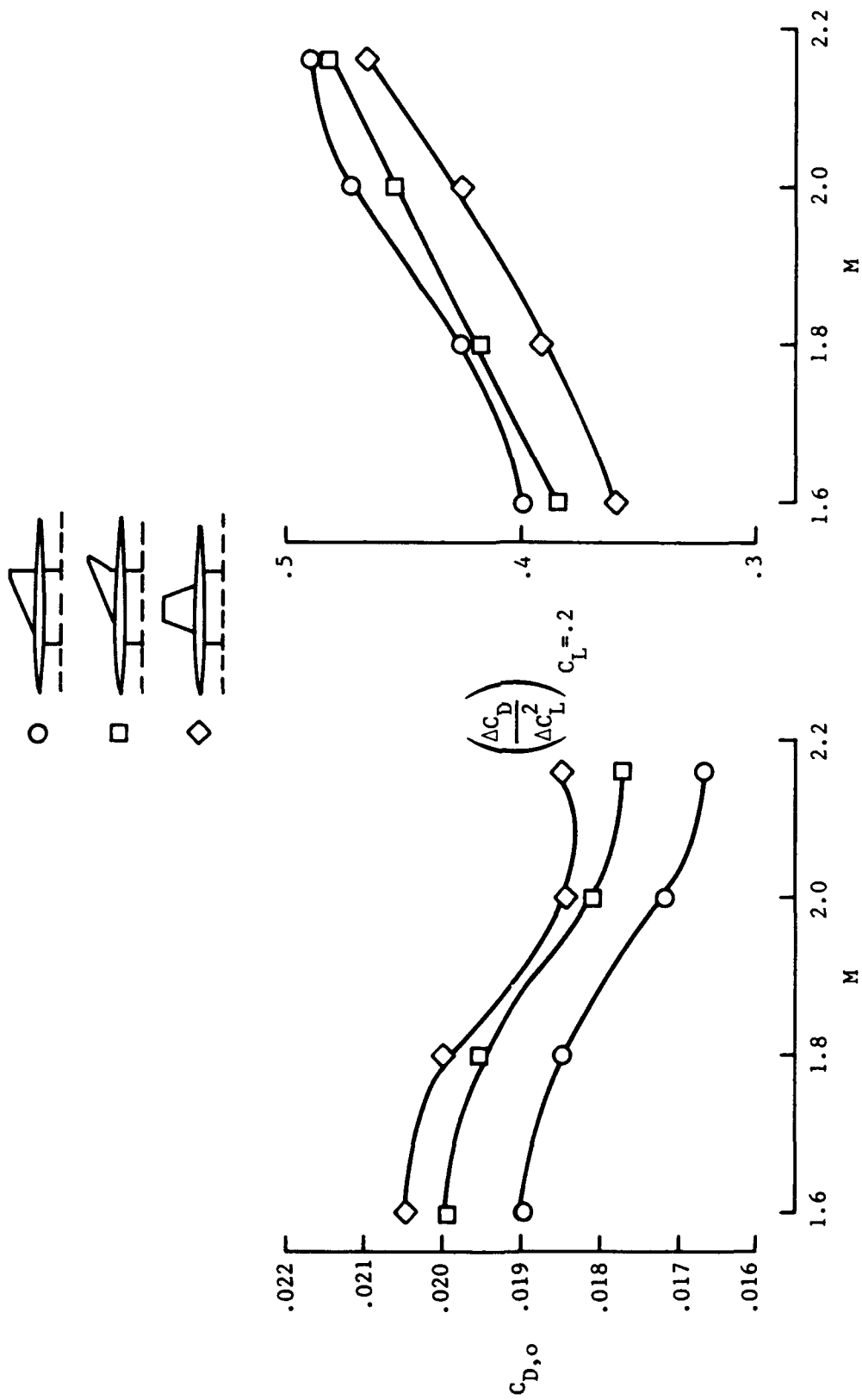


$M = 2.16$



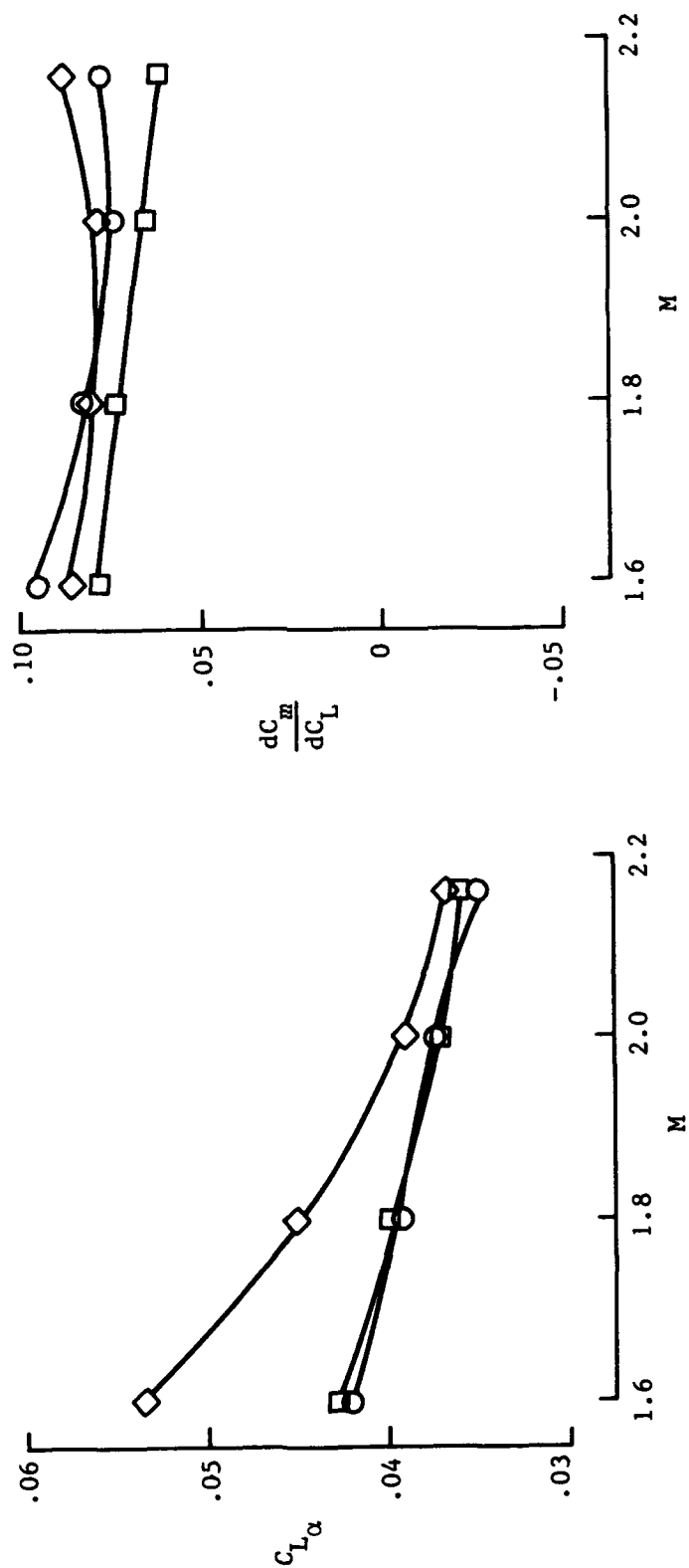
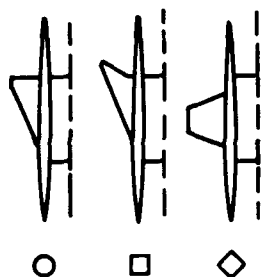
(c) Trapezoidal wing.

Figure 11. Concluded.



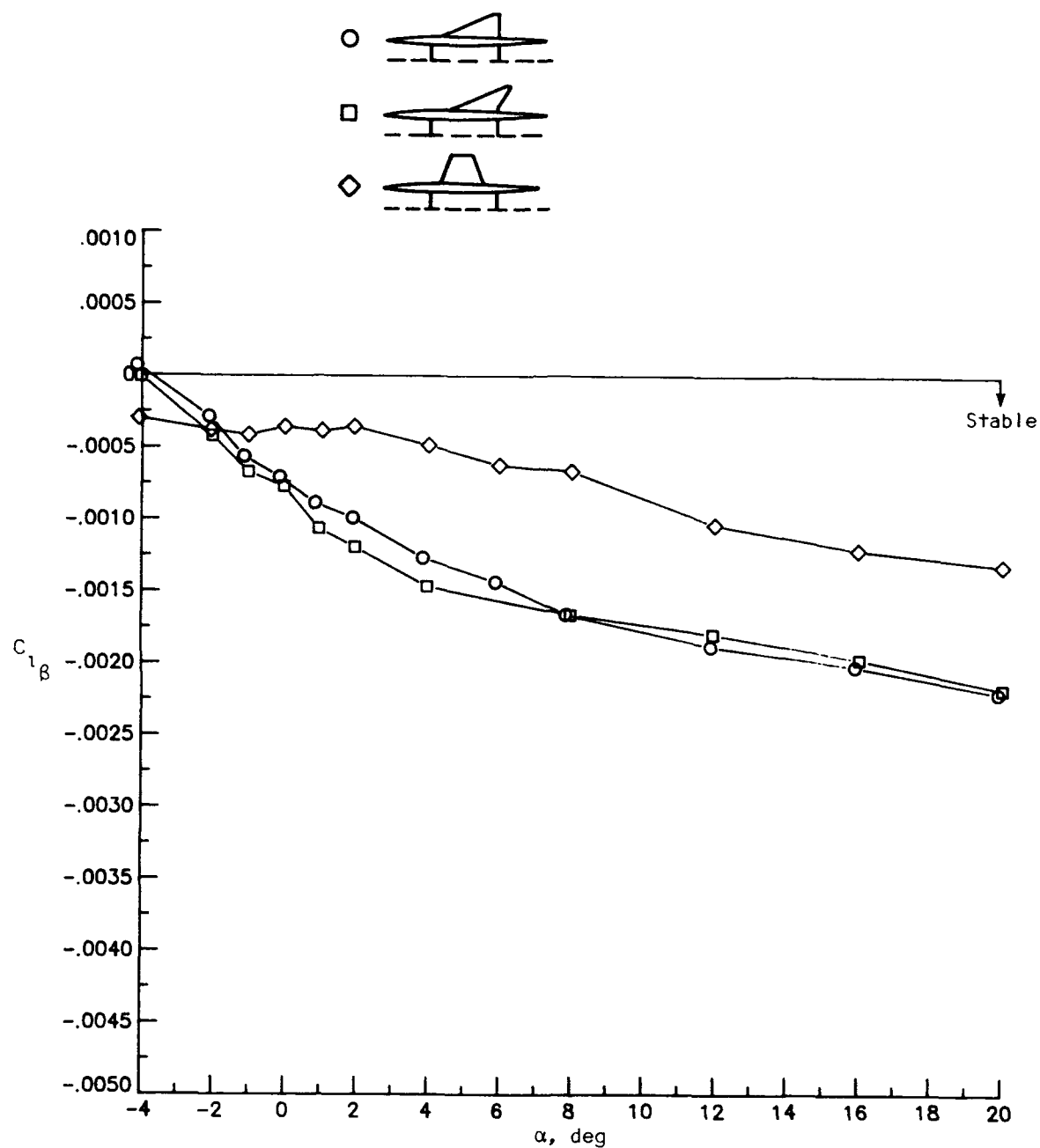
(a) Drag characteristics.

Figure 12. Effects of planform and Mach number on longitudinal aerodynamic characteristics. Vertical tails off.



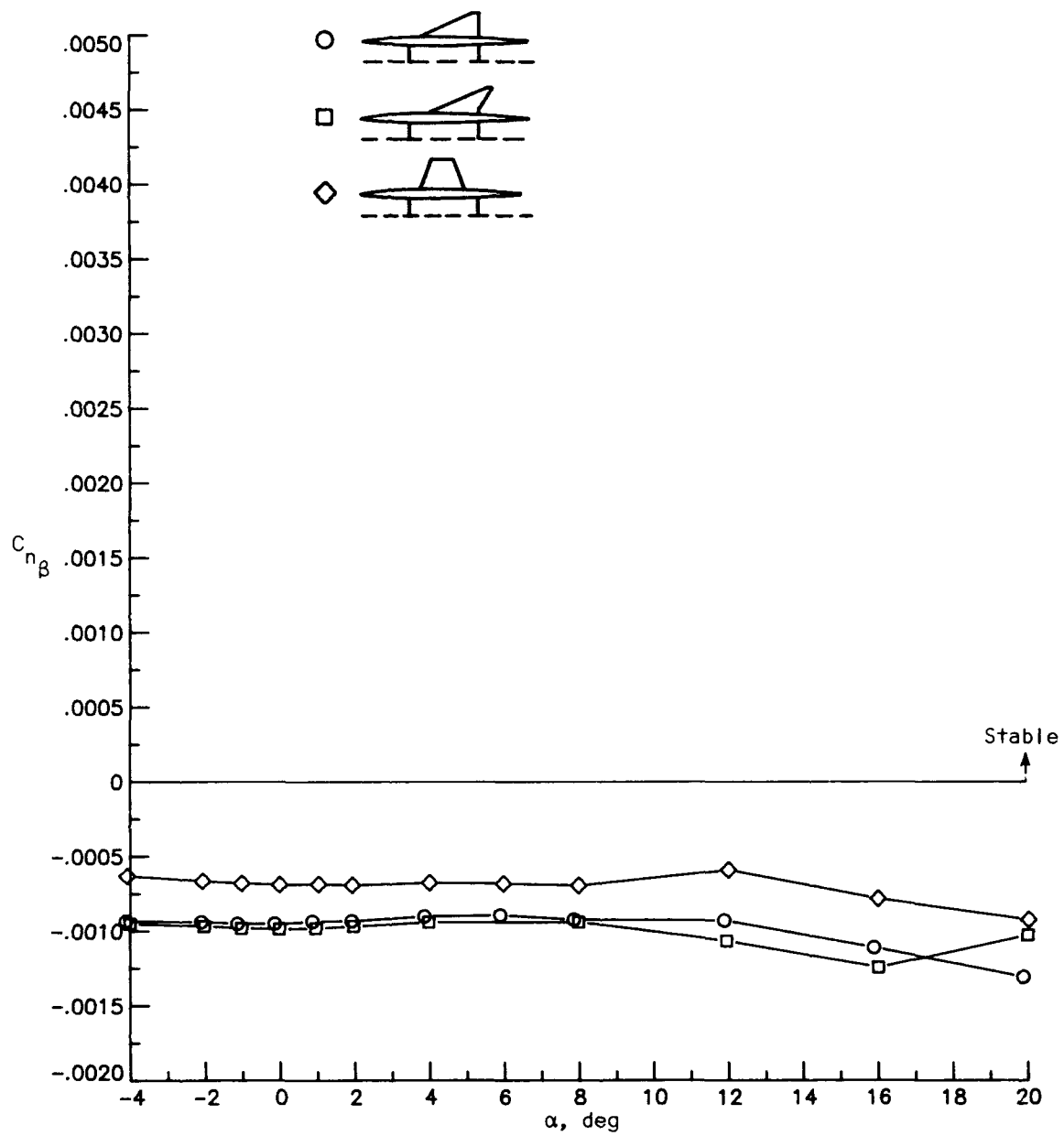
(b) Lift and pitching-moment characteristics.

Figure 12. Concluded.



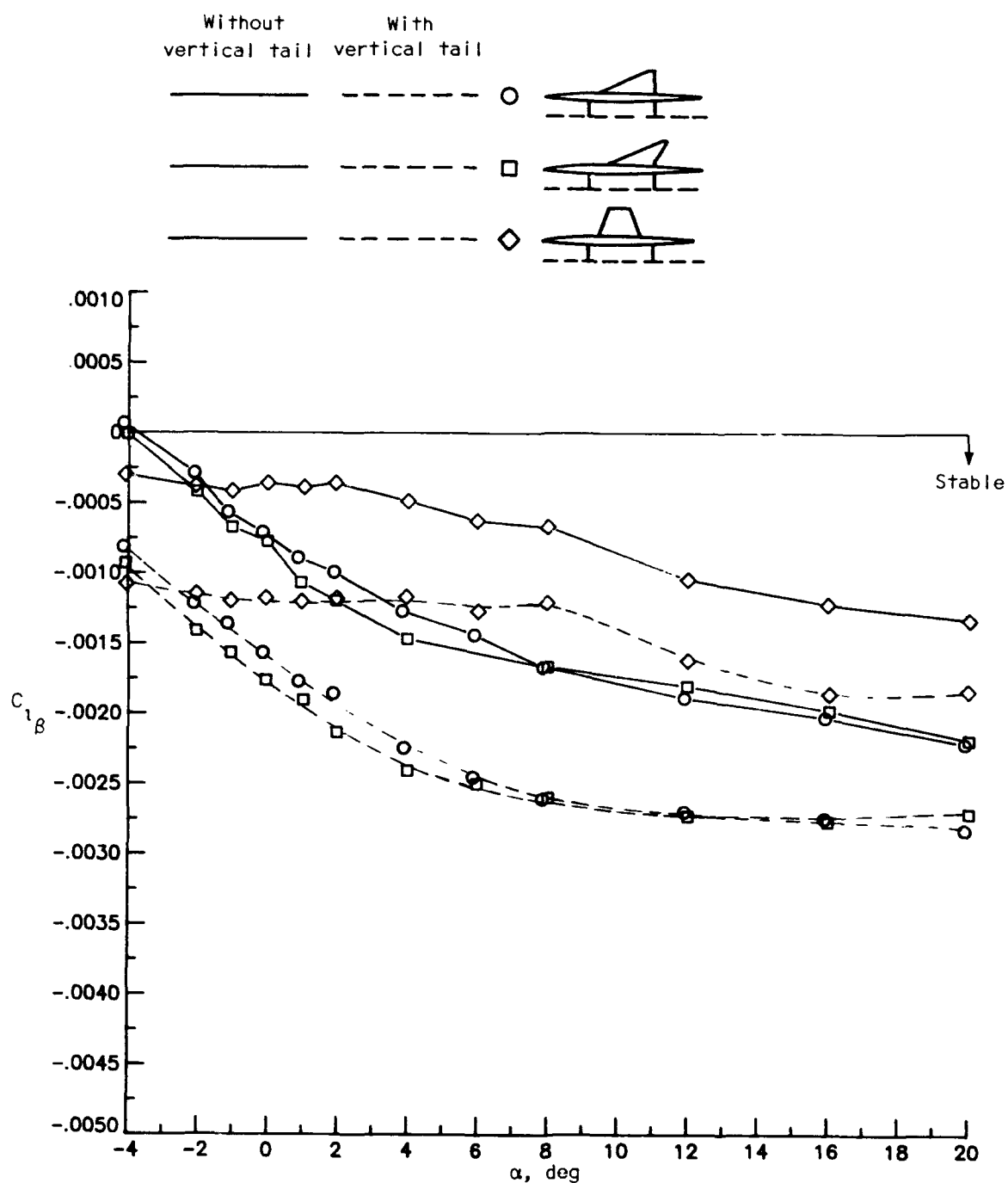
(a) Lateral stability characteristics.

Figure 13. Effect of planform on lateral-directional stability characteristics. Vertical tails off; $M = 1.80$.



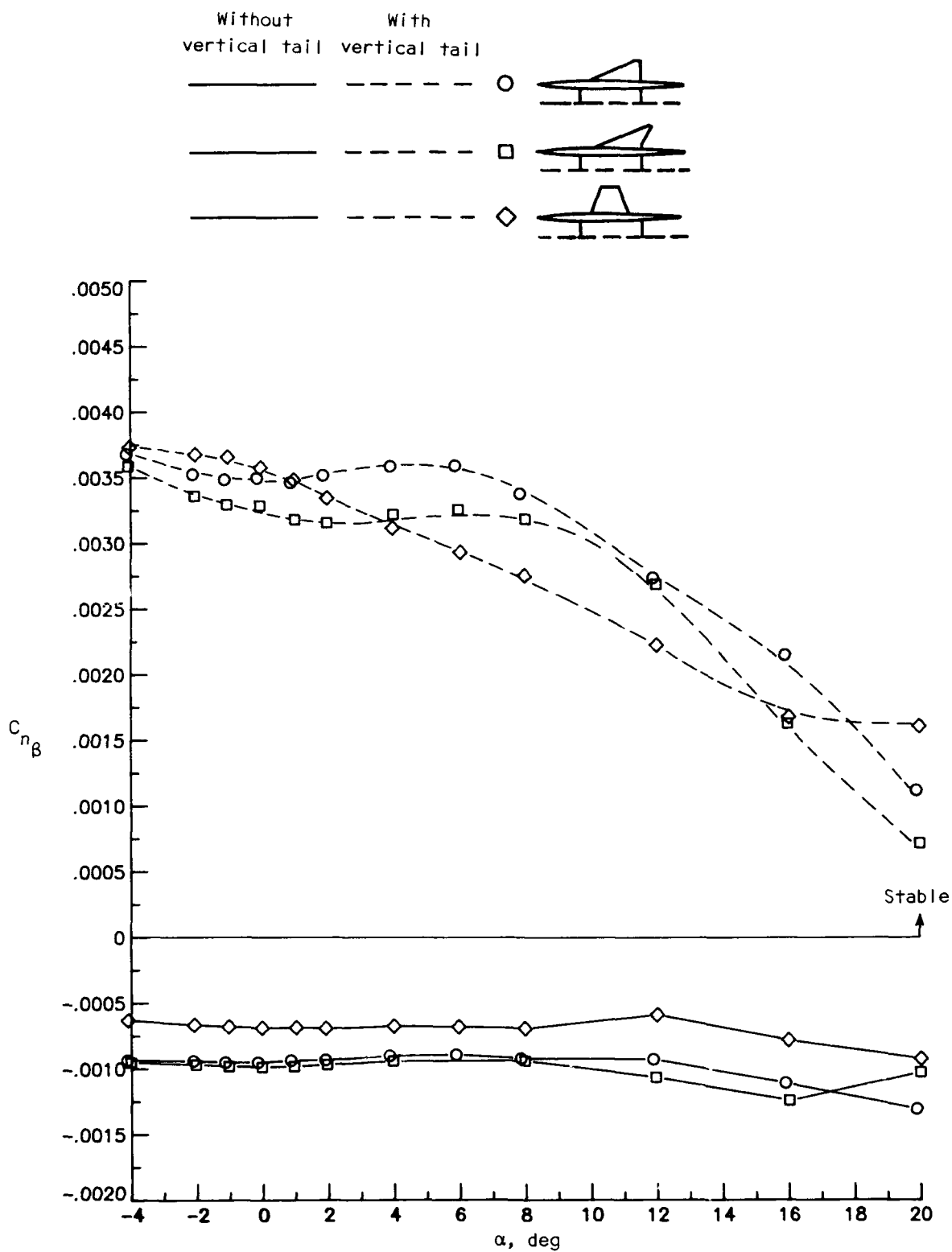
(b) Directional stability characteristics.

Figure 13. Concluded.



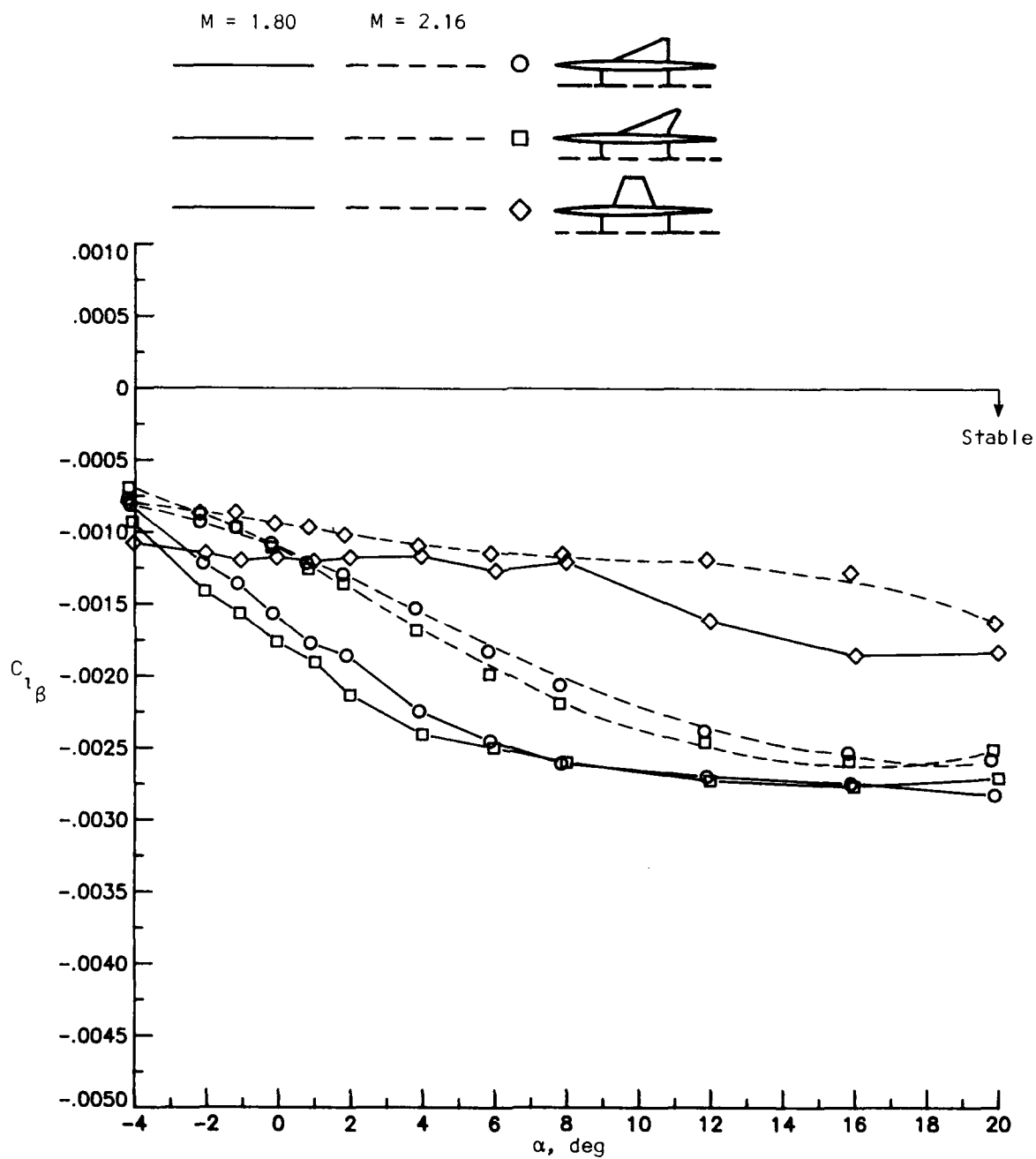
(a) Lateral stability characteristics.

Figure 14. Effect of vertical tails on lateral-directional stability characteristics. $M = 1.80$.



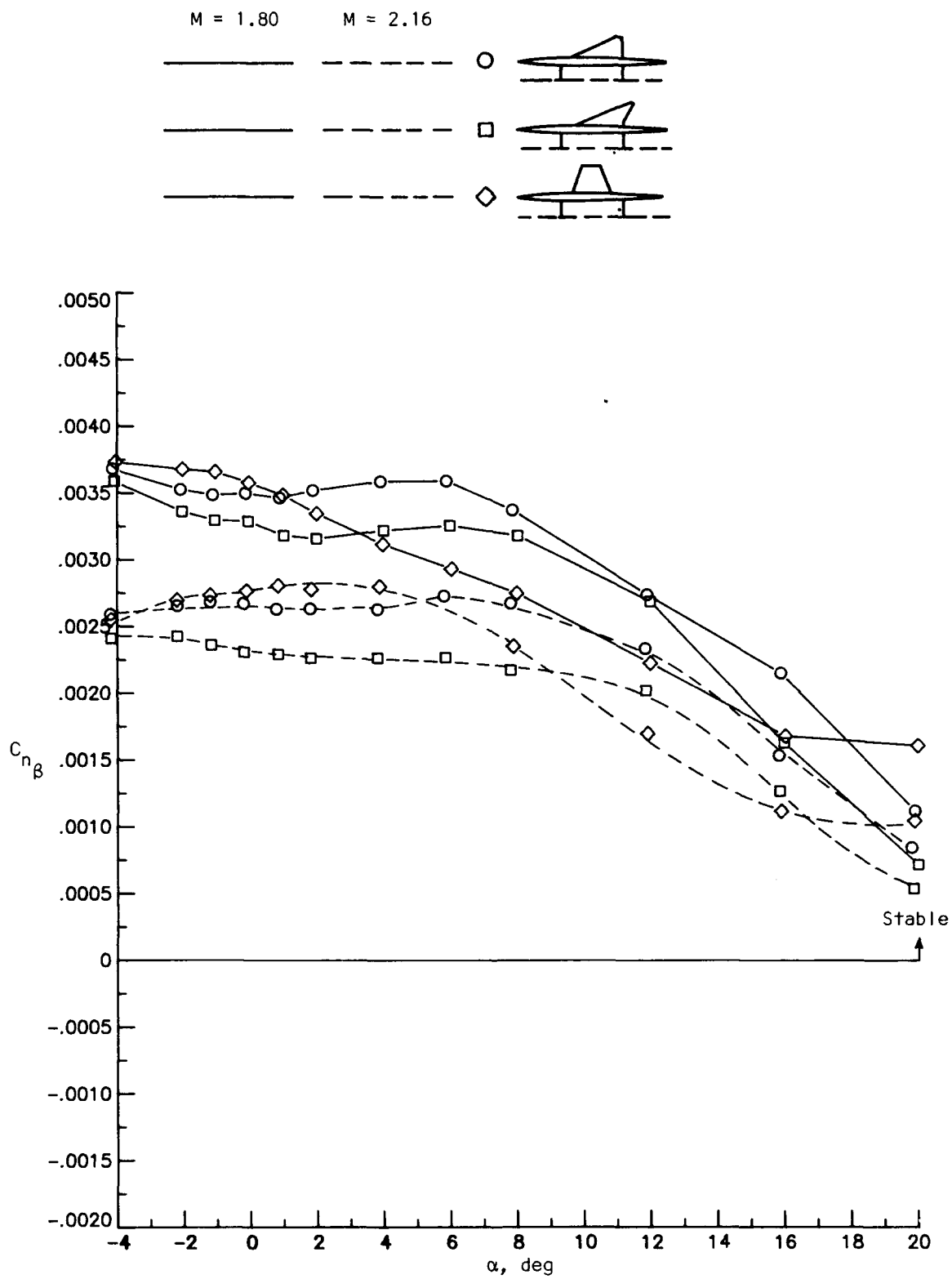
(b) Directional stability characteristics.

Figure 14. Concluded.



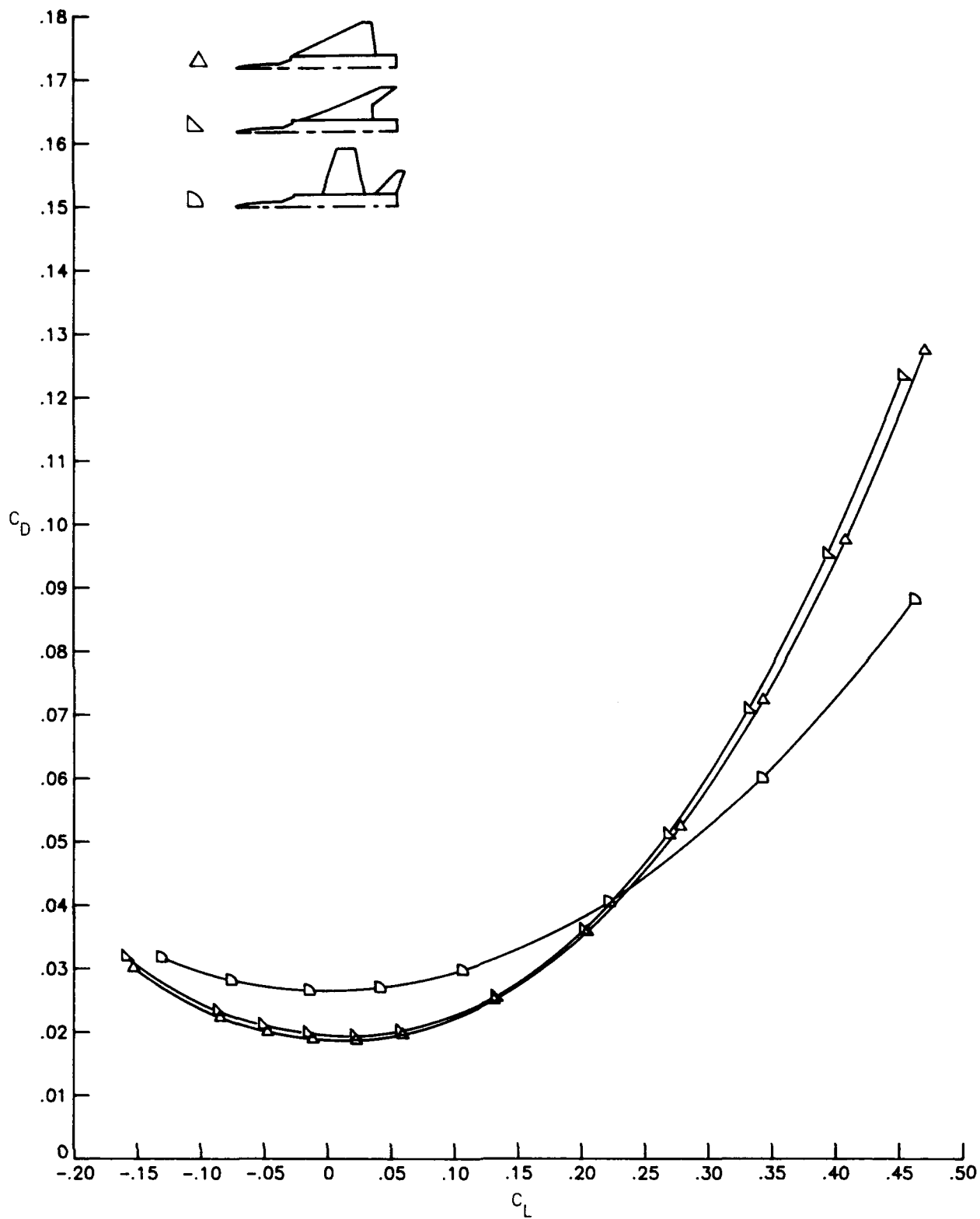
(a) Lateral stability characteristics.

Figure 15. Effect of Mach number on lateral-directional stability characteristics. Vertical tails on.



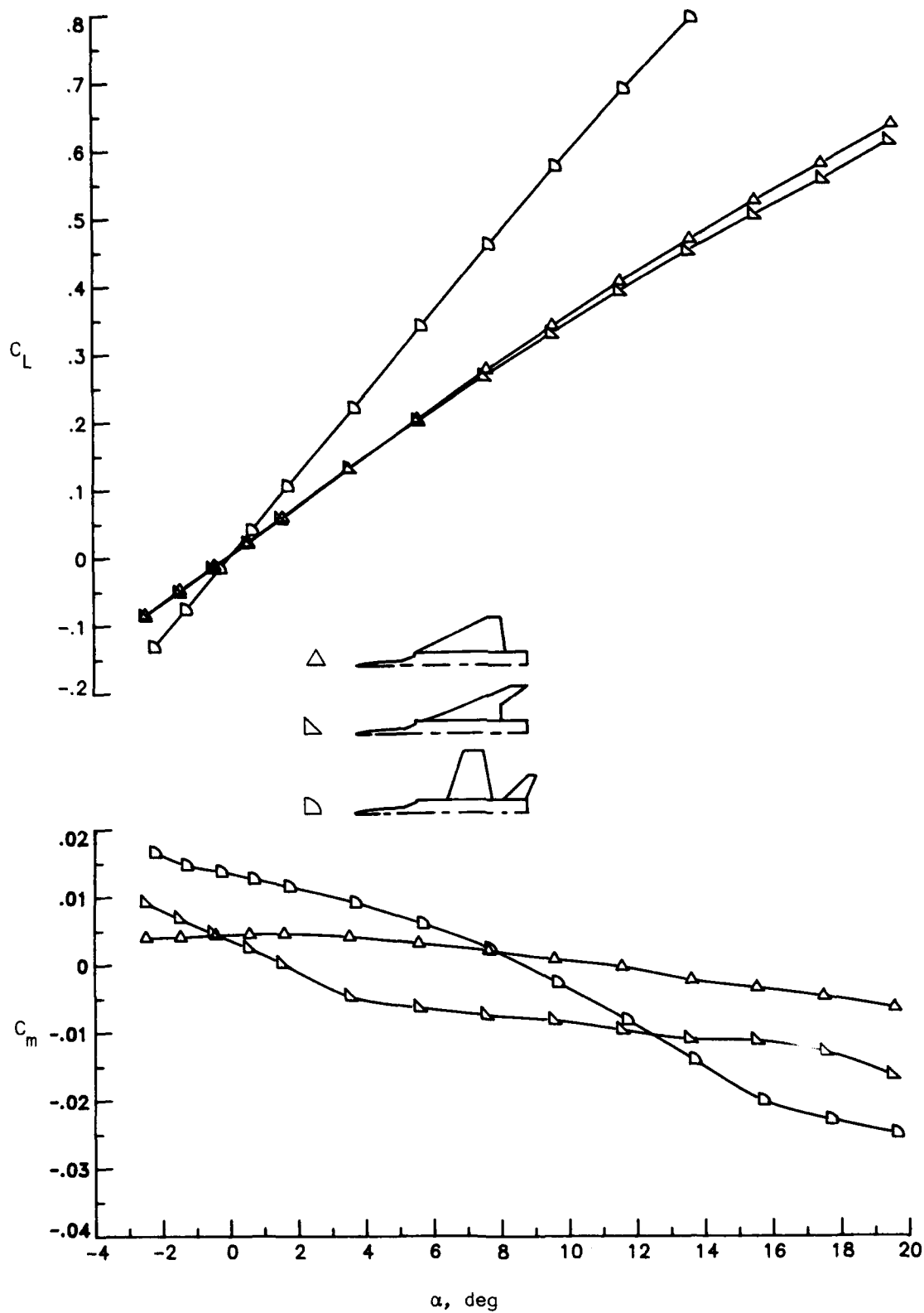
(b) Directional stability characteristics.

Figure 15. Concluded.



(a) Drag characteristics.

Figure 16. Effect of planform on longitudinal characteristics for single-body models at $M = 1.80$.



(b) Lift and pitching-moment characteristics.

Figure 16. Concluded.

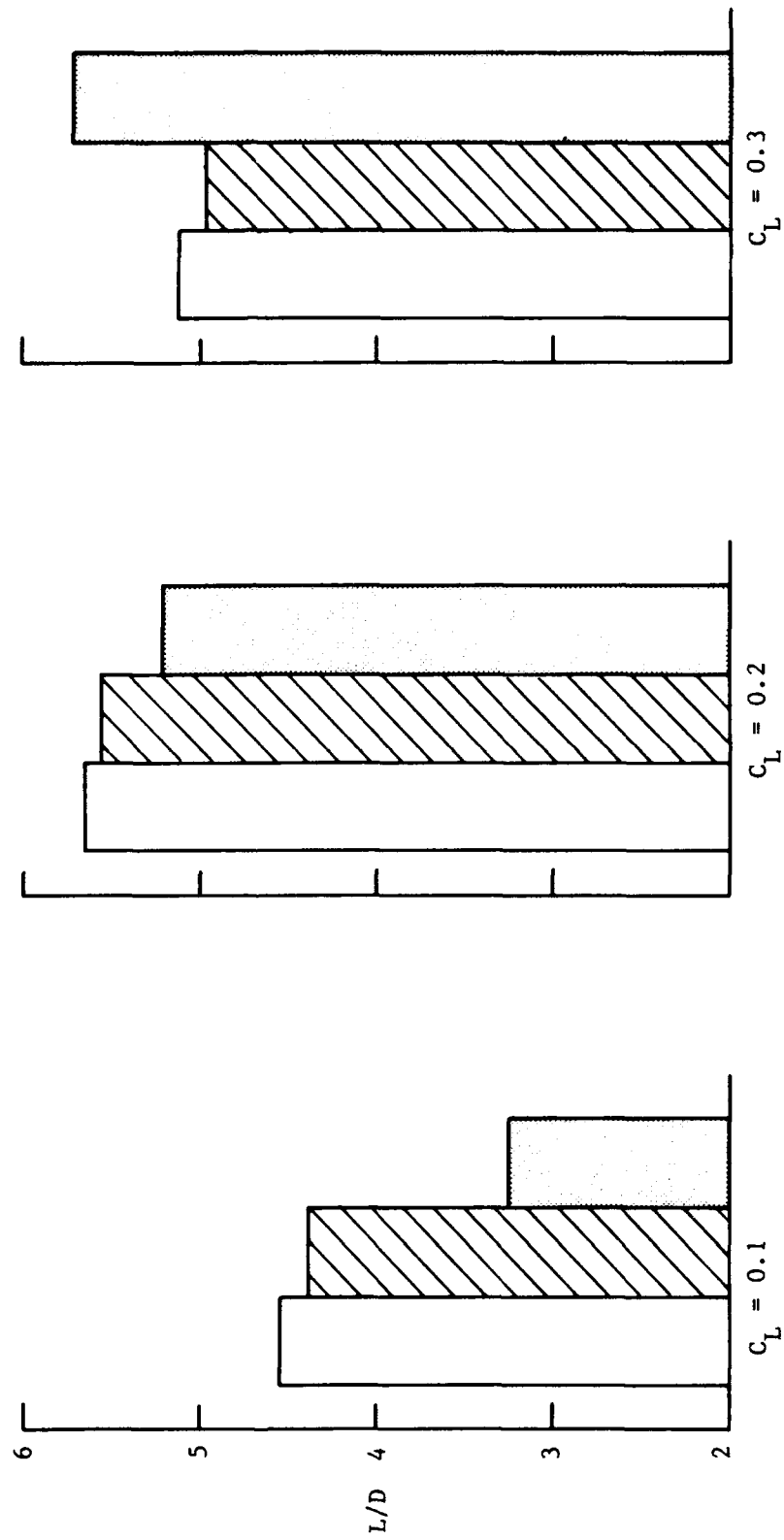
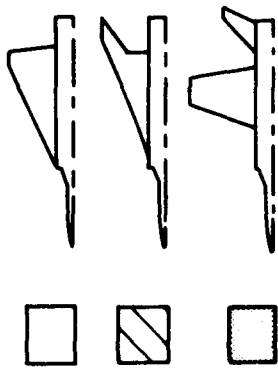


Figure 17. Effect of planform and lift coefficient on lift-drag ratio at $M = 1.80$ for single-body models.

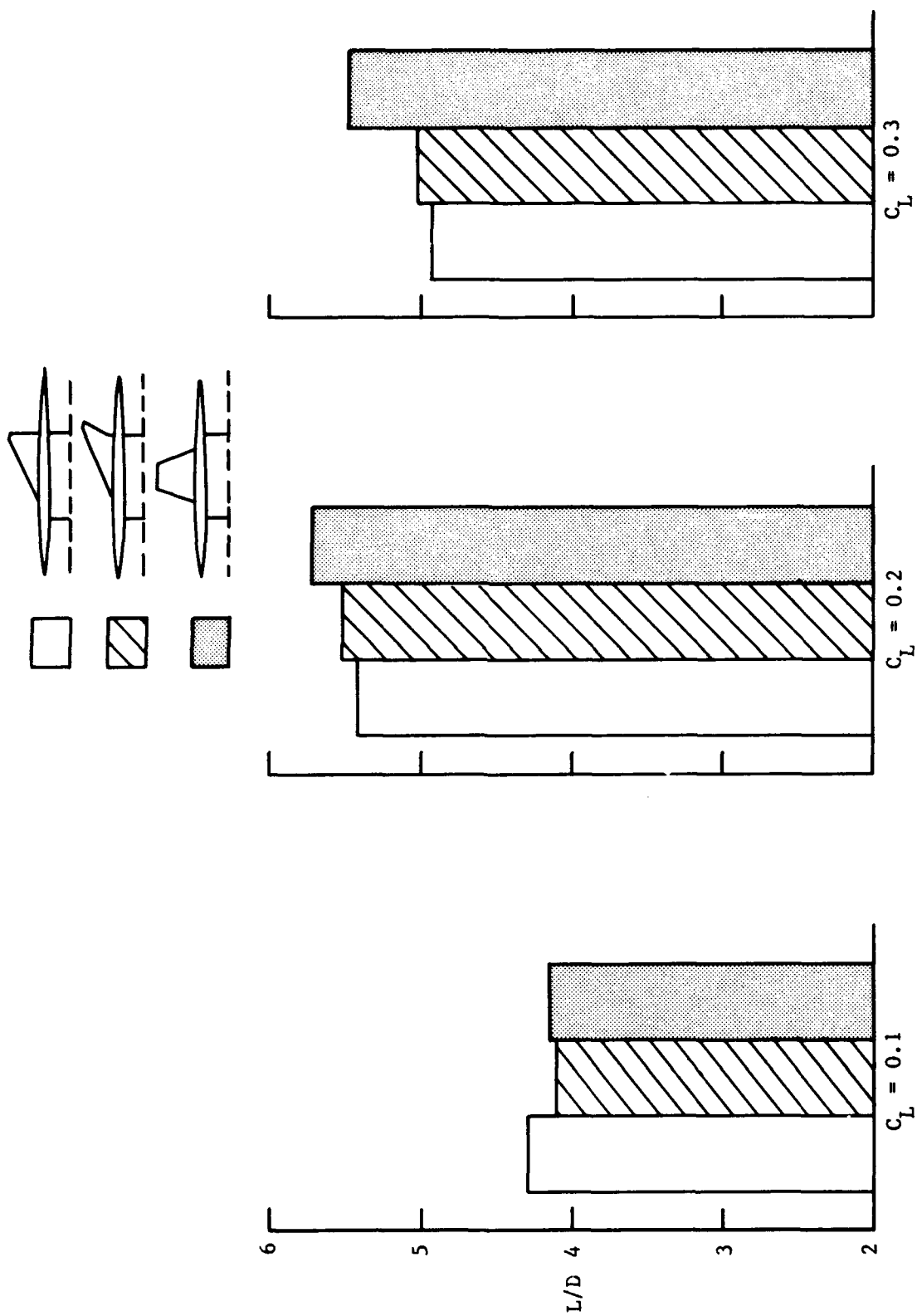


Figure 18. Effect of planform and lift coefficient on lift-drag ratio at $M = 1.80$ for multibody models.

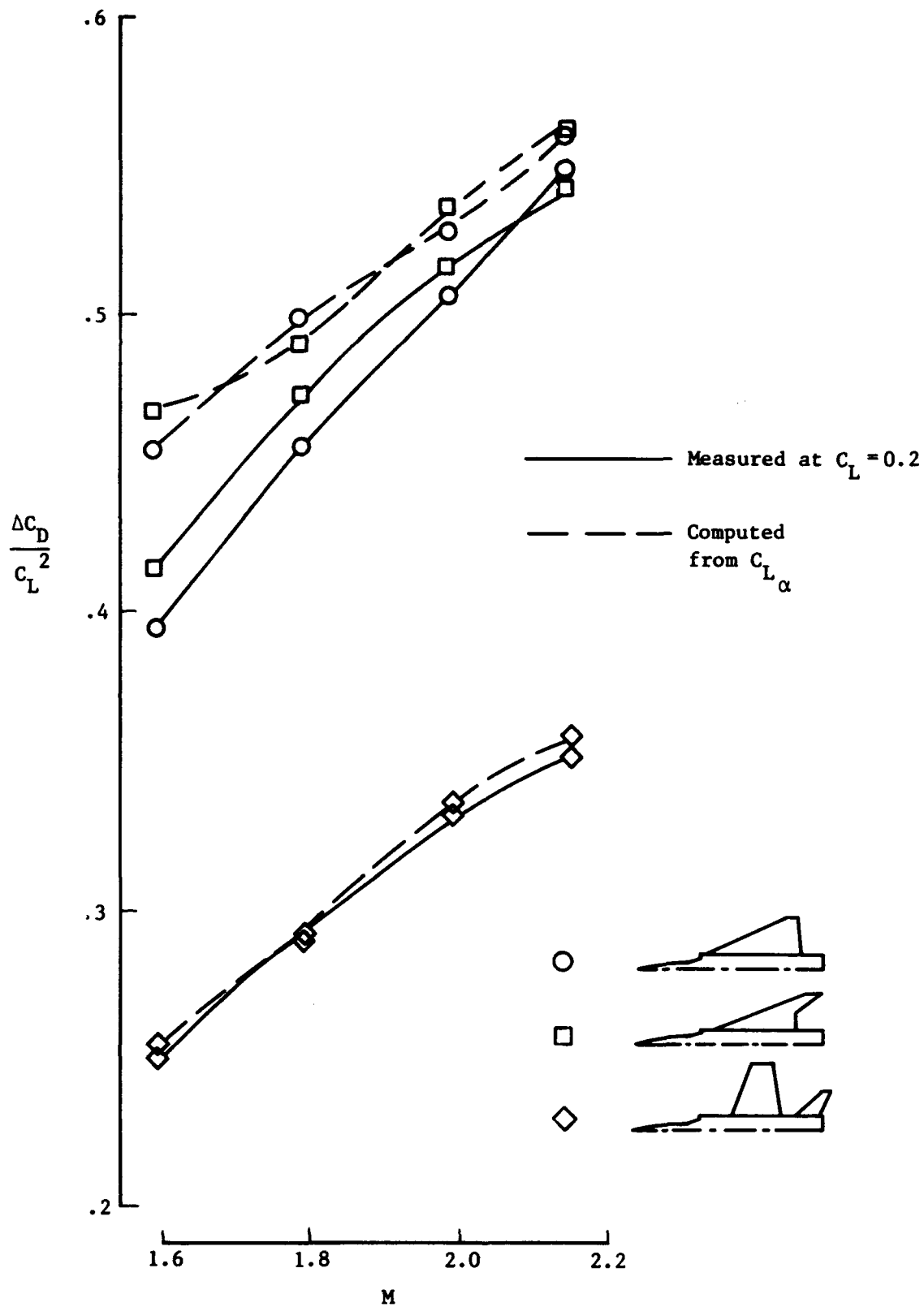


Figure 19. Variation of measured and computed drag-due-to-lift factor for single-body models.

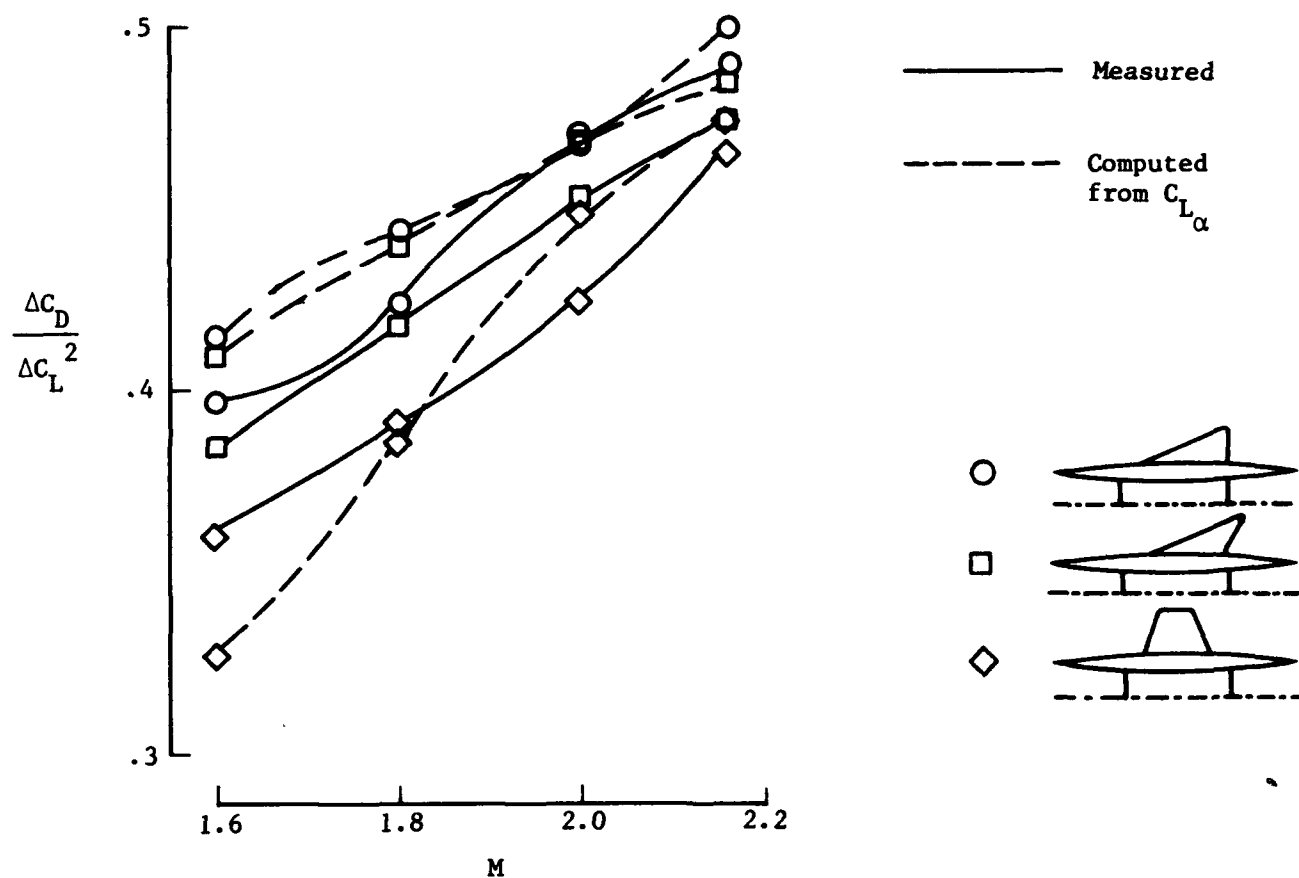


Figure 20. Variation of measured and computed drag-due-to-lift factor for multibody models.

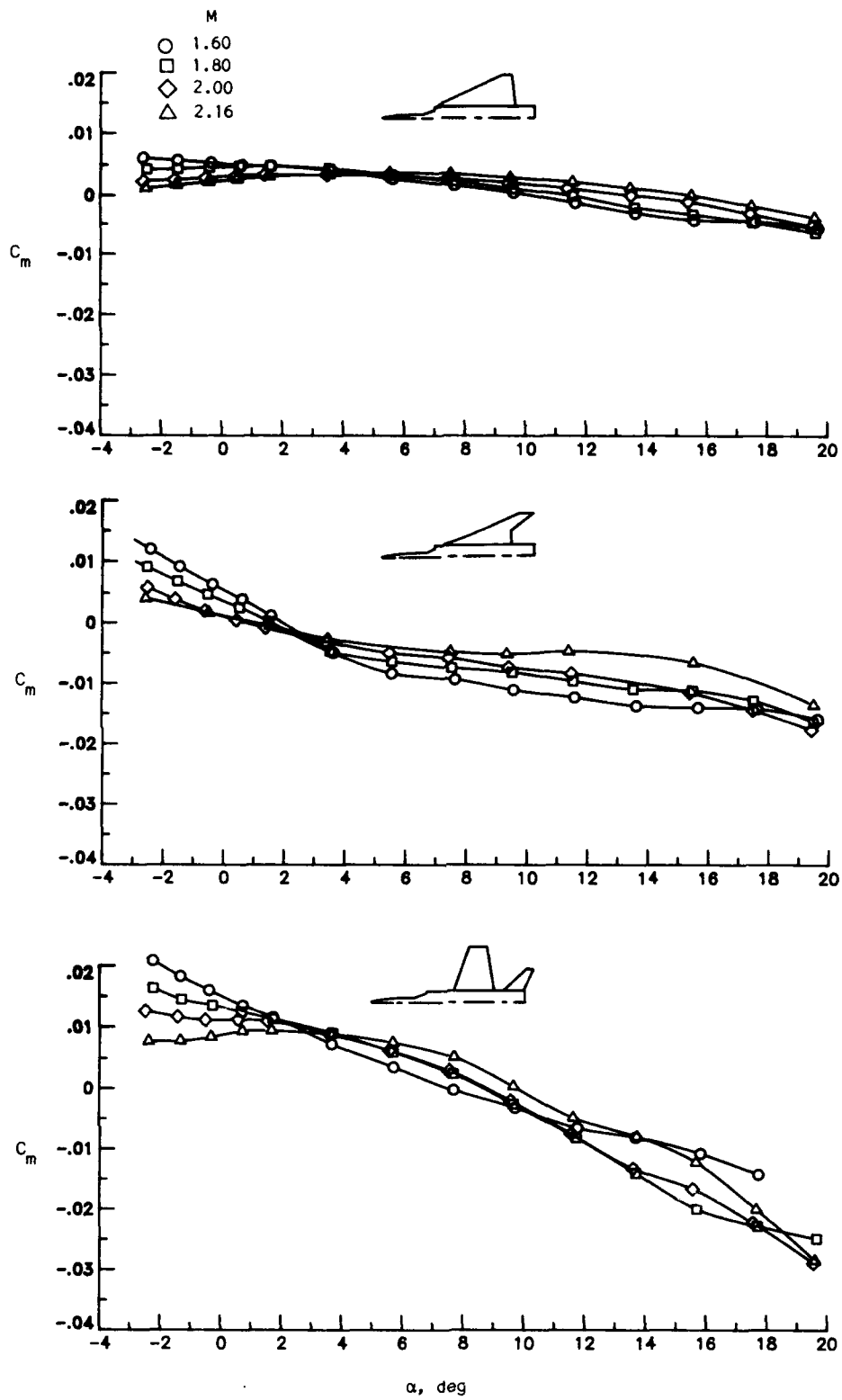
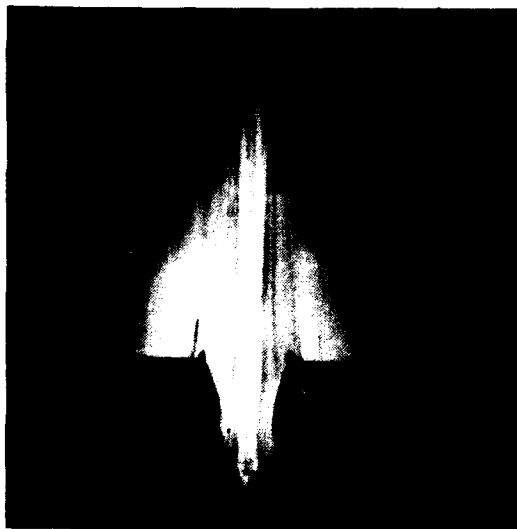


Figure 21. Effects of planform and Mach number on pitching-moment characteristics for single-body models.

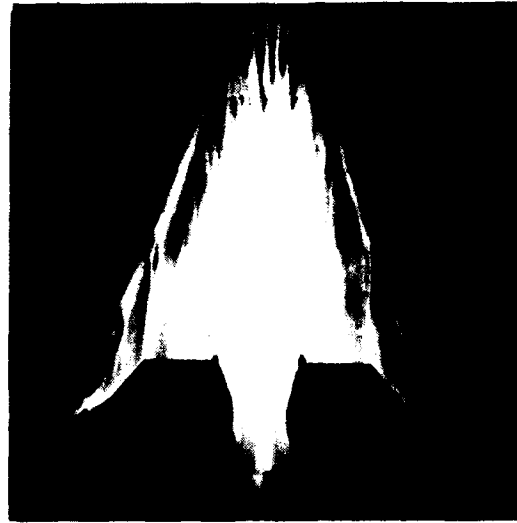
$\alpha = 0^\circ$



$\alpha = 2^\circ$



$\alpha = 4^\circ$



L-84-06

Figure 22. Oil-flow photographs of 70°/66° arrow wing model at $M = 1.80$.

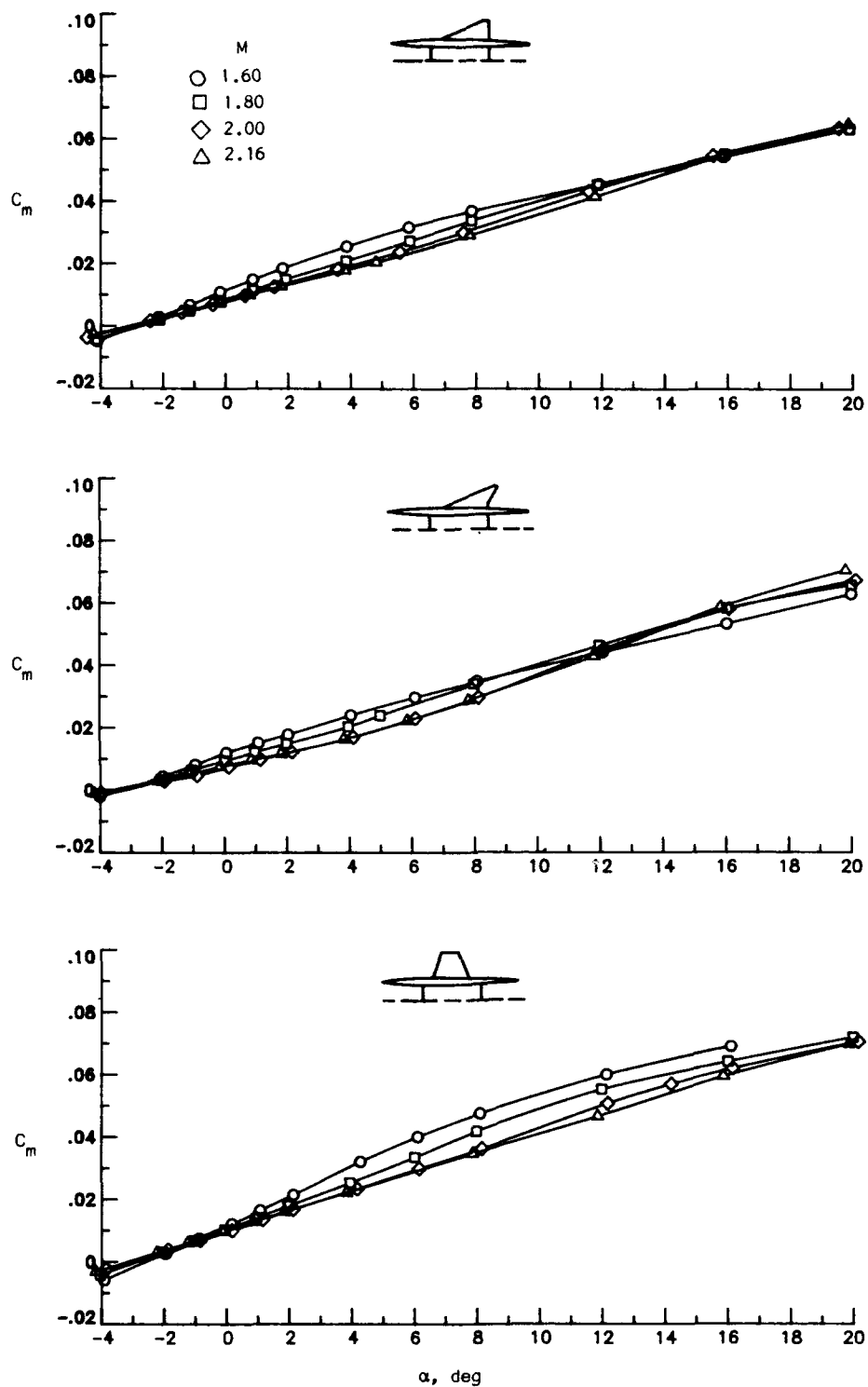


Figure 23. Effect of Mach number and planform on pitching moment for varying angle of attack for multibody models.

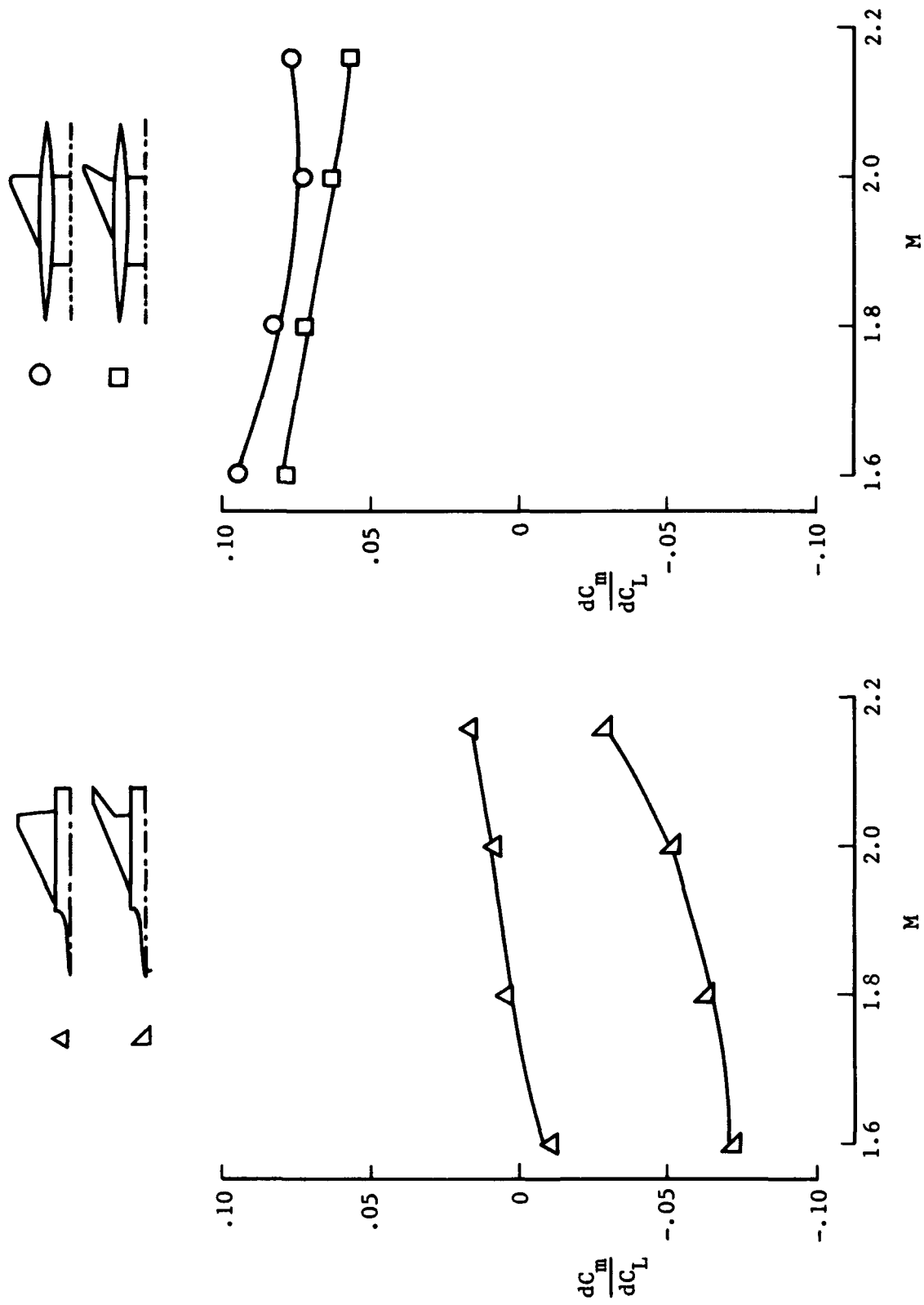
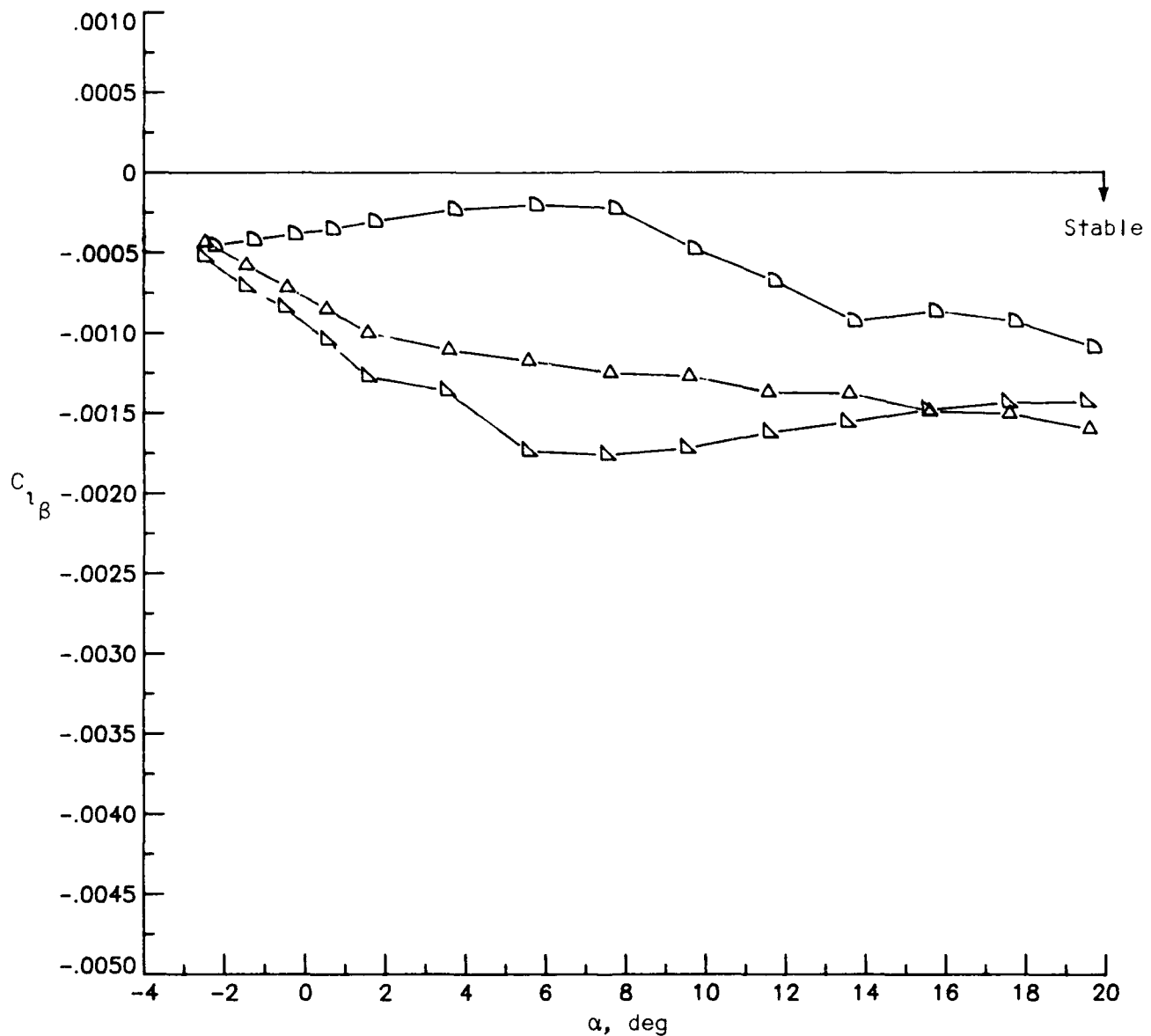
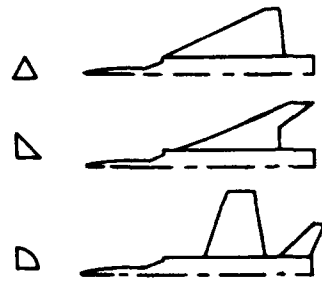
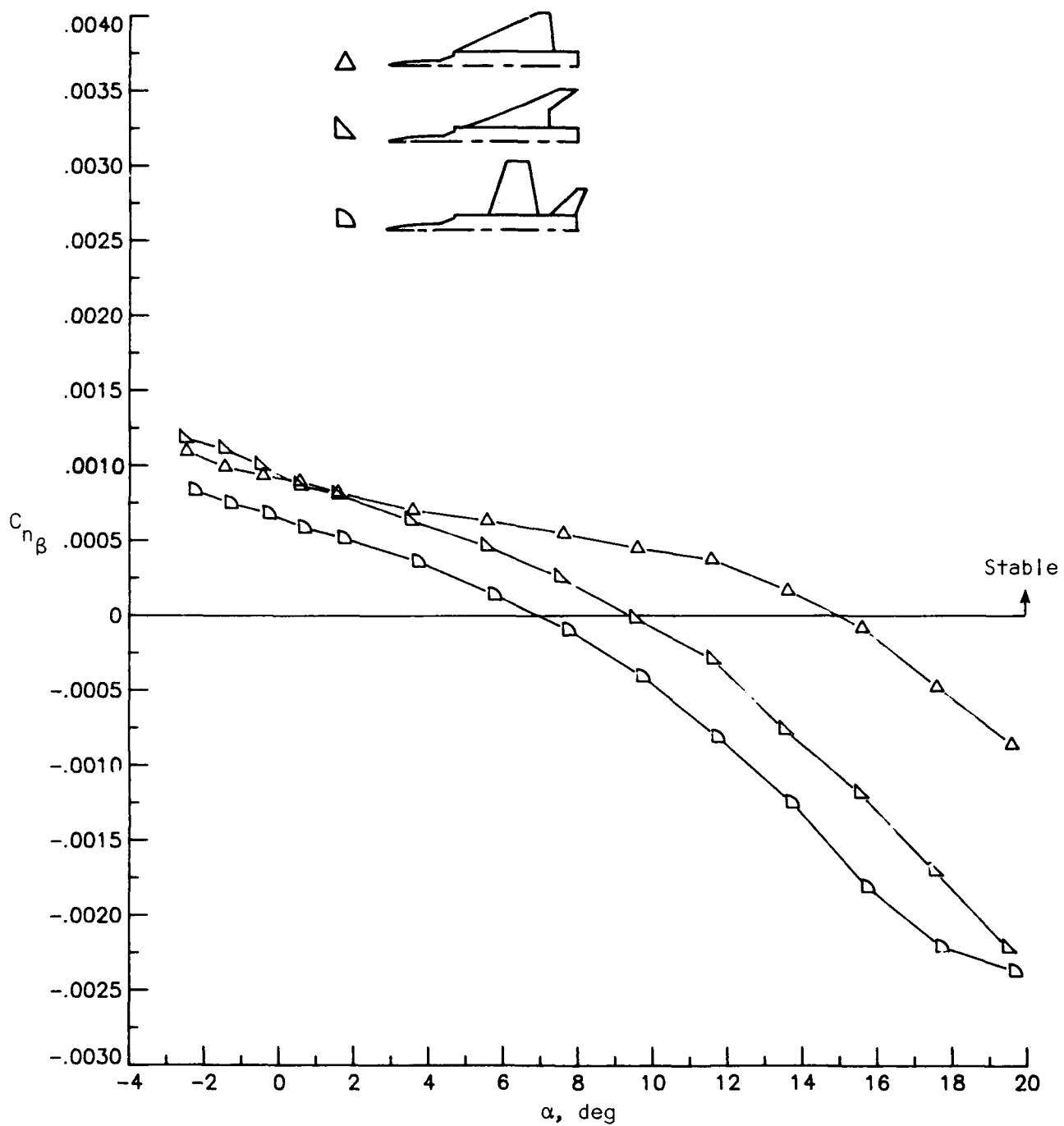


Figure 24. Effect of planform and Mach number on longitudinal stability parameter for single-body and multibody models.



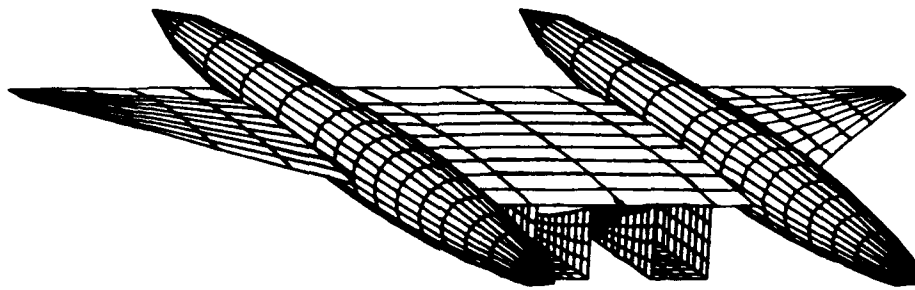
(a) Lateral stability characteristics.

Figure 25. Effect of planform on lateral-directional stability characteristics for single-body models at $M = 1.80$. Vertical tails on.

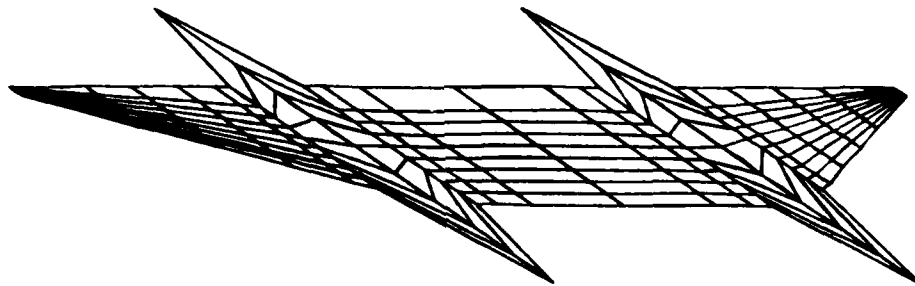


(b) Directional stability characteristics.

Figure 25. Concluded.



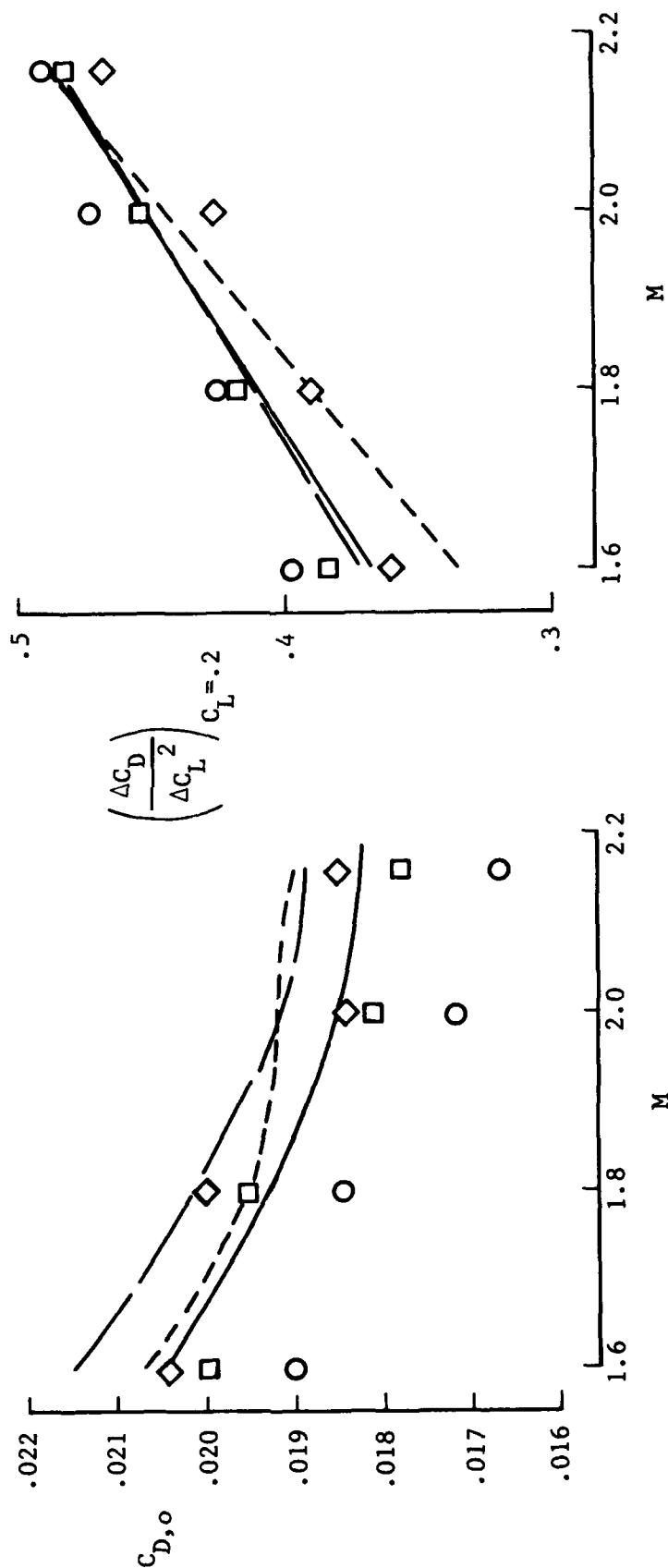
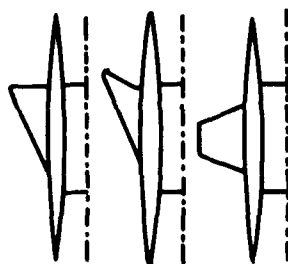
Zero-Lift Drag



Lift Analysis

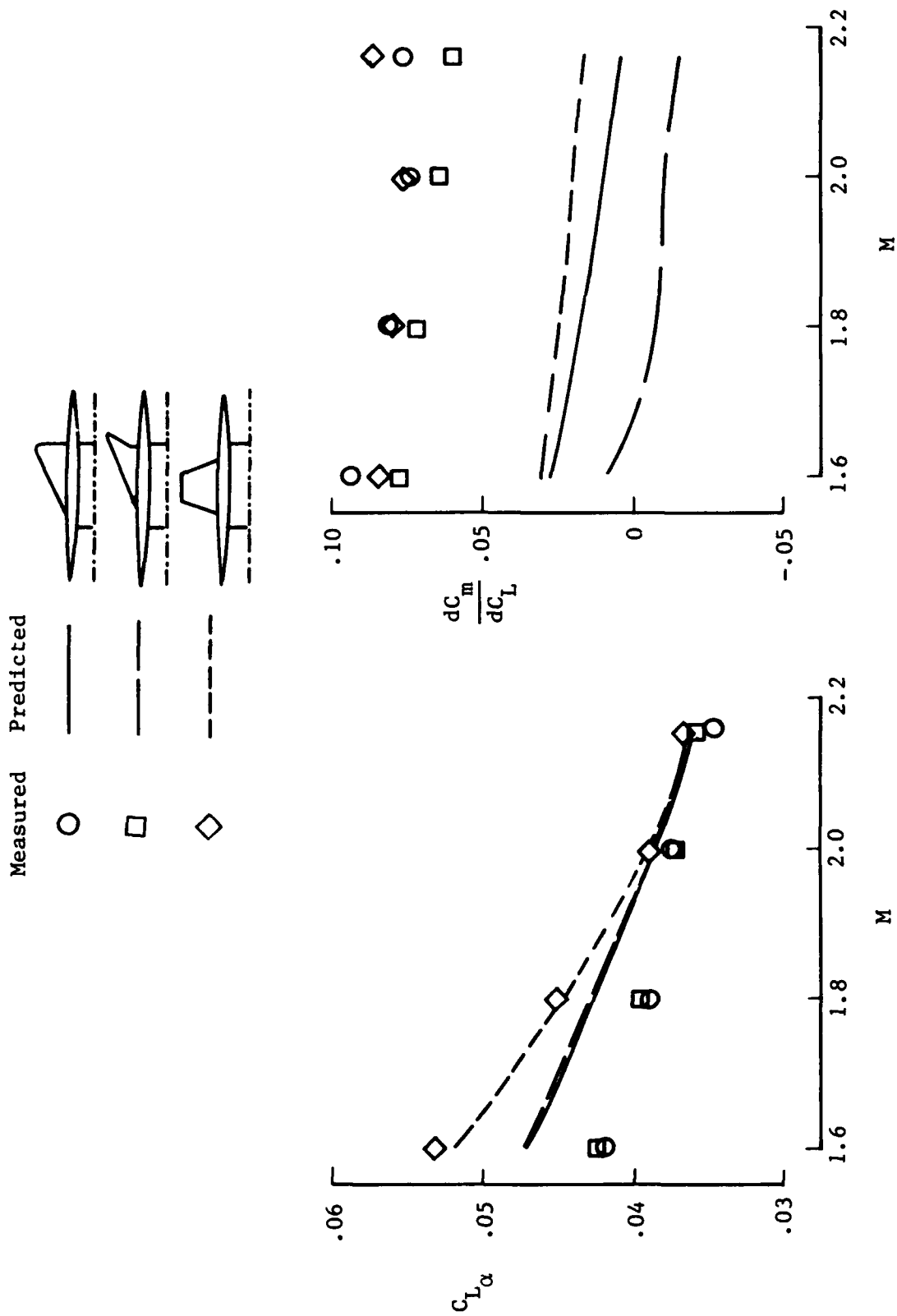
Figure 26. Computer graphics of computational models of multibody configuration used in linear-theory analysis.

Measured Predicted



(a) Drag characteristics.

Figure 27. Comparison between predicted and measured effects of planform and Mach number on multibody longitudinal aerodynamic characteristics. Vertical tails off.



(b) Lift and pitching-moment characteristics.

Figure 27. Concluded.

Appendix A

Internal Duct Friction Drag Correction

Experimental internal flow data were obtained for each configuration at all test conditions. The purpose of these measurements was to provide local flow conditions so as to calculate skin-friction drag. The two flow-through ducts were located on the lower surface of the inboard wing panel and bracketed the balance housing, as shown in figure A1. The two flow-through ducts were designed with a linear area growth of 1.13 to account for the boundary layer in order to maintain supersonic flow within the duct system. Cross-sectional views of the balance housing and duct system are presented in figure A1.

The duct Mach number was obtained by measuring the total pressure and the static pressure at approximately the center of the duct exit plane. The pressures were measured by a pressure transducer mounted externally to the wind-tunnel test section and connected by pressure tubing to a pressure probe located at the center of the duct exit plane.

The computed duct Mach number M_D was thus obtained for each configuration at all test conditions under the assumption that M_D did not vary down the length of the duct. The duct Mach number did not vary with configuration. This observation can be explained by examining the shock structure as represented in the schlieren photographs of figure A2. This figure shows the effect of planform, Mach number, and angle of attack on the shock structure at a sideslip angle of $\beta = 0^\circ$. Photographs are presented for angles of attack of 0° , 4° , and 8° at $M = 1.80$ and 2.16 for each test configuration. The photographs of figure A2 show that the shock structure between the bodies did not significantly vary with a change in outboard wing panel.

The variation of duct Mach number with angle of attack and free-stream Mach number is presented in figure A3. Duct Mach number is below the free-stream Mach number at $\alpha = 0^\circ$ because of the presence of the nose shocks ahead of the duct inlet. Figure A3 also shows that M_D decreases with increasing angle of attack, leveling off to a value of 1.3 at high angles of attack. The decreasing trend of M_D is the result of a shock occurring at the duct entrance, which becomes stronger as angle of attack increases. Figure A3 shows that the point at which M_D levels off occurs at higher angles of attack as free-stream Mach number increases. One explanation for this observation could be the interference of the bow shock from the balance housing on the duct system. The bow shock can be seen in the schlieren photographs of figures A2 and A4. In both of these

figures it is shown that at the free-stream Mach number of 2.16 the bow shock lies closer to the center body and does not detach as quickly as angle of attack increases than at the lower Mach number of 1.80. It should also be noted that there is a discontinuity occurring in the duct Mach number around $\alpha = 0^\circ$ for free-stream Mach numbers of 2.00 and 2.16 (see fig. A3). At these conditions, figure A4 shows that the bow shock from the balance housing would not significantly interfere with the duct inlet flow, as would occur at the lower Mach numbers. However, as angle of attack is increased, the bow shock becomes detached and interferes with the duct inlet flow, creating a condition similar to that observed at $\alpha = 0^\circ$ and $M = 1.80$. This drastic change in inlet flow conditions could account for the discontinuity in duct Mach number around $\alpha = 0^\circ$ at $M = 2.00$ and 2.16 .

As stated previously, in order to experimentally measure the duct Mach number, it was assumed that Mach number did not vary down the length of the duct. Thus M_D can be theoretically determined through the use of oblique shock relationships (ref. 21) to calculate the Mach number at the entrance of the duct for positive angles of attack, and expansion theory (ref. 21) is used to calculate M_D for negative angles of attack. For these calculations the duct Mach number measured at $\alpha = 0^\circ$ was used as the inlet entrance Mach number at all angles of attack, except for Mach numbers 2.00 and 2.16. Because of the discontinuity discussed above, the inlet Mach number for $M = 2.00$ and 2.16 was calculated by extrapolating to $\alpha = 0^\circ$ from the positive angles of attack. Simple shock and expansion relationships from reference 20 were then used to calculate the variation in duct Mach number with angle of attack resulting from the compression or expansion occurring at the inlet lip.

Presented in figure A5 is a comparison of the experimental and theoretical values of the duct Mach number. As was expected, because the body shock and the balance housing shocks were not accounted for, theory did not predict the leveling off of M_D with increasing angles of attack or the discontinuity at $\alpha = 0^\circ$ for the higher Mach numbers. However, theory did adequately predict the duct Mach number elsewhere, a fact substantiating the assumption of duct Mach number being constant throughout the duct.

The internal duct drag was calculated with the skin-friction code of reference 20. This code used the T' method in which flat-plate, adiabatic-wall, and turbulent boundary-layer conditions are assumed. Input into the code were the experimentally measured Mach number, the duct length, and the

wind-tunnel temperature and Reynolds number conditions. The duct geometry input was represented as a flat plate.

The internal duct drag was calculated for each configuration at all test conditions. The variation of

internal duct drag with Mach number and angle of attack is presented in figure A6. The variation of internal duct drag with Mach number and sideslip angle is shown in figure A7.

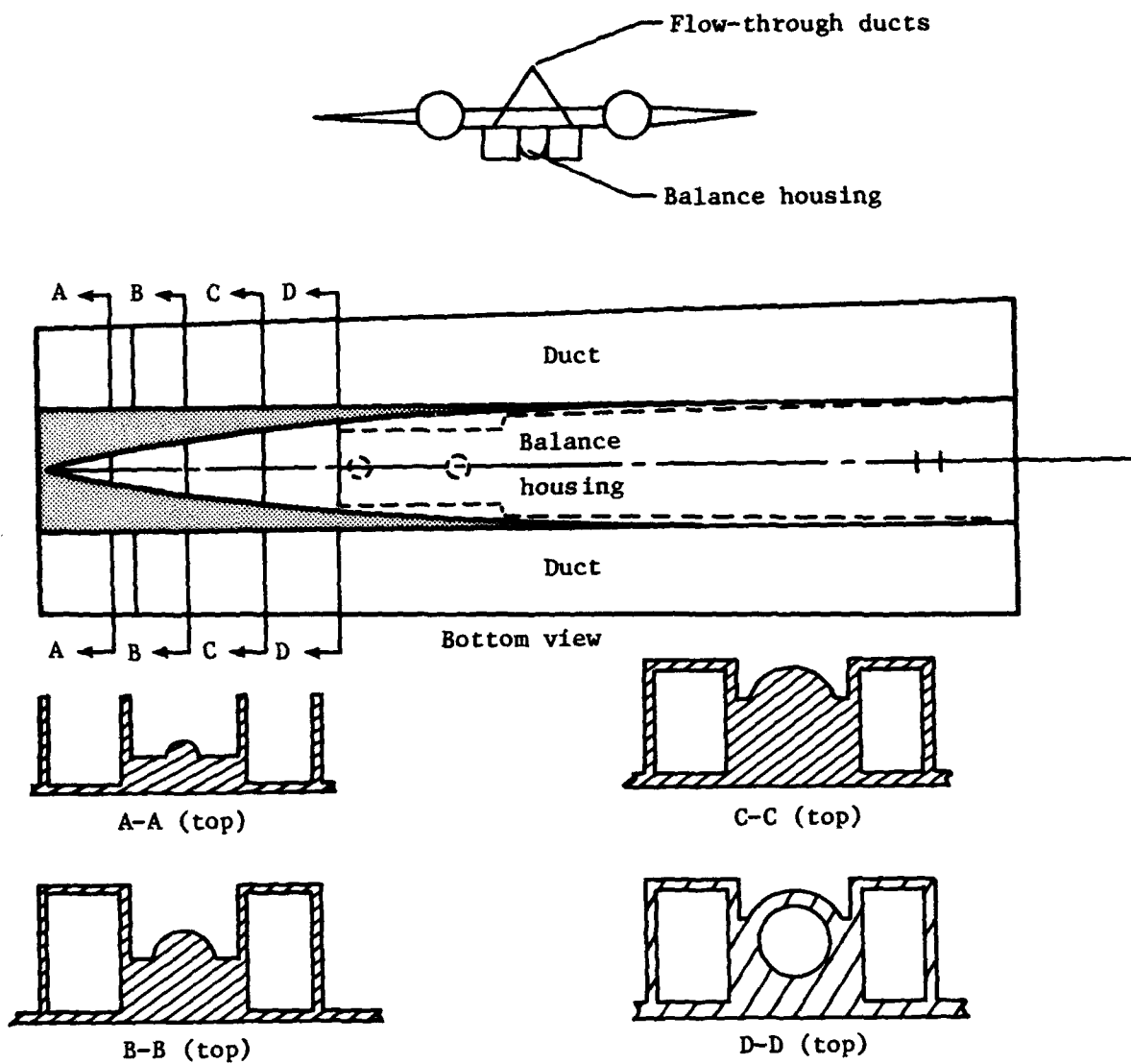
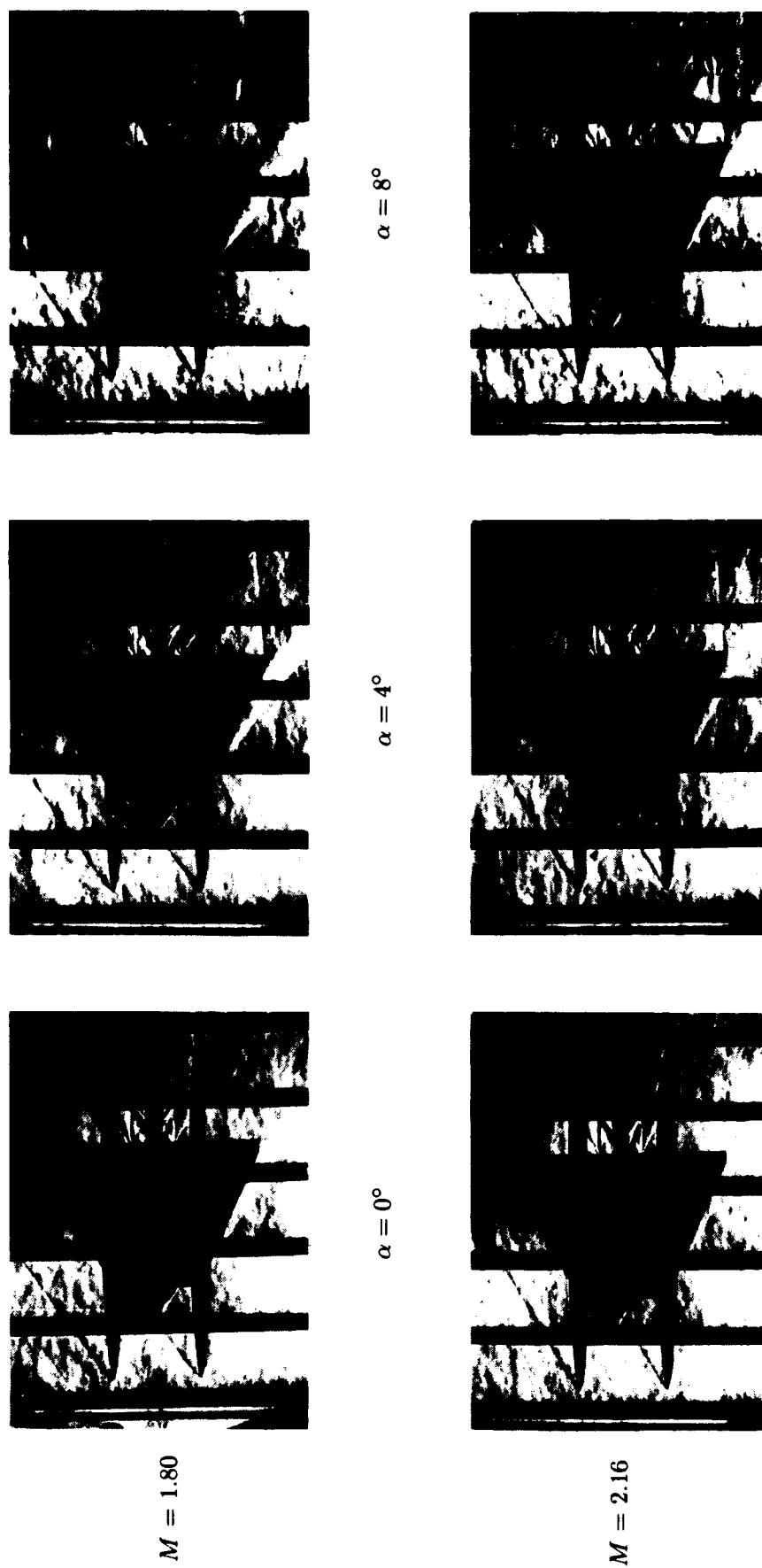


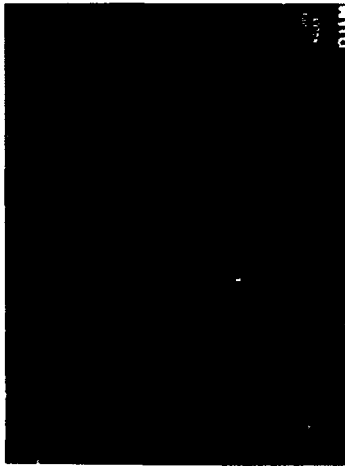
Figure A1. Cross sections of balance housing and flow-through ducts.



(a) Delta wing.

Figure A2. Schlieren photographs showing effects of Mach number and angle of attack for multibody models at $\beta = 0^\circ$.

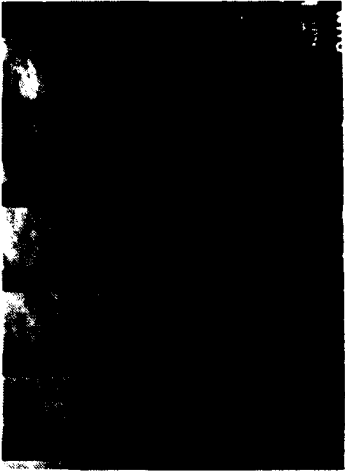
$M = 1.80$



$\alpha = 0^\circ$

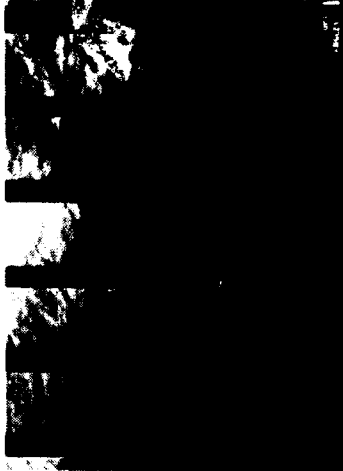
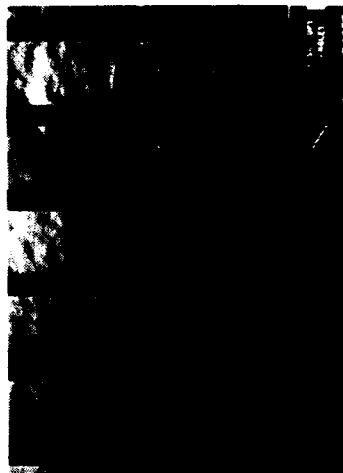


$\alpha = 4^\circ$

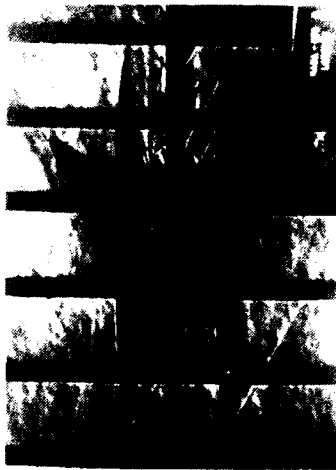


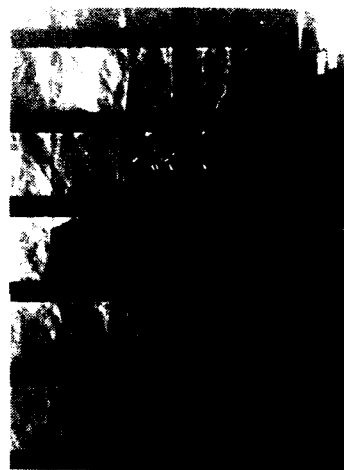
$\alpha = 8^\circ$

$M = 2.16$



(b) Arrow wing.
Figure A2. Continued.


 $M = 1.80$

 $\alpha = 0^\circ$
 $\alpha = 4^\circ$
 $\alpha = 8^\circ$

 $M = 2.16$


(d) Trapezoidal wing.

Figure A2. Concluded.

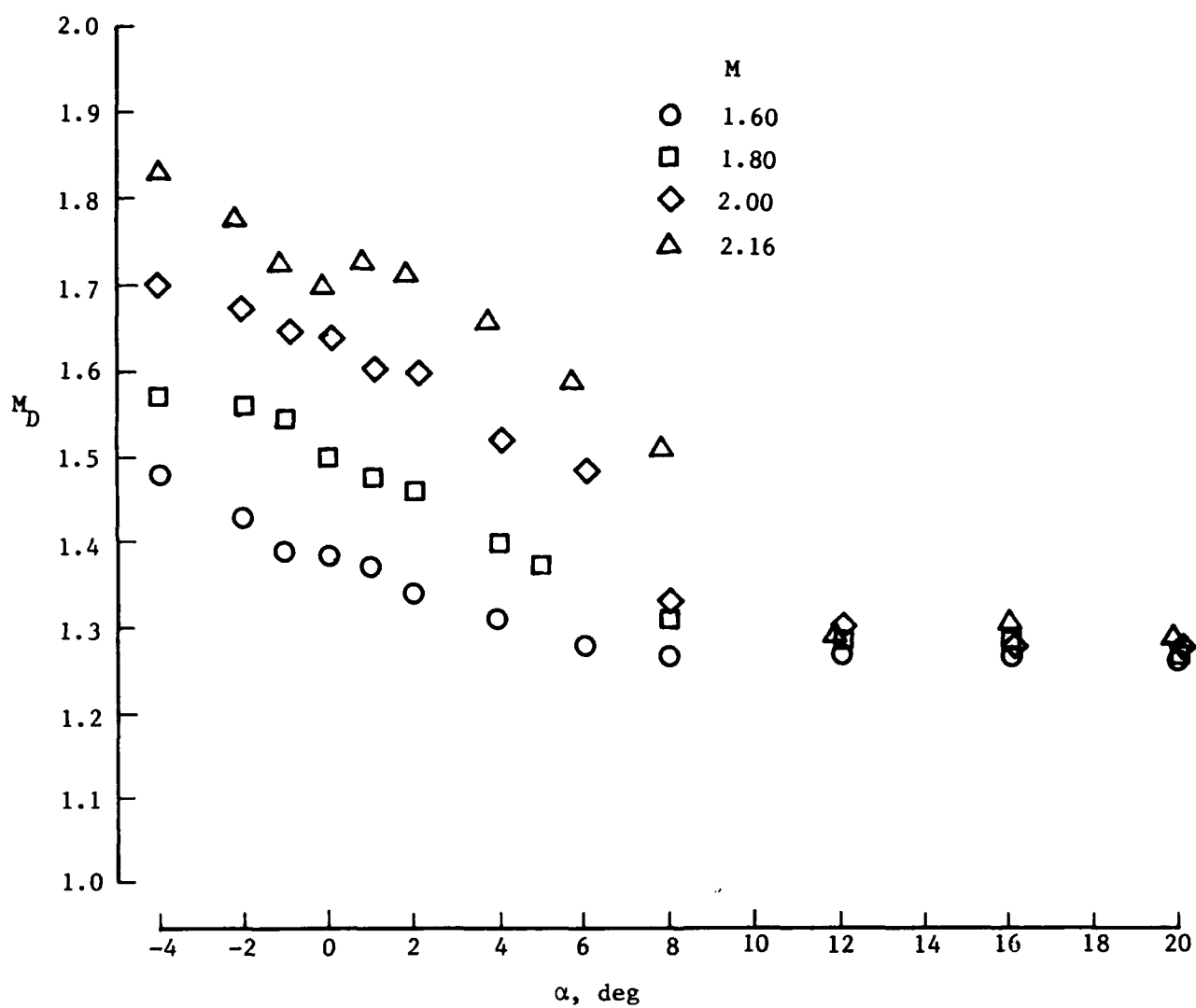


Figure A3. Effects of angle of attack and free-stream Mach number on duct Mach number.

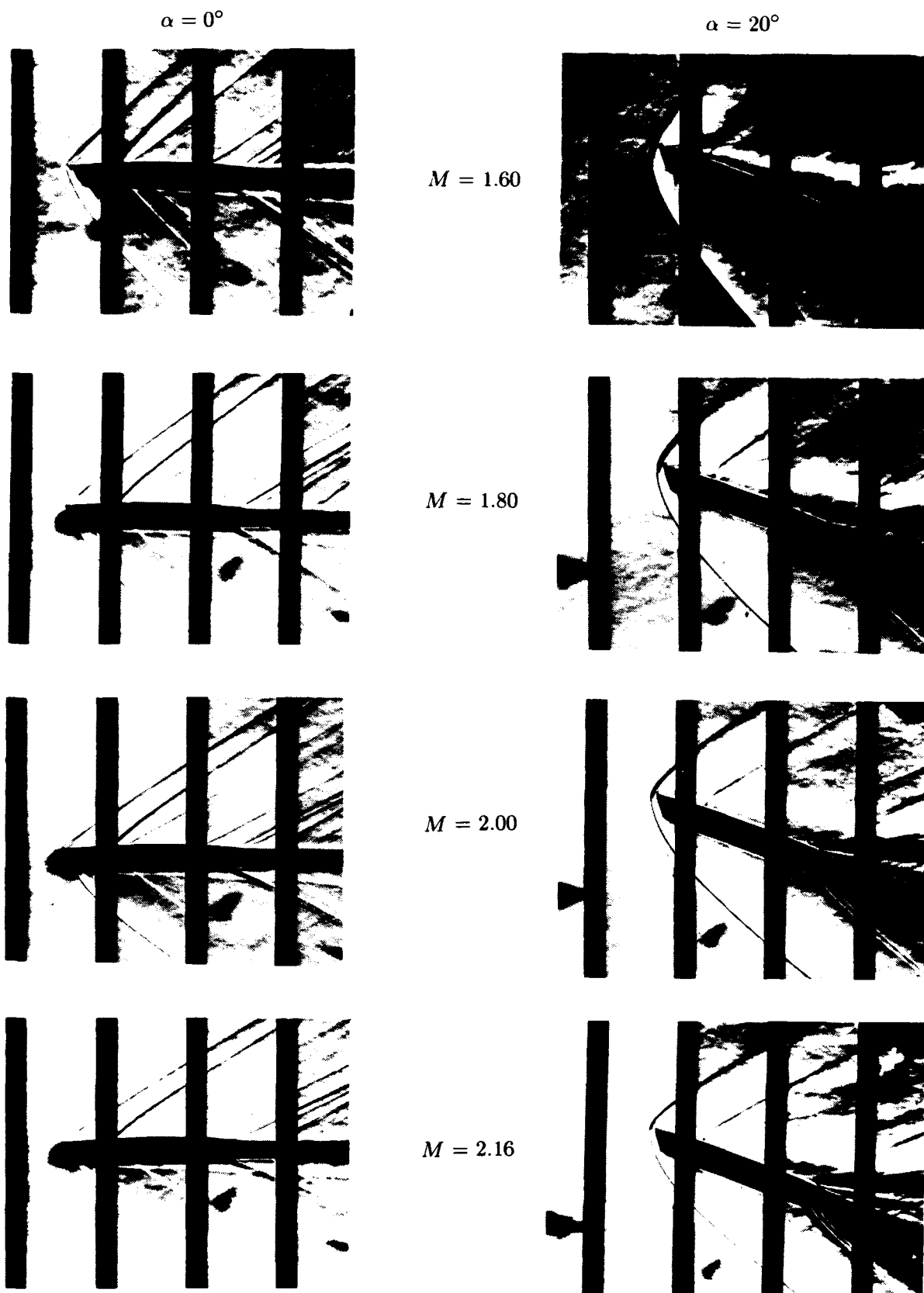
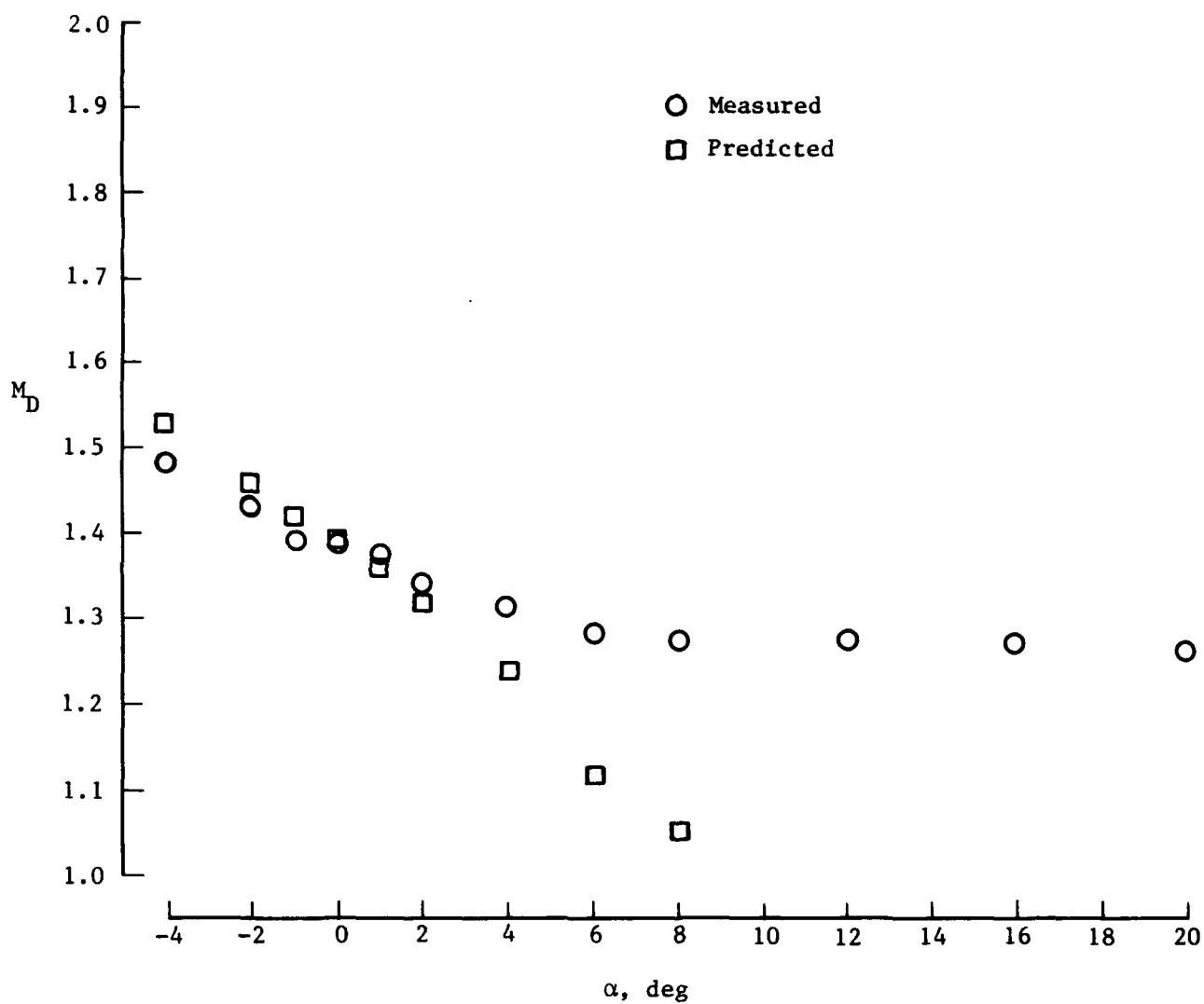
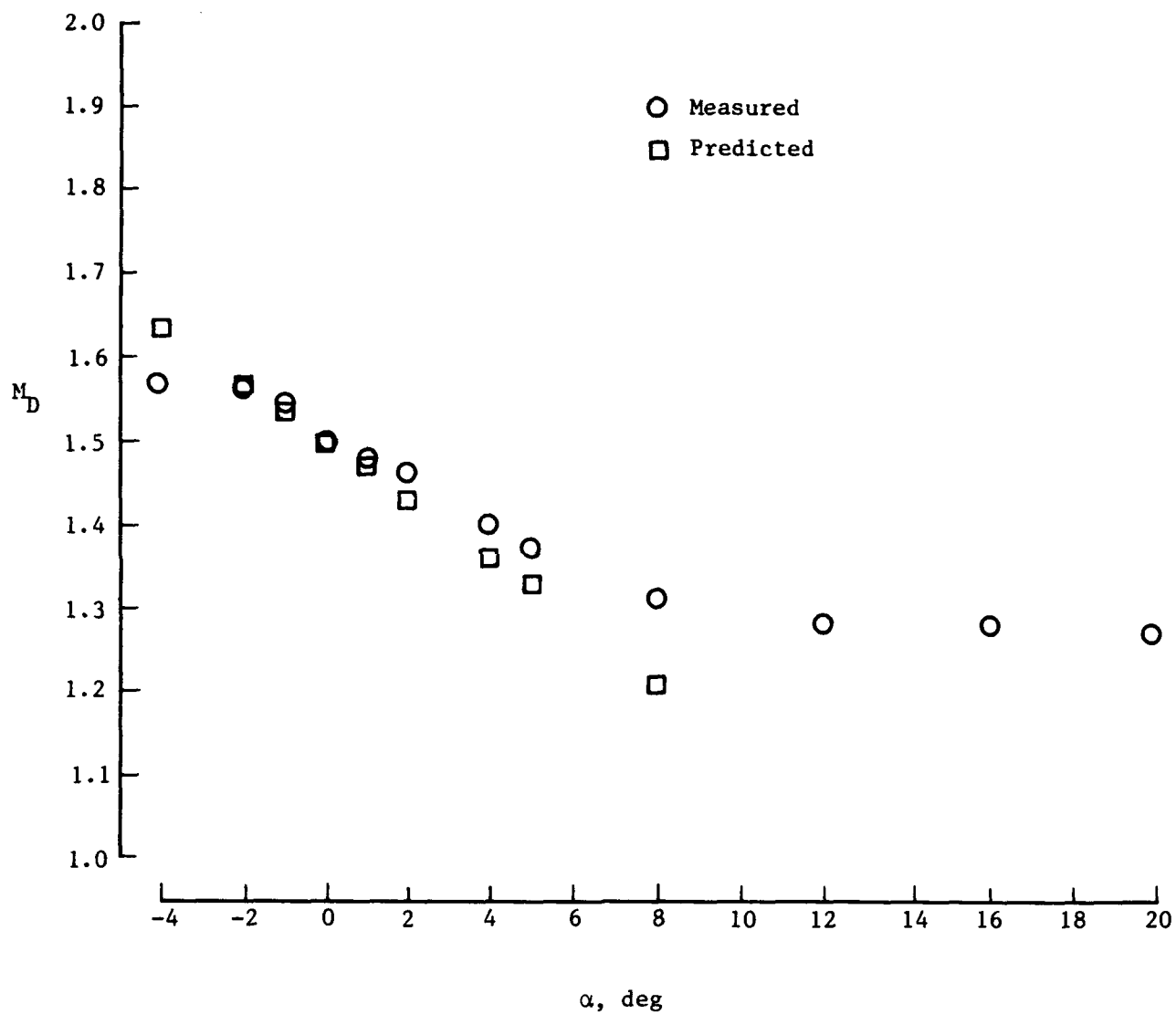


Figure A4. Schlieren photographs of strongback alone showing effects of Mach number and angle of attack at $\beta = 0^\circ$.



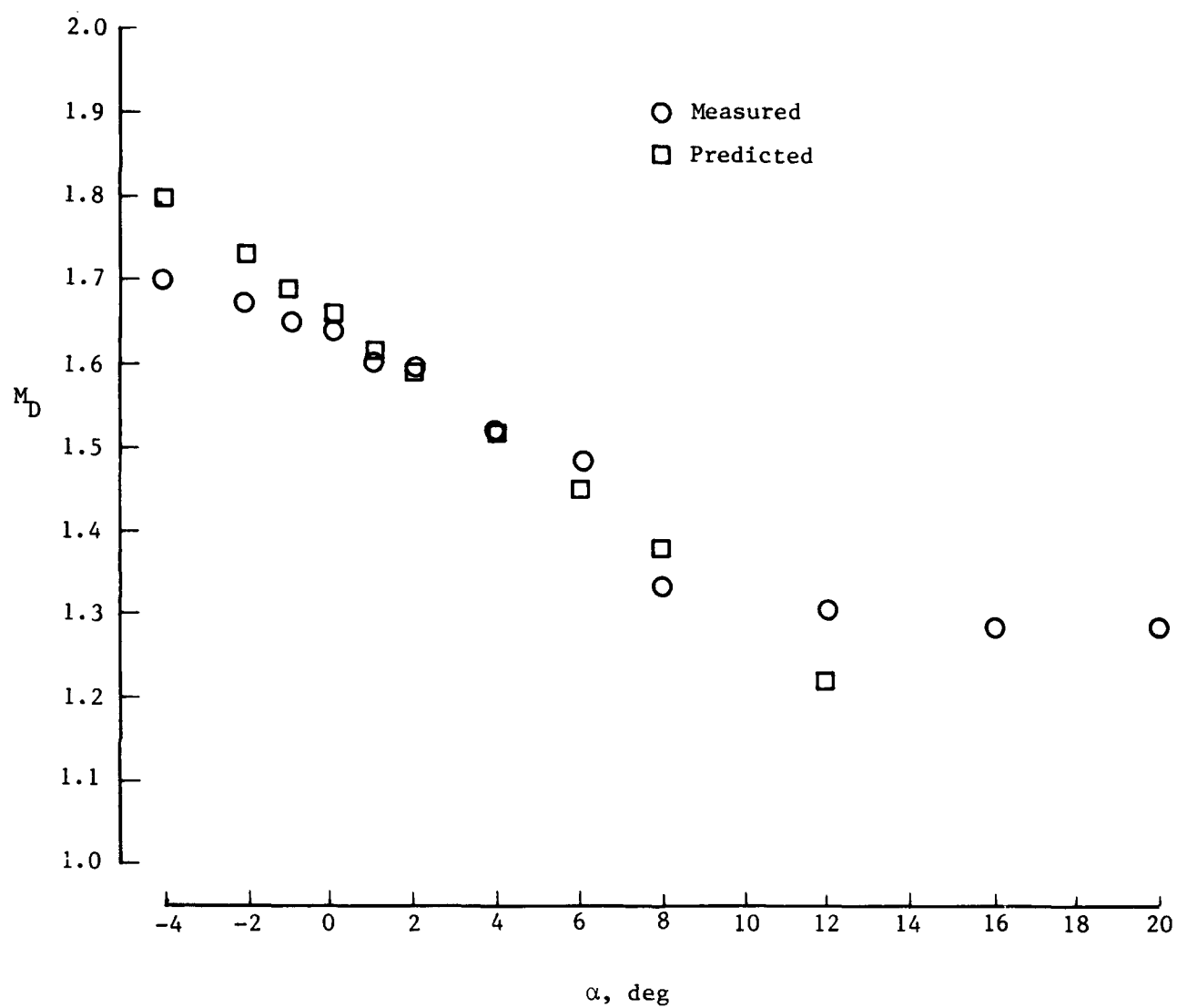
(a) $M = 1.60$.

Figure A5. Comparison of predicted and measured effects of free-stream Mach number and angle of attack on duct Mach number.



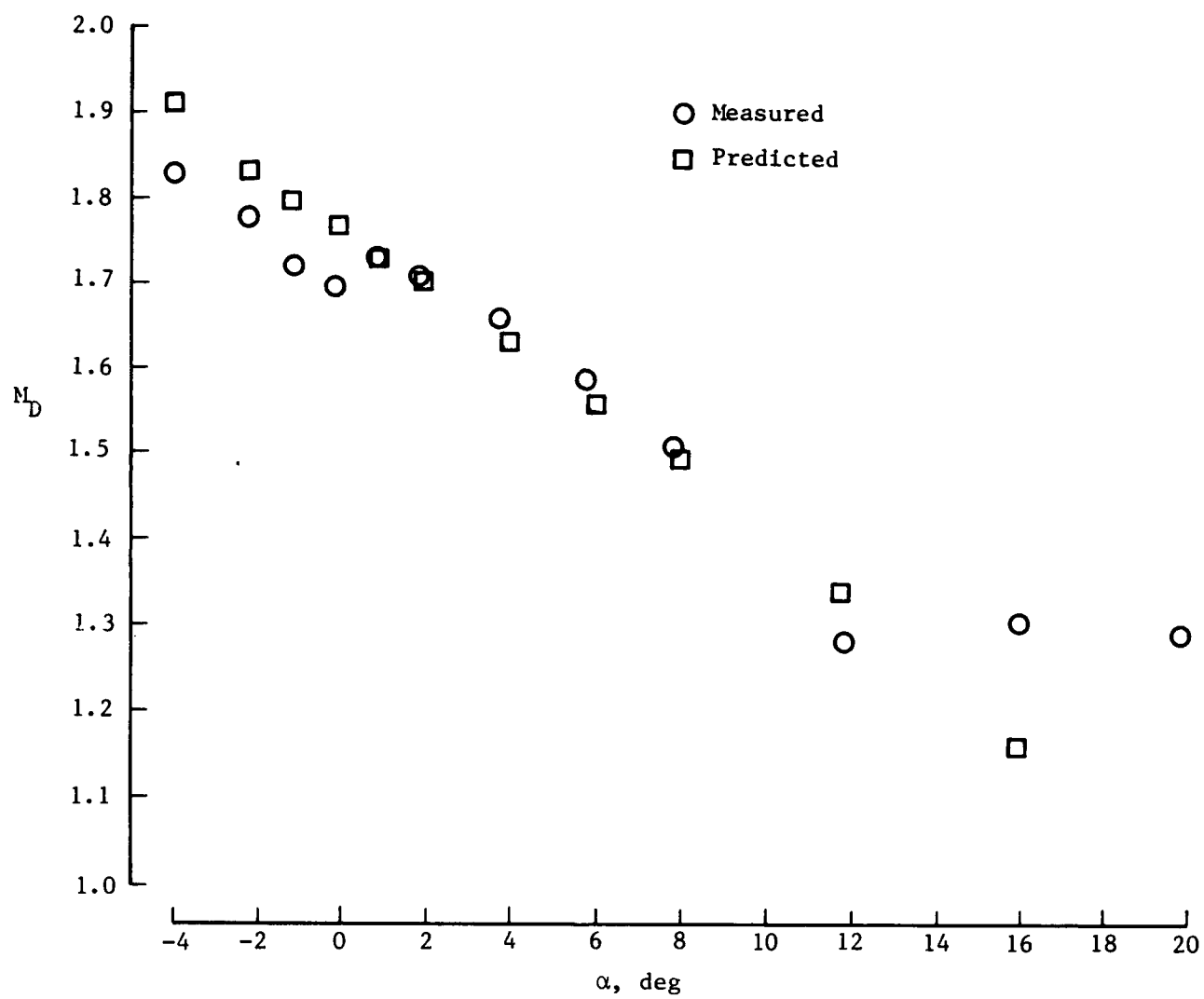
(b) $M = 1.80$.

Figure A5. Continued.



(c) $M = 2.00$.

Figure A5. Continued.



(d) $M = 2.16$.

Figure A5. Concluded.

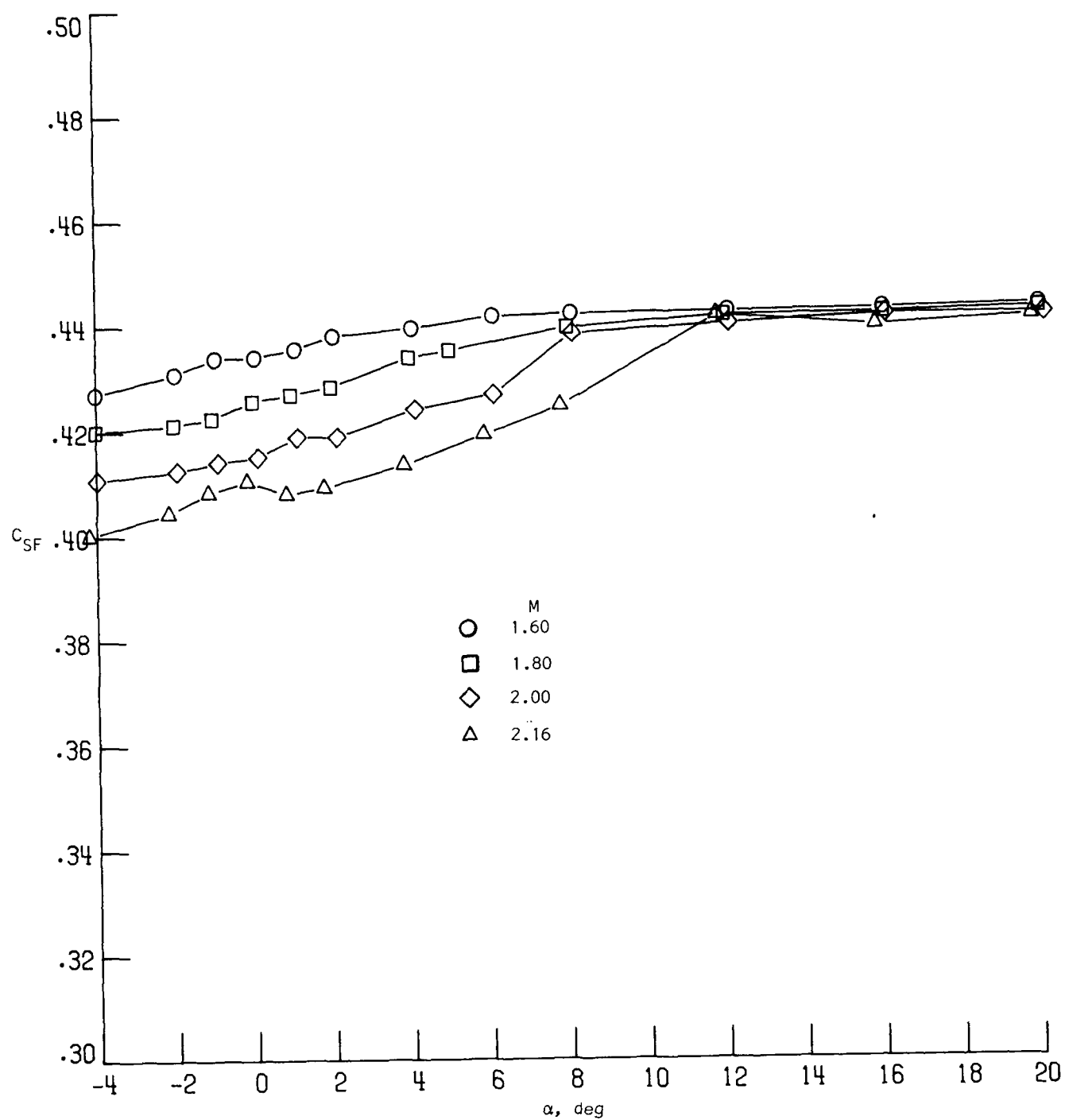


Figure A6. Effects of Mach number and angle of attack on internal duct drag.

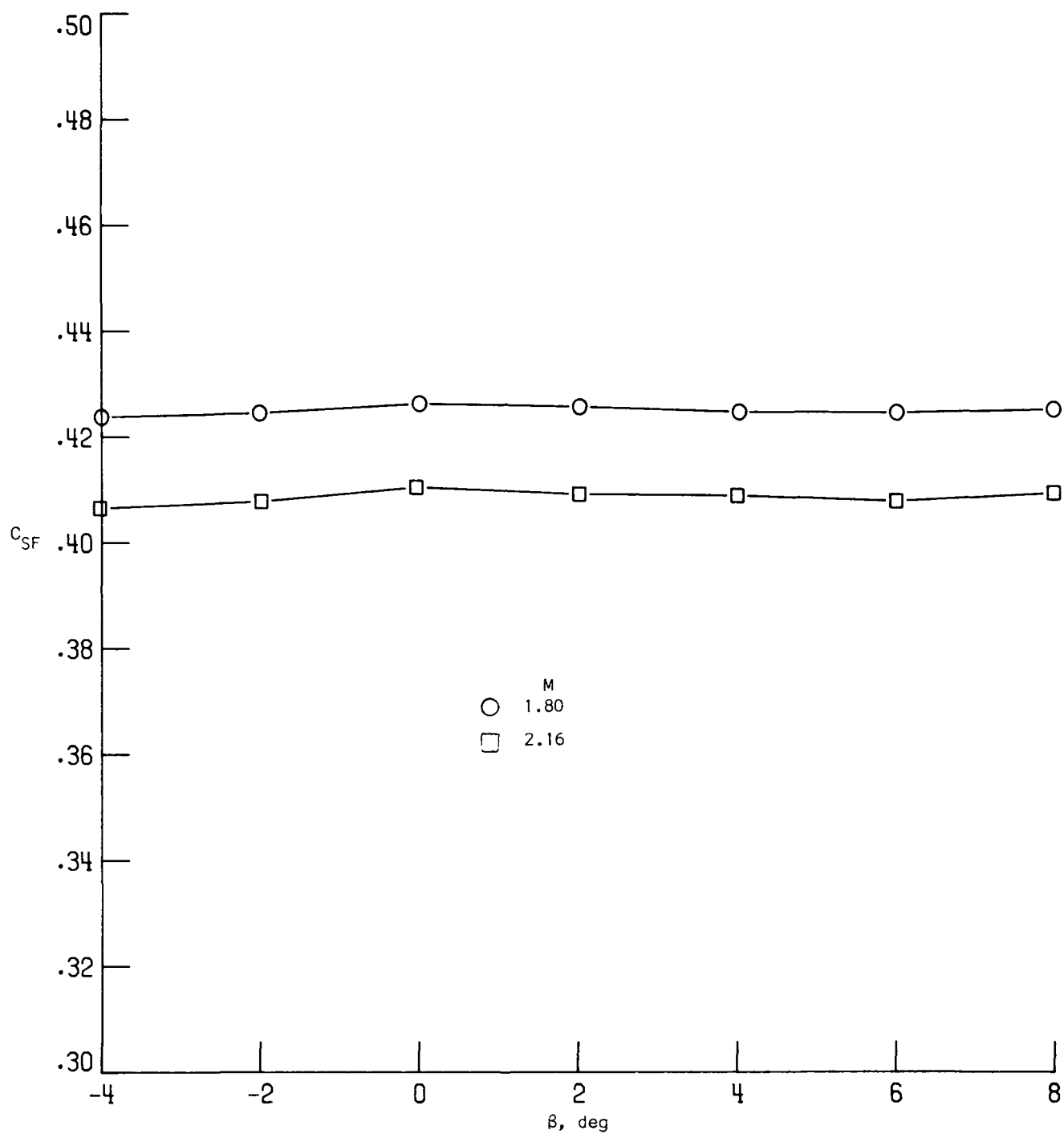


Figure A7. Effects of Mach number and sideslip angle of internal duct drag.

Appendix B

Force and Moment Data

The tabulated force and moment data were reduced with respect to the wing mean chord plane. Table B1 gives the column headings which appear in the tabulated data and identifies their corresponding symbols. Table BII is an index to the tabulated data which are presented in table BIII.

Table BI. Tabulated Data Symbols

Tabulated data heading	Definition
Both axis:	
ALPHA	α
BETA	β
CM	C_m
CY	C_Y
MACH	M
Body axis:	
CA	C_A
CAB	$C_{A,b}$
CAC	$C_{A,c}$
CLB	C_l
CN	C_N
CNB	C_n
R/FT	R
Stability axis:	
CD	C_D
CDB	$C_{D,b}$
CDC	$C_{D,c}$
CL	C_L
CLS	C_l
CNS	C_n
L/D	L/D

Table BII. Index to Tabulated Data

Page	Test	Run	Configuration	M	α , deg (a)	β , deg (b)
74	1460	23	BW ₁ F	1.60	Sweep	0
75	1460	24	BW ₁ F	1.80	Sweep	0
76	1460	25	BW ₁ F	1.80	0	Sweep
77	1460	26	BW ₁ F	1.80	8	Sweep
78	1460	27	BW ₁ F	1.80	Sweep	4
79	1460	29	BW ₁ F	2.00	Sweep	0
80	1460	30	BW ₁ F	2.16	Sweep	0
81	1460	31	BW ₁ F	2.16	0	Sweep
82	1460	32	BW ₁ F	2.16	8	Sweep
83	1460	33	BW ₁ F	2.16	Sweep	4
84	1460	35	BW ₁ FV	1.60	Sweep	0
85	1460	36	BW ₁ FV	1.80	Sweep	0
86	1460	37	BW ₁ FV	1.80	0	Sweep
87	1460	38	BW ₁ FV	1.80	8	Sweep
88	1460	39	BW ₁ FV	1.80	Sweep	4
89	1460	40	BW ₁ FV	2.00	Sweep	0
90	1460	41	BW ₁ FV	2.16	Sweep	0
91	1460	42	BW ₁ FV	2.16	0	Sweep
92	1460	43	BW ₁ FV	2.16	8	Sweep
93	1460	44	BW ₁ FV	2.16	Sweep	4
94	1532	9	BW ₂ F	1.60	Sweep	0
95	1532	12	BW ₂ F	1.80	Sweep	0
96	1532	13	BW ₂ F	1.80	0	Sweep
97	1532	14	BW ₂ F	1.80	8	Sweep
98	1532	15	BW ₂ F	1.80	Sweep	4
99	1532	17	BW ₂ F	2.00	Sweep	0
100	1532	20	BW ₂ F	2.16	Sweep	0
101	1532	21	BW ₂ F	2.16	0	Sweep
102	1532	22	BW ₂ F	2.16	8	Sweep
103	1532	23	BW ₂ F	2.16	Sweep	4

^a The term "Sweep" indicates data given for entire angle-of-attack range.

^b The term "Sweep" indicates data given for entire angle-of-sideslip range.

Table BII. Concluded

Page	Test	Run	Configuration	M	α , deg (a)	β , deg (b)
104	1532	25	BW ₂ FV	1.60	Sweep	0
105	1532	26	BW ₂ FV	1.80	Sweep	0
106	1532	27	BW ₂ FV	1.80	Sweep	4
107	1532	28	BW ₂ FV	1.80	0	Sweep
108	1532	29	BW ₂ FV	1.80	8	Sweep
109	1532	30	BW ₂ FV	2.00	Sweep	0
110	1532	31	BW ₂ FV	2.16	Sweep	0
111	1532	32	BW ₂ FV	2.16	Sweep	Sweep
112	1532	33	BW ₂ FV	2.16	0	Sweep
113	1532	34	BW ₂ FV	2.16	8	Sweep
114	1532	45	BW ₃ F	1.60	Sweep	0
115	1532	48	BW ₃ F	1.80	Sweep	0
116	1532	49	BW ₃ F	1.80	Sweep	4
117	1532	51	BW ₃ F	1.80	0	Sweep
118	1532	52	BW ₃ F	1.80	8	Sweep
119	1532	53	BW ₃ F	2.00	Sweep	0
120	1532	56	BW ₃ F	2.16	Sweep	0
121	1532	57	BW ₃ F	2.16	Sweep	Sweep
122	1532	58	BW ₃ F	2.16	0	Sweep
123	1532	59	BW ₃ F	2.16	8	Sweep
124	1532	35	BW ₃ FV	1.60	Sweep	0
125	1532	36	BW ₃ FV	1.80	Sweep	0
126	1532	37	BW ₃ FV	1.80	Sweep	4
127	1532	38	BW ₃ FV	1.80	0	Sweep
128	1532	39	BW ₃ FV	1.80	8	Sweep
129	1532	40	BW ₃ FV	2.00	Sweep	0
130	1532	41	BW ₃ FV	2.16	Sweep	0
131	1532	42	BW ₃ FV	2.16	Sweep	Sweep
132	1532	43	BW ₃ FV	2.16	0	Sweep
133	1532	44	BW ₃ FV	2.16	8	Sweep

^a The term "Sweep" indicates data given for entire angle-of-attack range.

^b The term "Sweep" indicates data given for entire angle-of-sideslip range.

Table BIII. Force and Moment Data

UPWT PROJECT 1460

RUN 23

MACH 1.60

BODY AXIS AXIAL FORCE CORRECTED FOR BASE AND CHAMBER PRESSURES

R/FT	BETA	ALPHA	CN	CA	CM	CLB	CNB	CY	CAC	CAB
2.002	.01	-4.11	-.1579	.0166	-.0049	.0003	-.0003	-.0007	.0020	.0006
2.005	.00	-2.15	-.0707	.0180	.0029	.0002	-.0003	-.0003	.0020	.0006
2.005	.00	-1.16	-.0293	.0186	.0068	.0001	-.0003	.0001	.0019	.0006
2.006	.00	-.17	.0133	.0191	.0109	.0001	-.0003	.0001	.0019	.0005
2.006	.00	.87	.0565	.0195	.0149	-.0000	-.0003	.0004	.0018	.0005
2.007	-.00	1.82	.0987	.0198	.0185	-.0000	-.0002	.0010	.0018	.0005
2.007	-.00	3.86	.1897	.0205	.0256	.0001	-.0001	.0014	.0017	.0005
2.008	-.01	5.84	.2778	.0211	.0318	-.0003	-.0001	.0017	.0016	.0005
2.010	-.01	7.84	.3634	.0216	.0368	-.0002	-.0000	.0023	.0015	.0004
2.006	-.01	11.88	.5338	.0230	.0457	-.0003	-.0001	.0030	.0012	.0004
1.995	-.01	15.85	.6929	.0244	.0545	-.0003	-.0000	.0035	.0014	.0004
1.987	-.02	19.86	.8603	.0266	.0635	-.0001	-.0002	.0053	.0013	.0004
1.975	-.00	-.17	.0134	.0192	.0113	.0002	-.0003	.0009	.0019	.0005

STABILITY AXIS DRAG CORRECTED FOR BASE AND CHAMBER PRESSURES

L/D	BETA	ALPHA	CL	CD	CM	CLS	CNS	CY	CDC	CDB
-5.5670	.01	-4.11	-.1551	.0279	-.0049	.0003	-.0003	-.0007	.0020	.0006
-3.3646	.00	-2.15	-.0694	.0206	.0029	.0003	-.0003	-.0003	.0020	.0006
-1.4846	.00	-1.16	-.0286	.0192	.0068	.0001	-.0003	.0001	.0019	.0006
.7049	.00	-.17	.0134	.0190	.0109	.0001	-.0003	.0001	.0019	.0005
2.7433	.00	.87	.0559	.0204	.0149	-.0000	-.0003	.0004	.0018	.0005
4.2582	-.00	1.82	.0975	.0229	.0185	-.0000	-.0002	.0010	.0018	.0005
5.6280	-.00	3.86	.1868	.0332	.0256	.0001	-.0001	.0014	.0017	.0005
5.5368	-.01	5.84	.2725	.0492	.0318	-.0003	-.0001	.0017	.0016	.0005
4.9980	-.01	7.84	.3548	.0710	.0368	-.0002	.0000	.0023	.0015	.0004
3.8816	-.01	11.88	.5141	.1325	.0457	-.0003	.0000	.0030	.0012	.0004
3.0811	-.01	15.85	.6553	.2127	.0545	-.0003	.0001	.0035	.0013	.0004
2.5036	-.02	19.86	.7944	.3173	.0635	-.0002	-.0002	.0053	.0013	.0004
.7042	-.00	-.17	.0135	.0191	.0113	.0002	-.0003	.0009	.0019	.0005

Table BIII. Continued

UPWT PROJECT 1460

RUN 24

MACH 1.80

BODY AXIS AXIAL FORCE CORRECTED FOR BASE AND CHAMBER PRESSURES

R/FT	BETA	ALPHA	CN	CA	CM	CLB	CNB	CY	CAC	CAB
1.998	.00	-4.14	-.1473	.0158	-.0044	.0001	-.0002	-.0004	.0017	.0005
1.996	.00	-2.12	-.0632	.0174	.0019	-.0001	-.0002	-.0000	.0016	.0005
1.996	.00	-1.16	-.0255	.0181	.0050	.0001	-.0002	.0002	.0015	.0005
1.999	.00	-.17	.0129	.0186	.0081	.0001	-.0002	.0004	.0015	.0004
2.004	.00	.87	.0541	.0192	.0115	-.0002	-.0002	.0003	.0014	.0004
2.003	-.00	1.92	.0979	.0196	.0150	-.0004	-.0002	.0008	.0014	.0004
2.000	-.00	3.84	.1749	.0202	.0210	-.0005	-.0002	.0010	.0013	.0004
2.001	-.00	5.87	.2539	.0210	.0274	-.0007	-.0001	.0014	.0013	.0004
2.001	-.01	7.84	.3302	.0217	.0338	-.0004	-.0000	.0017	.0011	.0003
2.002	-.01	11.84	.4809	.0236	.0455	-.0003	-.0001	.0027	.0011	.0003
2.003	-.01	15.89	.6311	.0257	.0553	-.0002	-.0001	.0030	.0012	.0003
2.003	-.01	19.88	.7822	.0282	.0634	-.0002	-.0001	.0039	.0011	.0003
2.006	.00	-.14	.0168	.0186	.0087	-.0001	-.0002	.0003	.0015	.0004

STABILITY AXIS DRAG CORRECTED FOR BASE AND CHAMBER PRESSURES

L/D	BETA	ALPHA	CL	CD	CM	CLS	CNS	CY	CDC	CDB
-5.4785	.00	-4.14	-.1446	.0264	-.0044	.0001	-.0002	-.0004	.0017	.0005
-3.1439	.00	-2.12	-.0620	.0197	.0019	-.0001	-.0002	-.0000	.0016	.0005
-1.3356	.00	-1.16	-.0249	.0186	.0050	.0001	-.0002	.0002	.0015	.0005
.6995	.00	-.17	.0130	.0186	.0081	.0001	-.0002	.0004	.0015	.0004
2.6799	.00	.87	.0536	.0200	.0115	-.0002	-.0002	.0003	.0014	.0004
4.2373	-.00	1.92	.0967	.0228	.0150	-.0004	-.0002	.0008	.0014	.0004
5.3950	-.00	3.84	.1721	.0319	.0210	-.0005	-.0002	.0010	.0013	.0004
5.3149	-.00	5.87	.2489	.0468	.0274	-.0007	.0000	.0014	.0013	.0004
4.8402	-.01	7.84	.3221	.0665	.0338	-.0004	.0000	.0017	.0011	.0003
3.8011	-.01	11.84	.4627	.1217	.0455	-.0003	-.0001	.0027	.0011	.0003
3.0170	-.01	15.89	.5958	.1975	.0553	-.0002	-.0001	.0030	.0012	.0003
2.4645	-.01	19.88	.7208	.2925	.0634	-.0002	-.0001	.0039	.0011	.0003
.9097	.00	-.14	.0169	.0186	.0087	-.0001	-.0002	.0003	.0015	.0004

Table BIII. Continued

UPWT PROJECT 1460

RUN 25

MACH 1.80

BODY AXIS AXIAL FORCE CORRECTED FOR BASE AND CHAMBER PRESSURES

R/FT	BETA	ALPHA	CN	CA	CM	CLB	CNB	CY	CAC	CAB
2.003	-4.10	-.13	.0168	.0186	.0089	.0027	.0038	.0137	.0015	.0004
2.004	-2.03	-.14	.0164	.0186	.0086	.0012	.0017	.0065	.0015	.0004
2.003	-.02	-.15	.0160	.0186	.0085	-.0002	-.0002	.0001	.0015	.0004
2.001	2.04	-.15	.0159	.0186	.0086	-.0015	-.0022	-.0061	.0015	.0004
2.002	4.11	-.15	.0146	.0187	.0085	-.0028	-.0041	-.0134	.0015	.0005
2.003	6.16	-.15	.0151	.0189	.0087	-.0042	-.0060	-.0212	.0016	.0005
2.004	8.23	-.15	.0144	.0191	.0087	-.0055	-.0082	-.0299	.0016	.0005
2.006	.00	-.14	.0168	.0187	.0086	-.0001	-.0002	.0001	.0015	.0004

STABILITY AXIS DRAG CORRECTED FOR BASE AND CHAMBER PRESSURES

L/D	BETA	ALPHA	CL	CD	CM	CLS	CNS	CY	CDC	CDB
.9108	-4.10	-.13	.0169	.0185	.0089	.0027	.0038	.0137	.0015	.0004
.8862	-2.03	-.14	.0164	.0186	.0086	.0012	.0017	.0065	.0015	.0004
.8654	-.02	-.15	.0161	.0186	.0085	-.0002	-.0002	.0001	.0015	.0004
.8597	2.04	-.15	.0160	.0186	.0086	-.0015	-.0022	-.0061	.0015	.0004
.7858	4.11	-.15	.0147	.0187	.0085	-.0028	-.0041	-.0134	.0015	.0005
.8047	6.16	-.15	.0152	.0188	.0087	-.0042	-.0060	-.0212	.0016	.0005
.7578	8.23	-.15	.0145	.0191	.0087	-.0055	-.0083	-.0299	.0016	.0005
.9078	.00	-.14	.0169	.0186	.0086	-.0001	-.0002	.0001	.0015	.0004

Table BIII. Continued

UPWT PROJECT 1460

RUN 26

MACH 1.80

BODY AXIS AXIAL FORCE CORRECTED FOR BASE AND CHAMBER PRESSURES

R/FT	BETA	ALPHA	CN	CA	CM	CLB	CNB	CY	CAC	CAB
2.002	-4.12	7.85	.3325	.0218	.0343	.0066	.0037	.0186	.0013	.0004
2.002	-2.04	7.85	.3329	.0216	.0344	.0031	.0017	.0101	.0012	.0004
2.005	-.01	7.85	.3318	.0216	.0339	-.0004	.0001	.0018	.0011	.0003
2.006	2.05	7.84	.3300	.0219	.0342	-.0041	-.0017	-.0064	.0012	.0003
2.006	4.11	7.84	.3299	.0221	.0340	-.0071	-.0038	-.0148	.0012	.0004
2.006	6.20	7.85	.3336	.0221	.0339	-.0102	-.0060	-.0241	.0013	.0004
2.004	8.27	7.85	.3322	.0222	.0338	-.0129	-.0086	-.0344	.0014	.0004
2.008	-.01	7.85	.3324	.0216	.0339	-.0004	.0000	.0020	.0011	.0003

STABILITY AXIS DRAG CORRECTED FOR BASE AND CHAMBER PRESSURES

L/D	BETA	ALPHA	CL	CD	CM	CLS	CNS	CY	CDC	CDB
4.8414	-4.12	7.85	.3243	.0670	.0343	.0071	.0028	.0186	.0013	.0004
4.8564	-2.04	7.85	.3247	.0669	.0344	.0033	.0012	.0101	.0012	.0004
4.8492	-.01	7.85	.3237	.0667	.0339	-.0004	.0001	.0018	.0011	.0003
4.8259	2.05	7.84	.3218	.0667	.0342	-.0043	-.0012	-.0064	.0011	.0003
4.8069	4.11	7.84	.3217	.0669	.0340	-.0075	-.0028	-.0148	.0012	.0004
4.8224	6.20	7.85	.3254	.0675	.0339	-.0110	-.0046	-.0241	.0013	.0004
4.8144	8.27	7.85	.3240	.0673	.0338	-.0139	-.0068	-.0344	.0013	.0004
4.8531	-.01	7.85	.3242	.0668	.0339	-.0004	.0001	.0020	.0011	.0003

Table BIII. Continued

UPWT PROJECT 1460

RUN 27

MACH 1.80

BODY AXIS AXIAL FORCE CORRECTED FOR BASE AND CHAMBER PRESSURES

R/FT	BETA	ALPHA	CN	CA	CM	CLB	CNR	CY	CAC	CAR
2.006	4.12	-4.13	-.1469	.0158	-.0039	.0004	-.0041	-.0150	.0017	.0005
2.001	4.11	-2.13	-.0638	.0174	.0022	-.0012	-.0041	-.0142	.0016	.0005
2.000	4.11	-1.15	-.0248	.0181	.0054	-.0022	-.0041	-.0140	.0016	.0005
2.000	4.11	-.16	.0140	.0186	.0085	-.0028	-.0041	-.0139	.0015	.0004
2.000	4.11	.82	.0531	.0190	.0116	-.0038	-.0041	-.0138	.0015	.0004
1.999	4.11	1.88	.0958	.0194	.0150	-.0045	-.0040	-.0139	.0014	.0004
1.994	4.11	3.85	.1754	.0201	.0210	-.0057	-.0039	-.0140	.0014	.0004
1.988	4.11	5.88	.2553	.0211	.0276	-.0066	-.0037	-.0144	.0013	.0004
1.985	4.12	7.85	.3310	.0221	.0339	-.0072	-.0038	-.0156	.0012	.0004
1.985	4.13	11.89	.4828	.0239	.0460	-.0081	-.0040	-.0182	.0012	.0003
1.989	4.16	15.89	.6325	.0259	.0563	-.0086	-.0048	-.0220	.0013	.0003
1.994	4.18	19.88	.7832	.0283	.0649	-.0094	-.0056	-.0238	.0011	.0004
1.993	4.11	-.13	.0170	.0186	.0088	-.0029	-.0041	-.0139	.0015	.0004

STABILITY AXIS DRAG CORRECTED FOR BASE AND CHAMBER PRESSURES

L/D	BETA	ALPHA	CL	CD	CM	CLS	CNS	CY	CDC	CDB
-5.4805	4.12	-4.13	-.1443	.0263	-.0039	.0007	-.0040	-.0150	.0017	.0005
-3.1689	4.11	-2.13	-.0626	.0198	.0022	-.0011	-.0041	-.0142	.0016	.0005
-1.2984	4.11	-1.15	-.0242	.0186	.0054	-.0021	-.0042	-.0140	.0016	.0005
.7597	4.11	-.16	.0141	.0186	.0085	-.0028	-.0041	-.0139	.0015	.0004
2.6545	4.11	.82	.0526	.0198	.0116	-.0039	-.0040	-.0138	.0015	.0004
4.2089	4.11	1.88	.0946	.0225	.0150	-.0046	-.0039	-.0139	.0014	.0004
5.4306	4.11	3.85	.1727	.0318	.0210	-.0060	-.0035	-.0140	.0014	.0004
5.3103	4.11	5.88	.2502	.0471	.0276	-.0070	-.0030	-.0144	.0013	.0004
4.8122	4.12	7.85	.3228	.0671	.0339	-.0077	-.0028	-.0156	.0012	.0003
3.7783	4.13	11.89	.4643	.1229	.0460	-.0087	-.0022	-.0182	.0012	.0003
3.0137	4.16	15.89	.5970	.1981	.0563	-.0096	-.0022	-.0220	.0012	.0003
2.4632	4.18	19.88	.7216	.2930	.0649	-.0108	-.0021	-.0238	.0010	.0003
.9177	4.11	-.13	.0171	.0186	.0088	-.0029	-.0041	-.0139	.0015	.0004

Table BIII. Continued

UPWT PROJECT 1460

RUN 29

MACH 2.00

BODY AXIS AXIAL FORCE CORRECTED FOR BASE AND CHAMBER PRESSURES

R/FT	BETA	ALPHA	CN	CA	CM	CLB	CNB	CY	CAC	CAB
2.003	.00	-4.44	-.1454	.0143	-.0037	.0003	-.0001	-.0009	.0014	.0004
2.006	.00	-2.42	-.0679	.0158	.0017	.0003	-.0001	-.0006	.0013	.0004
2.007	.00	-1.42	-.0292	.0167	.0045	.0003	-.0001	-.0003	.0013	.0004
2.013	.00	-.42	.0077	.0173	.0070	.0001	-.0001	-.0001	.0013	.0004
2.017	.00	.61	.0471	.0179	.0099	.0002	-.0001	.0000	.0012	.0004
2.019	-.00	1.55	.0833	.0185	.0126	.0003	-.0001	.0003	.0011	.0003
2.002	-.00	3.57	.1570	.0193	.0183	-.0000	-.0000	.0006	.0011	.0003
1.991	-.00	5.55	.2301	.0203	.0239	-.0000	.0000	.0009	.0010	.0003
1.985	-.00	7.57	.3027	.0212	.0300	-.0002	.0000	.0013	.0009	.0003
1.994	-.01	11.56	.4434	.0232	.0433	-.0001	-.0001	.0023	.0009	.0003
1.996	-.01	15.52	.5835	.0259	.0549	-.0002	-.0000	.0025	.0010	.0003
1.998	-.01	19.53	.7244	.0285	.0638	-.0003	.0000	.0026	.0010	.0003
1.998	.00	-.49	.0070	.0173	.0072	.0001	-.0001	.0003	.0013	.0004

STABILITY AXIS DRAG CORRECTED FOR BASE AND CHAMBER PRESSURES

L/D	BETA	ALPHA	CL	CD	CM	CLS	CNS	CY	CDC	CDB
-5.5895	.00	-4.44	-.1427	.0255	-.0037	.0003	-.0001	-.0009	.0014	.0004
-3.5646	.00	-2.42	-.0666	.0187	.0017	.0003	-.0001	-.0006	.0013	.0004
-1.6335	.00	-1.42	-.0284	.0174	.0045	.0003	-.0001	-.0003	.0013	.0004
.4621	.00	-.42	.0080	.0172	.0070	.0001	-.0001	-.0001	.0013	.0004
2.5349	.00	.61	.0467	.0184	.0099	.0002	-.0001	.0000	.0012	.0004
3.9767	-.00	1.55	.0824	.0207	.0126	.0003	-.0001	.0003	.0011	.0003
5.3158	-.00	3.57	.1546	.0291	.0183	-.0000	-.0000	.0006	.0011	.0003
5.3127	-.00	5.55	.2255	.0425	.0239	-.0000	.0000	.0009	.0010	.0003
4.8488	-.00	7.57	.2952	.0609	.0300	-.0002	.0000	.0013	.0009	.0003
3.8230	-.01	11.56	.4267	.1116	.0433	-.0001	-.0001	.0023	.0009	.0003
3.0434	-.01	15.52	.5512	.1811	.0549	-.0002	.0000	.0025	.0010	.0003
2.4826	-.01	19.53	.6680	.2691	.0638	-.0002	.0001	.0026	.0010	.0003
.4241	.00	-.49	.0073	.0173	.0072	.0001	-.0001	.0003	.0013	.0004

Table BIII. Continued

UPWT PROJECT 1460

RUN 30

MACH 2.16

BODY AXIS AXIAL FORCE CORRECTED FOR BASE AND CHAMBER PRESSURES

R/FT	BETA	ALPHA	CN	CA	CM	CLB	CNB	CY	CAC	CAB
2.000	.00	-4.22	-.1314	.0138	-.0028	.0003	-.0002	-.0006	.0013	.0004
2.002	.00	-2.17	-.0569	.0155	.0023	.0001	-.0002	-.0002	.0013	.0004
2.003	.00	-1.21	-.0223	.0162	.0046	-.0000	-.0002	.0000	.0013	.0004
2.004	.00	-.18	.0146	.0170	.0074	.0001	-.0001	.0002	.0013	.0004
2.005	.00	.77	.0476	.0177	.0100	-.0002	-.0001	.0002	.0012	.0003
2.005	.00	1.78	.0829	.0183	.0128	-.0001	-.0001	.0002	.0011	.0003
2.005	-.00	3.81	.1564	.0195	.0179	-.0001	-.0001	.0008	.0010	.0003
2.003	-.00	4.81	.1924	.0201	.0206	-.0001	-.0001	.0009	.0010	.0003
2.003	-.01	7.79	.2939	.0217	.0290	-.0000	-.0000	.0015	.0009	.0003
2.005	-.01	11.78	.4289	.0239	.0417	-.0001	.0000	.0022	.0008	.0002
2.002	-.01	15.79	.5678	.0262	.0547	-.0000	.0000	.0023	.0008	.0003
2.003	-.01	19.85	.7053	.0288	.0650	-.0003	.0001	.0026	.0010	.0003
2.003	.00	-.17	.0159	.0170	.0076	-.0001	-.0002	.0005	.0013	.0003

STABILITY AXIS DRAG CORRECTED FOR BASE AND CHAMBER PRESSURES

L/D	BETA	ALPHA	CL	CD	CM	CLS	CNS	CY	CDC	CDB
-5.4983	.00	-4.22	-.1289	.0234	-.0028	.0003	-.0002	-.0006	.0013	.0004
-3.1687	.00	-2.17	-.0558	.0176	.0023	.0001	-.0002	-.0002	.0013	.0004
-1.2947	.00	-1.21	-.0216	.0167	.0046	-.0000	-.0002	.0000	.0013	.0004
.8699	.00	-.18	.0147	.0169	.0074	.0001	-.0001	.0002	.0013	.0004
2.5715	.00	.77	.0471	.0183	.0100	-.0002	-.0001	.0002	.0012	.0003
3.9243	.00	1.78	.0818	.0209	.0128	-.0002	-.0001	.0002	.0011	.0003
5.1438	-.00	3.81	.1538	.0299	.0179	-.0001	-.0001	.0008	.0010	.0003
5.2281	-.00	4.81	.1888	.0361	.0206	-.0001	-.0001	.0009	.0010	.0003
4.5675	-.01	7.79	.2862	.0613	.0290	-.0000	-.0000	.0015	.0009	.0003
3.7115	-.01	11.78	.4120	.1110	.0417	-.0001	.0000	.0022	.0008	.0002
2.9783	-.01	15.79	.5352	.1797	.0547	-.0000	.0000	.0023	.0008	.0002
2.4328	-.01	19.85	.6485	.2666	.0650	-.0002	.0002	.0026	.0009	.0003
.9396	.00	-.17	.0160	.0170	.0076	-.0001	-.0002	.0005	.0013	.0003

Table BIII. Continued

UPWT PROJECT 1460

RUN 31

MACH 2.16

BODY AXIS AXIAL FORCE CORRECTED FOR BASE AND CHAMBER PRESSURES

R/FT	BETA	ALPHA	CN	CA	CM	CLB	CNB	CY	CAC	CAB
2.000	-4.09	-.17	.0168	.0171	.0080	.0016	.0038	.0135	.0012	.0003
2.002	-2.03	-.18	.0154	.0169	.0076	.0009	.0019	.0068	.0012	.0003
2.003	.00	-.19	.0157	.0170	.0076	.0000	-.0002	.0002	.0013	.0004
2.005	2.05	-.19	.0156	.0170	.0077	-.0008	-.0021	-.0057	.0012	.0004
2.008	4.11	-.19	.0142	.0171	.0078	-.0015	-.0041	-.0132	.0012	.0003
2.009	6.18	-.19	.0143	.0175	.0079	-.0023	-.0060	-.0210	.0012	.0003
2.004	8.24	-.19	.0155	.0176	.0080	-.0030	-.0084	-.0301	.0013	.0003
2.007	.00	-.19	.0152	.0170	.0075	.0001	-.0002	.0003	.0013	.0004

STABILITY AXIS DRAG CORRECTED FOR BASE AND CHAMBER PRESSURES

L/D	BETA	ALPHA	CL	CD	CM	CLS	CNS	CY	CDC	CDB
.9931	-4.09	-.17	.0169	.0170	.0080	.0016	.0038	.0135	.0012	.0003
.9171	-2.03	-.18	.0155	.0169	.0076	.0009	.0019	.0068	.0012	.0003
.9311	.00	-.19	.0158	.0170	.0076	.0000	-.0002	.0002	.0013	.0004
.9230	2.05	-.19	.0157	.0170	.0077	-.0008	-.0021	-.0057	.0012	.0004
.8368	4.11	-.19	.0143	.0171	.0078	-.0015	-.0041	-.0132	.0012	.0003
.8273	6.18	-.19	.0144	.0174	.0079	-.0022	-.0060	-.0210	.0012	.0003
.8917	8.24	-.19	.0156	.0175	.0080	-.0029	-.0084	-.0301	.0013	.0003
.9034	.00	-.19	.0153	.0170	.0075	.0001	-.0002	.0003	.0013	.0004

Table BIII. Continued

UPWT PROJECT 1460

RUN 32

MACH 2.16

BODY AXIS AXIAL FORCE CORRECTED FOR BASE AND CHAMBER PRESSURES

R/FT	BETA	ALPHA	CN	CA	CM	CLB	CNB	CY	CAC	CAB
2.004	-4.12	7.81	.2946	.0215	.0293	.0051	.0042	.0189	.0009	.0003
2.005	-2.05	7.81	.2940	.0215	.0292	.0027	.0022	.0101	.0009	.0002
2.004	-.01	7.81	.2950	.0217	.0292	-.0001	-.0001	.0017	.0009	.0003
2.003	2.06	7.81	.2939	.0218	.0291	-.0029	-.0022	-.0065	.0009	.0003
2.004	4.10	7.80	.2929	.0219	.0294	-.0054	-.0043	-.0156	.0009	.0003
2.005	6.18	7.80	.2925	.0217	.0295	-.0073	-.0068	-.0244	.0010	.0002
2.003	8.27	7.80	.2909	.0216	.0305	-.0091	-.0096	-.0343	.0011	.0003
1.992	-.01	7.79	.2946	.0217	.0292	-.0001	-.0001	.0017	.0009	.0003

STABILITY AXIS DRAG CORRECTED FOR BASE AND CHAMBER PRESSURES

L/D	BETA	ALPHA	CL	CD	CM	CLS	CNS	CY	CDC	CDB
4.6749	-4.12	7.81	.2869	.0614	.0293	.0057	.0035	.0189	.0009	.0002
4.6729	-2.05	7.81	.2863	.0613	.0292	.0030	.0018	.0101	.0009	.0002
4.6641	-.01	7.81	.2873	.0616	.0292	-.0001	-.0001	.0017	.0009	.0003
4.6532	2.06	7.81	.2862	.0615	.0291	-.0032	-.0018	-.0065	.0009	.0003
4.6433	4.10	7.80	.2852	.0614	.0294	-.0060	-.0035	-.0156	.0009	.0002
4.6531	6.18	7.80	.2849	.0612	.0295	-.0082	-.0057	-.0244	.0010	.0002
4.6536	8.27	7.80	.2832	.0609	.0305	-.0103	-.0083	-.0343	.0010	.0003
4.6680	-.01	7.79	.2869	.0615	.0292	-.0001	-.0000	.0017	.0009	.0003

Table BIII. Continued

UPWT PROJECT 1460

RUN 33

MACH 2.16

BODY AXIS AXIAL FORCE CORRECTED FOR BASE AND CHAMBER PRESSURES

R/FT	BETA	ALPHA	CN	CA	CM	CLB	CNB	CY	CAC	CAB
1.991	4.11	-4.22	-.1307	.0141	-.0023	-.0001	-.0042	-.0139	.0014	.0004
1.994	4.11	-2.21	-.0589	.0158	.0024	-.0007	-.0041	-.0134	.0013	.0004
1.995	4.10	-1.19	-.0216	.0165	.0051	-.0011	-.0041	-.0131	.0013	.0003
1.996	4.11	-.19	.0127	.0171	.0076	-.0017	-.0041	-.0131	.0012	.0003
1.994	4.10	.83	.0482	.0177	.0102	-.0020	-.0041	-.0130	.0012	.0003
1.995	4.11	1.81	.0834	.0183	.0128	-.0024	-.0041	-.0133	.0011	.0003
1.997	4.11	3.80	.1546	.0195	.0181	-.0034	-.0042	-.0137	.0011	.0003
1.997	4.11	5.77	.2240	.0206	.0234	-.0044	-.0042	-.0144	.0010	.0003
1.997	4.12	7.76	.2913	.0219	.0291	-.0053	-.0044	-.0158	.0009	.0003
1.998	4.14	11.80	.4285	.0240	.0418	-.0069	-.0052	-.0179	.0008	.0002
1.998	4.16	15.83	.5652	.0264	.0566	-.0081	-.0060	-.0198	.0009	.0003
2.002	4.18	19.82	.7001	.0293	.0666	-.0091	-.0066	-.0220	.0008	.0004
2.002	4.11	-.19	.0150	.0171	.0079	-.0016	-.0041	-.0131	.0012	.0003

STABILITY AXIS DRAG CORRECTED FOR BASE AND CHAMBER PRESSURES

L/D	BETA	ALPHA	CL	CD	CM	CLS	CNS	CY	CDC	CDB
-5.4277	4.11	-4.22	-.1282	.0236	-.0023	.0002	-.0042	-.0139	.0014	.0004
-3.2027	4.11	-2.21	-.0577	.0180	.0024	-.0006	-.0041	-.0134	.0013	.0004
-1.2361	4.10	-1.19	-.0210	.0170	.0051	-.0010	-.0041	-.0131	.0013	.0003
.7555	4.11	-.19	.0129	.0170	.0076	-.0017	-.0041	-.0131	.0012	.0003
2.5874	4.10	.83	.0477	.0184	.0102	-.0021	-.0041	-.0130	.0012	.0003
3.9346	4.11	1.81	.0823	.0209	.0128	-.0026	-.0040	-.0133	.0011	.0003
5.1264	4.11	3.80	.1520	.0296	.0181	-.0037	-.0039	-.0137	.0011	.0003
5.0984	4.11	5.77	.2194	.0430	.0234	-.0048	-.0038	-.0144	.0010	.0003
4.6502	4.12	7.76	.2836	.0610	.0291	-.0058	-.0036	-.0158	.0009	.0002
3.7016	4.14	11.80	.4115	.1112	.0418	-.0078	-.0037	-.0179	.0008	.0002
2.9647	4.16	15.83	.5324	.1796	.0566	-.0094	-.0036	-.0198	.0009	.0003
2.4289	4.18	19.82	.6436	.2650	.0666	-.0108	-.0032	-.0220	.0007	.0003
.8839	4.11	-.19	.0151	.0171	.0079	-.0016	-.0041	-.0131	.0012	.0003

Table BIII. Continued

UPWT PROJECT 1460

RUN 35

MACH 1.60

BODY AXIS AXIAL FORCE CORRECTED FOR BASE AND CHAMBER PRESSURES

R/FT	BETA	ALPHA	CN	CA	CM	CLB	CNB	CY	CAC	CAB
2.005	-.00	-4.13	-.1601	.0196	-.0037	.0000	.0013	-.0033	.0020	.0006
2.005	-.00	-2.15	-.0746	.0206	.0037	-.0001	.0012	-.0024	.0019	.0005
2.003	-.01	-1.17	-.0323	.0210	.0078	-.0001	.0012	-.0021	.0019	.0005
2.004	-.01	-.20	.0098	.0213	.0119	-.0001	.0012	-.0020	.0019	.0005
2.001	-.01	.83	.0544	.0216	.0161	-.0003	.0011	-.0013	.0018	.0005
2.001	-.01	1.85	.0996	.0217	.0201	-.0001	.0009	-.0007	.0018	.0005
2.002	-.01	3.88	.1911	.0220	.0272	.0001	.0010	-.0003	.0017	.0005
2.004	-.01	5.87	.2778	.0222	.0334	-.0005	.0006	.0009	.0016	.0005
2.006	-.01	7.84	.3611	.0222	.0382	-.0003	.0007	.0013	.0015	.0004
2.005	-.02	11.89	.5296	.0229	.0471	-.0003	.0007	.0019	.0012	.0004
2.005	-.02	15.82	.6875	.0237	.0558	-.0002	.0006	.0028	.0013	.0004
2.000	-.02	19.84	.8519	.0251	.0643	-.0003	.0000	.0051	.0013	.0004
2.004	-.01	-.16	.0114	.0214	.0124	-.0001	.0012	-.0016	.0019	.0005

STABILITY AXIS DRAG CORRECTED FOR BASE AND CHAMBER PRESSURES

L/D	BETA	ALPHA	CL	CD	CM	CLS	CNS	CY	CDC	CDB
-5.0498	-.00	-4.13	-.1570	.0311	-.0037	-.0001	.0013	-.0033	.0020	.0006
-3.1284	-.00	-2.15	-.0731	.0234	.0037	-.0001	.0012	-.0024	.0019	.0005
-1.4542	-.01	-1.17	-.0315	.0217	.0078	-.0001	.0012	-.0021	.0019	.0005
.4647	-.01	-.20	.0099	.0213	.0119	-.0001	.0012	-.0020	.0019	.0005
2.4084	-.01	.83	.0538	.0223	.0161	-.0002	.0011	-.0013	.0018	.0005
3.9465	-.01	1.85	.0983	.0249	.0201	-.0001	.0009	-.0007	.0018	.0005
5.3934	-.01	3.88	.1880	.0349	.0272	.0001	.0010	-.0003	.0017	.0005
5.3996	-.01	5.87	.2724	.0504	.0334	-.0004	.0007	.0009	.0016	.0005
4.9487	-.01	7.84	.3525	.0712	.0382	-.0002	.0007	.0013	.0015	.0004
3.8788	-.02	11.89	.5100	.1315	.0471	-.0001	.0007	.0019	.0012	.0003
3.0943	-.02	15.82	.6505	.2102	.0558	-.0000	.0007	.0028	.0013	.0004
2.5168	-.02	19.84	.7871	.3127	.0643	-.0002	.0001	.0051	.0012	.0004
.5378	-.01	-.16	.0115	.0213	.0124	-.0001	.0012	-.0016	.0019	.0005

Table BIII. Continued

UPWT PROJECT 1460

RUN 36

MACH 1.80

BODY AXIS AXIAL FORCE CORRECTED FOR BASE AND CHAMBER PRESSURES

R/FT	BETA	ALPHA	CN	CA	CM	CLB	CNB	CY	CAC	CAB
2.001	-.00	-4.15	-.1486	.0187	-.0030	-.0002	.0008	-.0024	.0017	.0005
2.000	-.00	-2.07	-.0617	.0199	.0033	-.0002	.0009	-.0020	.0015	.0004
1.999	-.00	-1.12	-.0233	.0204	.0064	-.0002	.0009	-.0019	.0015	.0004
2.000	-.00	-.16	.0142	.0207	.0095	-.0003	.0007	-.0013	.0014	.0004
2.000	-.00	.88	.0548	.0211	.0127	-.0003	.0008	-.0012	.0014	.0004
2.001	-.01	1.84	.0930	.0212	.0159	-.0006	.0007	-.0006	.0014	.0004
2.003	-.01	3.89	.1754	.0215	.0222	-.0004	.0006	.0000	.0013	.0004
1.999	-.01	5.85	.2517	.0217	.0284	-.0005	.0006	.0006	.0012	.0004
1.997	-.01	7.83	.3283	.0221	.0349	-.0003	.0008	.0009	.0011	.0003
1.999	-.01	11.88	.4804	.0232	.0469	-.0004	.0006	.0020	.0011	.0003
2.001	-.02	15.85	.6257	.0245	.0562	-.0005	.0004	.0029	.0012	.0003
2.003	-.02	19.89	.7768	.0263	.0651	-.0002	.0004	.0037	.0011	.0003
2.004	-.00	-.13	.0153	.0208	.0097	-.0003	.0008	-.0013	.0014	.0004

STABILITY AXIS DRAG CORRECTED FOR BASE AND CHAMBER PRESSURES

L/D	BETA	ALPHA	CL	CD	CM	CLS	CNS	CY	CDC	CDB
-4.9549	-.00	-4.15	-.1458	.0294	-.0030	-.0002	.0008	-.0024	.0017	.0005
-2.7280	-.00	-2.07	-.0604	.0221	.0033	-.0002	.0009	-.0020	.0015	.0004
-1.0839	-.00	-1.12	-.0226	.0209	.0064	-.0003	.0009	-.0019	.0015	.0004
.6923	-.00	-.16	.0143	.0207	.0095	-.0003	.0007	-.0013	.0014	.0004
2.4768	-.00	.88	.0542	.0219	.0127	-.0002	.0008	-.0012	.0014	.0004
3.7889	-.01	1.84	.0918	.0242	.0159	-.0006	.0007	-.0006	.0014	.0004
5.1785	-.01	3.89	.1725	.0333	.0222	-.0004	.0006	.0000	.0013	.0004
5.2200	-.01	5.85	.2466	.0472	.0284	-.0004	.0006	.0006	.0012	.0003
4.8059	-.01	7.83	.3201	.0666	.0349	-.0002	.0008	.0009	.0011	.0003
3.8012	-.01	11.88	.4622	.1216	.0469	-.0003	.0007	.0020	.0011	.0003
3.0395	-.02	15.85	.5910	.1944	.0562	-.0003	.0006	.0029	.0012	.0003
2.4784	-.02	19.89	.7163	.2890	.0651	-.0000	.0005	.0037	.0010	.0003
.7444	-.00	-.13	.0154	.0207	.0097	-.0003	.0008	-.0013	.0014	.0004

Table BIII. Continued

UPWT PROJECT 1460

RUN 37

MACH 1.80

BODY AXIS AXIAL FORCE CORRECTED FOR BASE AND CHAMBER PRESSURES

R/FT	BETA	ALPHA	CN	CA	CM	CLB	CNB	CY	CAC	CAB
2.002	-4.00	-.10	.0177	.0212	.0108	.0062	-.0133	.0400	.0015	.0004
2.003	-1.99	-.12	.0167	.0210	.0099	.0030	-.0061	.0189	.0015	.0004
2.005	-.00	-.14	.0152	.0207	.0096	-.0003	.0009	-.0017	.0015	.0004
2.004	2.00	-.13	.0165	.0205	.0099	-.0034	.0077	-.0216	.0015	.0004
2.001	4.01	-.13	.0154	.0204	.0104	-.0066	.0149	-.0430	.0015	.0005
2.000	6.03	-.12	.0157	.0203	.0113	-.0096	.0216	-.0640	.0015	.0005
2.000	8.05	-.12	.0158	.0203	.0125	-.0124	.0276	-.0854	.0016	.0005
2.004	-.00	-.14	.0158	.0207	.0096	-.0005	.0009	-.0019	.0015	.0004

STABILITY AXIS DRAG CORRECTED FOR BASE AND CHAMBER PRESSURES

L/D	BETA	ALPHA	CL	CD	CM	CLS	CNS	CY	CDC	CDB
.8382	-4.00	-.10	.0178	.0212	.0108	.0062	-.0132	.0400	.0015	.0004
.8037	-1.99	-.12	.0168	.0209	.0099	.0030	-.0061	.0189	.0015	.0004
.7387	-.00	-.14	.0153	.0207	.0096	-.0003	.0009	-.0017	.0015	.0004
.8140	2.00	-.13	.0166	.0204	.0099	-.0034	.0077	-.0216	.0015	.0004
.7623	4.01	-.13	.0155	.0203	.0104	-.0067	.0149	-.0430	.0015	.0005
.7779	6.03	-.12	.0158	.0203	.0113	-.0097	.0215	-.0640	.0015	.0005
.7842	8.05	-.12	.0159	.0203	.0125	-.0125	.0276	-.0854	.0016	.0005
.7681	-.00	-.14	.0159	.0207	.0096	-.0005	.0009	-.0019	.0015	.0004

Table BIII. Continued

UPWT PROJECT 1460

RUN 38

MACH 1.80

BODY AXIS AXIAL FORCE CORRECTED FOR BASE AND CHAMBER PRESSURES

R/FT	BETA	ALPHA	CN	CA	CM	CLB	CNB	CY	CAC	CAB
1.997	-4.02	7.86	.3314	.0229	.0361	.0102	-.0129	.0417	.0012	.0004
2.000	-2.00	7.85	.3300	.0224	.0356	.0050	-.0062	.0224	.0012	.0004
2.003	-.01	7.85	.3295	.0221	.0351	-.0003	.0006	.0010	.0011	.0003
2.002	2.00	7.85	.3298	.0222	.0355	-.0056	.0073	-.0207	.0011	.0003
2.002	4.01	7.85	.3297	.0222	.0356	-.0108	.0142	-.0429	.0012	.0003
2.001	6.03	7.85	.3302	.0219	.0355	-.0156	.0206	-.0652	.0012	.0004
2.001	8.08	7.85	.3307	.0217	.0358	-.0199	.0257	-.0874	.0013	.0004
1.999	-.01	7.85	.3302	.0221	.0353	-.0005	.0006	.0008	.0011	.0003

STABILITY AXIS DRAG CORRECTED FOR BASE AND CHAMBER PRESSURES

L/D	BETA	ALPHA	CL	CD	CM	CLS	CNS	CY	CDC	CDB
4.7511	-4.02	7.86	.3230	.0680	.0361	.0084	-.0142	.0447	.0012	.0004
4.7807	-2.00	7.85	.3217	.0673	.0356	.0041	-.0068	.0224	.0012	.0003
4.8027	-.01	7.85	.3213	.0669	.0351	-.0003	.0006	.0010	.0011	.0003
4.7942	2.00	7.85	.3216	.0671	.0355	-.0046	.0080	-.0207	.0011	.0003
4.7936	4.01	7.85	.3215	.0671	.0356	-.0087	.0156	-.0429	.0012	.0003
4.8199	6.03	7.85	.3220	.0668	.0355	-.0126	.0225	-.0652	.0012	.0004
4.8389	8.08	7.85	.3225	.0666	.0358	-.0163	.0282	-.0874	.0013	.0004
4.8056	-.01	7.85	.3220	.0670	.0353	-.0004	.0007	.0008	.0011	.0003

Table BIII. Continued

UPWT PROJECT 1460

RUN 39

MACH 1.80

BODY AXIS AXIAL FORCE CORRECTED FOR BASE AND CHAMBER PRESSURES

R/FT	BETA	ALPHA	CN	CA	CM	CLB	CNB	CY	CAC	CAB
1.998	4.01	-4.13	-.1488	.0181	-.0019	-.0034	.0155	-.0451	.0017	.0005
1.998	4.01	-2.15	-.0671	.0194	.0036	-.0051	.0150	-.0436	.0016	.0005
1.998	4.01	-1.17	-.0274	.0200	.0069	-.0057	.0149	-.0429	.0016	.0005
1.999	4.01	-.16	.0126	.0203	.0102	-.0066	.0147	-.0424	.0015	.0005
1.999	4.01	.84	.0514	.0205	.0132	-.0073	.0147	-.0426	.0015	.0004
2.001	4.01	1.87	.0934	.0207	.0165	-.0080	.0148	-.0426	.0014	.0004
2.002	4.01	3.89	.1737	.0210	.0225	-.0094	.0150	-.0432	.0014	.0004
2.003	4.01	5.87	.2511	.0216	.0287	-.0103	.0150	-.0435	.0013	.0004
2.005	4.01	7.85	.3288	.0222	.0355	-.0108	.0143	-.0434	.0012	.0004
2.004	4.04	11.88	.4794	.0233	.0476	-.0114	.0117	-.0426	.0012	.0004
2.001	4.07	15.91	.6264	.0245	.0576	-.0117	.0092	-.0434	.0013	.0003
1.995	4.12	19.87	.7739	.0262	.0664	-.0119	.0050	-.0404	.0012	.0004
1.992	4.01	-.16	.0137	.0203	.0103	-.0066	.0148	-.0426	.0015	.0005

STABILITY AXIS DRAG CORRECTED FOR BASE AND CHAMBER PRESSURES

L/D	BETA	ALPHA	CL	CD	CM	CLS	CNS	CY	CDC	CDB
-5.0690	4.01	-4.13	-.1460	.0288	-.0019	-.0045	.0153	-.0451	.0017	.0005
-3.0094	4.01	-2.15	-.0658	.0219	.0036	-.0056	.0148	-.0436	.0016	.0005
-1.3020	4.01	-1.17	-.0267	.0205	.0069	-.0060	.0148	-.0429	.0016	.0005
.6303	4.01	-.16	.0127	.0202	.0102	-.0067	.0147	-.0424	.0015	.0005
2.3936	4.01	.84	.0508	.0212	.0132	-.0071	.0148	-.0426	.0015	.0004
3.8918	4.01	1.87	.0922	.0237	.0165	-.0075	.0150	-.0426	.0014	.0004
5.2209	4.01	3.89	.1709	.0327	.0225	-.0084	.0156	-.0432	.0013	.0004
5.2187	4.01	5.87	.2460	.0471	.0287	-.0087	.0160	-.0435	.0013	.0004
4.7902	4.01	7.85	.3206	.0669	.0355	-.0087	.0157	-.0434	.0012	.0003
3.7977	4.04	11.88	.4612	.1214	.0476	-.0087	.0138	-.0426	.0012	.0003
3.0282	4.07	15.91	.5915	.1953	.0576	-.0087	.0121	-.0434	.0012	.0003
2.4813	4.12	19.87	.7137	.2876	.0664	-.0095	.0088	-.0404	.0011	.0003
.6818	4.01	-.16	.0138	.0203	.0103	-.0066	.0147	-.0426	.0015	.0005

Table BIII. Continued

UPWT PROJECT 1460

RUN 40

MACH 2.00

BODY AXIS AXIAL FORCE CORRECTED FOR BASE AND CHAMBER PRESSURES

R/FT	BETA	ALPHA	CN	CA	CM	CLB	CNB	CY	CAC	CAB
2.004	-.00	-4.43	-.1440	.0171	-.0014	.0003	.0008	-.0025	.0014	.0004
2.000	-.00	-2.43	-.0679	.0182	.0036	.0002	.0007	-.0016	.0013	.0004
1.999	-.00	-1.45	-.0299	.0188	.0063	.0003	.0006	-.0013	.0013	.0004
2.000	-.00	-.50	.0051	.0192	.0086	.0001	.0006	-.0010	.0012	.0004
2.000	-.00	.54	.0439	.0197	.0113	.0001	.0006	-.0008	.0012	.0004
2.001	-.00	1.53	.0809	.0200	.0140	.0001	.0005	-.0005	.0011	.0003
2.002	-.01	3.52	.1555	.0206	.0197	.0001	.0004	.0001	.0011	.0003
2.003	-.01	5.62	.2316	.0210	.0255	-.0001	.0005	.0002	.0010	.0003
2.004	-.01	7.54	.3000	.0214	.0313	-.0002	.0005	.0007	.0009	.0003
2.004	-.01	11.58	.4411	.0230	.0448	-.0002	.0005	.0013	.0009	.0003
2.004	-.02	15.58	.5805	.0246	.0565	-.0002	.0010	.0013	.0010	.0003
2.003	-.02	19.57	.7202	.0262	.0658	-.0002	.0002	.0034	.0010	.0003
2.003	-.00	-.47	.0071	.0192	.0089	.0001	.0006	-.0011	.0012	.0004

STABILITY AXIS DRAG CORRECTED FOR BASE AND CHAMBER PRESSURES

L/D	BETA	ALPHA	CL	CD	CM	CLS	CNS	CY	CDC	CDB
-5.0043	-.00	-4.43	-.1411	.0282	-.0014	.0002	.0009	-.0025	.0014	.0004
-3.1571	-.00	-2.43	-.0664	.0210	.0036	.0002	.0007	-.0016	.0013	.0004
-1.4878	-.00	-1.45	-.0291	.0195	.0063	.0003	.0007	-.0013	.0013	.0004
.2798	-.00	-.50	.0054	.0191	.0086	.0001	.0006	-.0010	.0012	.0004
2.1703	-.00	.54	.0436	.0201	.0113	.0001	.0006	-.0008	.0012	.0004
3.6105	-.00	1.53	.0799	.0221	.0140	.0001	.0005	-.0005	.0011	.0003
5.0865	-.01	3.52	.1530	.0301	.0197	.0001	.0004	.0001	.0010	.0003
5.2046	-.01	5.62	.2270	.0436	.0255	-.0000	.0005	.0002	.0010	.0003
4.8261	-.01	7.54	.2925	.0606	.0313	-.0001	.0005	.0007	.0009	.0003
3.8203	-.01	11.58	.4244	.1111	.0448	-.0001	.0005	.0013	.0009	.0003
3.0542	-.02	15.58	.5484	.1796	.0565	.0001	.0010	.0013	.0009	.0003
2.4988	-.02	19.57	.6646	.2660	.0658	-.0001	.0003	.0034	.0009	.0003
.3865	-.00	-.47	.0074	.0192	.0089	.0001	.0006	-.0011	.0012	.0004

Table BIII. Continued

UPWT PROJECT 1460

RUN 41

MACH 2.16

BODY AXIS AXIAL FORCE CORRECTED FOR BASE AND CHAMBER PRESSURES

R/FT	BETA	ALPHA	CN	CA	CM	CLB	CNB	CY	CAC	CAB
1.999	.00	-4.20	-.1324	.0168	-.0014	-.0000	.0005	-.0018	.0013	.0004
1.995	-.00	-2.20	-.0599	.0179	.0033	.0001	.0005	-.0014	.0013	.0004
1.990	-.00	-1.20	-.0237	.0185	.0058	-.0000	.0005	-.0012	.0013	.0004
1.986	-.00	-.21	.0120	.0190	.0083	-.0001	.0004	-.0007	.0013	.0004
1.982	-.00	.74	.0450	.0195	.0109	.0001	.0004	-.0007	.0012	.0003
1.981	-.00	1.78	.0814	.0199	.0137	-.0000	.0004	-.0005	.0011	.0003
1.985	-.00	3.81	.1558	.0208	.0188	-.0000	.0003	-.0000	.0010	.0003
1.990	-.00	5.79	.2246	.0214	.0241	.0000	.0003	.0003	.0009	.0003
1.995	-.01	7.77	.2918	.0221	.0297	.0000	.0003	.0008	.0009	.0003
2.000	-.01	11.79	.4272	.0235	.0425	-.0001	.0005	.0011	.0008	.0002
2.000	-.01	15.83	.5652	.0247	.0563	-.0001	.0009	.0008	.0008	.0003
1.999	-.01	19.78	.6972	.0264	.0664	-.0001	.0002	.0025	.0009	.0003
1.999	-.00	-.21	.0134	.0190	.0085	.0000	.0005	-.0009	.0012	.0004

STABILITY AXIS DRAG CORRECTED FOR BASE AND CHAMBER PRESSURES

L/D	BETA	ALPHA	CL	CD	CM	CLS	CNS	CY	CDC	CDB
-4.9008	.00	-4.20	-.1297	.0265	-.0014	-.0000	.0005	-.0018	.0013	.0004
-2.9080	-.00	-2.20	-.0586	.0202	.0033	.0001	.0005	-.0014	.0013	.0004
-1.2116	-.00	-1.20	-.0230	.0190	.0058	-.0000	.0005	-.0012	.0013	.0004
.6391	-.00	-.21	.0121	.0189	.0083	-.0001	.0004	-.0007	.0013	.0004
2.2195	-.00	.74	.0446	.0201	.0109	.0001	.0004	-.0007	.0012	.0003
3.5798	-.00	1.78	.0803	.0224	.0137	-.0000	.0004	-.0005	.0011	.0003
4.9246	-.00	3.81	.1531	.0311	.0188	-.0000	.0003	-.0000	.0010	.0003
5.0052	-.00	5.79	.2199	.0439	.0241	.0001	.0003	.0003	.0009	.0003
4.6348	-.01	7.77	.2842	.0613	.0297	.0000	.0003	.0008	.0009	.0003
3.7185	-.01	11.79	.4103	.1103	.0425	.0000	.0005	.0011	.0008	.0002
2.9943	-.01	15.83	.5330	.1780	.0563	.0001	.0009	.0008	.0008	.0002
2.4626	-.01	19.78	.6421	.2607	.0664	-.0001	.0002	.0025	.0009	.0003
.7132	-.00	-.21	.0135	.0190	.0085	.0000	.0005	-.0009	.0012	.0004

Table BIII. Continued

UPWT PROJECT 1460

RUN 42

MACH 2.16

BODY AXIS AXIAL FORCE CORRECTED FOR BASE AND CHAMBER PRESSURES

R/FT	BETA	ALPHA	CN	CA	CM	CLB	CNB	CY	CAC	CAB
2.000	-4.00	-.19	.0135	.0196	.0095	.0043	-.0102	.0351	.0012	.0003
2.000	-1.99	-.20	.0124	.0192	.0086	.0022	-.0049	.0171	.0012	.0003
2.001	-.00	-.21	.0134	.0191	.0085	-.0002	.0005	-.0010	.0013	.0004
2.001	2.01	-.21	.0124	.0189	.0086	-.0021	.0058	-.0185	.0012	.0004
2.003	4.03	-.21	.0127	.0189	.0092	-.0043	.0111	-.0372	.0012	.0003
2.003	6.04	-.20	.0125	.0190	.0099	-.0064	.0160	-.0556	.0012	.0003
2.004	8.09	-.19	.0132	.0191	.0107	-.0084	.0204	-.0749	.0012	.0004
2.006	-.00	-.21	.0129	.0190	.0084	.0001	.0005	-.0011	.0013	.0004

STABILITY AXIS DRAG CORRECTED FOR BASE AND CHAMBER PRESSURES

L/D	BETA	ALPHA	CL	CD	CM	CLS	CNS	CY	CDC	CDB
.6957	-4.00	-.19	.0136	.0195	.0095	.0044	-.0102	.0351	.0012	.0003
.6554	-1.99	-.20	.0126	.0192	.0086	.0022	-.0049	.0171	.0012	.0003
.7120	-.00	-.21	.0135	.0190	.0085	-.0002	.0005	-.0010	.0013	.0004
.6626	2.01	-.21	.0125	.0189	.0086	-.0021	.0058	-.0185	.0012	.0004
.6777	4.03	-.21	.0128	.0189	.0092	-.0044	.0111	-.0372	.0012	.0003
.6650	6.04	-.20	.0126	.0190	.0099	-.0064	.0159	-.0556	.0012	.0003
.7014	8.09	-.19	.0133	.0190	.0107	-.0085	.0203	-.0749	.0012	.0004
.6862	-.00	-.21	.0130	.0190	.0084	.0000	.0005	-.0011	.0013	.0004

Table BIII. Continued

UPWT PROJECT 1460

RUN 43

MACH 2.16

BODY AXIS AXIAL FORCE CORRECTED FOR BASE AND CHAMBER PRESSURES

R/FT	BETA	ALPHA	CN	CA	CM	CLB	CNB	CY	CAC	CAB
2.002	-4.04	7.81	.2925	.0224	.0307	.0083	-.0107	.0412	.0008	.0003
2.003	-2.00	7.80	.2927	.0221	.0301	.0044	-.0056	.0217	.0009	.0003
2.004	-.01	7.81	.2938	.0221	.0300	-.0001	.0003	.0008	.0009	.0003
2.003	2.01	7.81	.2937	.0220	.0302	-.0043	.0059	-.0193	.0009	.0003
2.001	4.04	7.80	.2927	.0219	.0307	-.0084	.0111	-.0397	.0009	.0003
2.002	6.08	7.80	.2913	.0216	.0310	-.0117	.0152	-.0589	.0010	.0003
2.002	8.10	7.80	.2898	.0214	.0322	-.0147	.0179	-.0772	.0011	.0003
2.002	-.01	7.80	.2930	.0220	.0299	-.0000	.0003	.0008	.0009	.0003

STABILITY AXIS DRAG CORRECTED FOR BASE AND CHAMBER PRESSURES

L/D	BETA	ALPHA	CL	CD	CM	CLS	CNS	CY	CDC	CDB
4.5953	-4.04	7.81	.2848	.0620	.0307	.0067	-.0117	.0412	.0008	.0003
4.6214	-2.00	7.80	.2850	.0617	.0301	.0036	-.0061	.0217	.0009	.0003
4.6297	-.01	7.81	.2861	.0618	.0300	-.0001	.0003	.0008	.0009	.0003
4.6358	2.01	7.81	.2860	.0617	.0302	-.0034	.0064	-.0193	.0009	.0003
4.6419	4.04	7.80	.2850	.0614	.0307	-.0068	.0122	-.0397	.0009	.0003
4.6605	6.08	7.80	.2837	.0609	.0310	-.0095	.0167	-.0589	.0010	.0002
4.6670	8.10	7.80	.2822	.0605	.0322	-.0122	.0198	-.0772	.0010	.0003
4.6324	-.01	7.80	.2853	.0616	.0299	.0000	.0003	.0008	.0009	.0003

Table BIII. Continued

UPWT PROJECT 1460

RUN 44

MACH 2.16

BODY AXIS AXIAL FORCE CORRECTED FOR BASE AND CHAMBER PRESSURES

R/FT	BETA	ALPHA	CN	CA	CM	CLB	CNB	CY	CAC	CAB
2.002	4.03	-4.22	-.1322	.0167	-.0004	-.0031	.0109	-.0374	.0014	.0004
2.003	4.03	-2.21	-.0595	.0180	.0043	-.0037	.0112	-.0374	.0013	.0004
2.004	4.03	-1.23	-.0250	.0185	.0066	-.0039	.0113	-.0374	.0013	.0003
2.004	4.03	-.22	.0105	.0188	.0091	-.0044	.0111	-.0372	.0012	.0003
2.001	4.03	.79	.0467	.0192	.0117	-.0048	.0110	-.0371	.0012	.0003
2.001	4.03	1.77	.0818	.0196	.0142	-.0053	.0110	-.0372	.0011	.0003
2.001	4.03	3.79	.1528	.0203	.0192	-.0062	.0109	-.0377	.0011	.0003
2.002	4.03	5.79	.2235	.0210	.0245	-.0073	.0113	-.0389	.0010	.0003
2.003	4.04	7.81	.2908	.0218	.0303	-.0083	.0111	-.0396	.0009	.0003
1.997	4.06	11.83	.4284	.0233	.0435	-.0098	.0100	-.0417	.0008	.0002
1.992	4.08	15.79	.5604	.0248	.0581	-.0105	.0072	-.0403	.0009	.0003
1.991	4.12	19.80	.6952	.0269	.0684	-.0108	.0036	-.0381	.0008	.0004

STABILITY AXIS DRAG CORRECTED FOR BASE AND CHAMBER PRESSURES

L/D	BETA	ALPHA	CL	CD	CM	CLS	CNS	CY	CDC	CDB
-4.9131	4.03	-4.22	-.1296	.0264	-.0004	-.0039	.0106	-.0374	.0014	.0004
-2.8786	4.03	-2.21	-.0583	.0202	.0043	-.0041	.0110	-.0374	.0013	.0004
-1.2812	4.03	-1.23	-.0243	.0190	.0066	-.0041	.0112	-.0374	.0013	.0003
.5675	4.03	-.22	.0107	.0188	.0091	-.0045	.0111	-.0372	.0012	.0003
2.3284	4.03	.79	.0463	.0199	.0117	-.0046	.0111	-.0371	.0012	.0003
3.6424	4.03	1.77	.0807	.0221	.0142	-.0049	.0111	-.0372	.0011	.0003
4.9555	4.03	3.79	.1502	.0303	.0192	-.0055	.0113	-.0377	.0011	.0003
5.0394	4.03	5.79	.2187	.0434	.0245	-.0061	.0120	-.0389	.0010	.0003
4.6330	4.04	7.81	.2831	.0611	.0303	-.0067	.0121	-.0396	.0009	.0003
3.7201	4.06	11.83	.4114	.1106	.0435	-.0075	.0118	-.0417	.0008	.0002
2.9967	4.08	15.79	.5285	.1764	.0581	-.0082	.0098	-.0403	.0009	.0003
2.4537	4.12	19.80	.6400	.2608	.0684	-.0089	.0071	-.0381	.0008	.0003

Table BIII. Continued

UPWT PROJECT 1532

RUN 9

MACH 1.60

BODY AXIS AXIAL FORCE CORRECTED FOR BASE AND CHAMBER PRESSURES

R/FT	BETA	ALPHA	CN	CA	CM	CLB	CNB	CY	CAC	CAB
1.997	-.00	-4.01	-.1474	.0178	-.0021	.0002	-.0001	.0005	.0017	.0004
2.000	-.00	-1.99	-.0606	.0193	.0044	.0004	-.0000	.0013	.0017	.0005
2.000	-.01	-.97	-.0173	.0198	.0082	.0002	.0001	.0020	.0016	.0005
2.000	-.01	.04	.0260	.0201	.0119	.0004	.0001	.0025	.0016	.0005
2.000	-.01	1.06	.0697	.0203	.0151	.0000	.0001	.0028	.0016	.0005
2.001	-.01	2.03	.1140	.0203	.0177	-.0000	.0001	.0030	.0016	.0004
2.000	-.01	4.03	.2001	.0204	.0239	-.0001	.0001	.0039	.0015	.0004
2.000	-.01	6.08	.2916	.0207	.0297	-.0000	.0001	.0042	.0014	.0004
2.001	-.02	8.06	.3744	.0212	.0347	-.0001	.0001	.0052	.0012	.0004
2.002	-.02	12.06	.5340	.0216	.0441	.0001	.0001	.0051	.0011	.0003
2.002	-.03	16.02	.6898	.0213	.0532	-.0001	.0002	.0079	.0013	.0004
2.002	-.04	19.99	.8505	.0197	.0627	-.0002	.0001	.0106	.0012	.0004
2.002	-.01	.03	.0278	.0201	.0125	-.0001	.0000	.0022	.0016	.0005

STABILITY AXIS DRAG CORRECTED FOR BASE AND CHAMBER PRESSURES

L/D	BETA	ALPHA	CL	CD	CM	CLS	CNS	CY	CDC	CDB
-5.1440	-.00	-4.01	-.1446	.0281	-.0021	.0002	-.0000	.0005	.0017	.0004
-2.7742	-.00	-1.99	-.0593	.0214	.0044	.0004	-.0000	.0013	.0017	.0005
-.8307	-.01	-.97	-.0167	.0201	.0082	.0002	.0001	.0020	.0016	.0005
1.2880	-.01	.04	.0260	.0202	.0119	.0004	.0001	.0025	.0016	.0005
3.2001	-.01	1.06	.0690	.0216	.0151	.0000	.0001	.0028	.0016	.0005
4.6355	-.01	2.03	.1126	.0243	.0177	-.0000	.0001	.0030	.0016	.0004
5.7264	-.01	4.03	.1969	.0344	.0239	-.0000	.0001	.0039	.0015	.0004
5.5550	-.01	6.08	.2859	.0515	.0297	-.0000	.0001	.0042	.0014	.0004
4.9748	-.02	8.06	.3654	.0734	.0347	-.0001	.0001	.0052	.0012	.0004
3.8738	-.02	12.06	.5141	.1327	.0441	.0001	.0001	.0051	.0011	.0003
3.0947	-.03	16.02	.6525	.2108	.0532	-.0000	.0002	.0079	.0012	.0003
2.5428	-.04	19.99	.7867	.3094	.0627	-.0002	.0002	.0106	.0012	.0004
1.3774	-.01	.03	.0277	.0201	.0125	-.0001	.0000	.0022	.0016	.0005

Table BIII. Continued

UPWT PROJECT 1532

RUN 12

MACH 1.80

BODY AXIS AXIAL FORCE CORRECTED FOR BASE AND CHAMBER PRESSURES

R/FT	BETA	ALPHA	CN	CA	CM	CLB	CNB	CY	CAC	CAB
2.001	.00	-4.01	-.1351	.0172	-.0016	.0005	-.0000	-.0002	.0015	.0004
2.002	-.00	-2.04	-.0542	.0188	.0032	.0002	-.0000	.0002	.0015	.0004
2.004	-.00	-1.07	-.0131	.0193	.0064	.0002	.0000	.0008	.0014	.0004
2.005	-.01	-.02	.0280	.0199	.0094	.0001	.0001	.0015	.0013	.0004
2.004	-.01	.95	.0663	.0201	.0121	.0001	.0001	.0017	.0013	.0004
2.004	-.01	1.97	.1083	.0203	.0148	.0000	.0001	.0019	.0012	.0003
2.003	-.01	3.95	.1869	.0206	.0202	-.0002	.0001	.0025	.0011	.0003
2.002	-.01	4.97	.2269	.0209	.0238	.0001	.0001	.0028	.0011	.0003
2.003	-.01	7.96	.3417	.0215	.0338	-.0001	.0002	.0038	.0010	.0003
2.003	-.02	11.95	.4844	.0226	.0462	-.0001	.0003	.0047	.0009	.0002
2.003	-.03	16.02	.6320	.0238	.0581	-.0001	.0005	.0063	.0011	.0003
2.002	-.03	19.99	.7799	.0232	.0656	-.0001	.0002	.0082	.0010	.0003
2.004	-.01	-.06	.0305	.0200	.0097	.0002	.0001	.0016	.0013	.0004

STABILITY AXIS DRAG CORRECTED FOR BASE AND CHAMBER PRESSURES

L/D	BETA	ALPHA	CL	CD	CM	CLS	CNS	CY	CDC	CDB
-4.9771	.00	-4.01	-.1325	.0266	-.0016	.0005	.0000	-.0002	.0015	.0004
-2.5606	-.00	-2.04	-.0530	.0207	.0032	.0002	-.0000	.0002	.0015	.0004
-.6357	-.00	-1.07	-.0124	.0196	.0064	.0002	.0000	.0008	.0014	.0004
1.4065	-.01	-.02	.0280	.0199	.0094	.0001	.0001	.0015	.0013	.0004
3.1016	-.01	.95	.0657	.0212	.0121	.0001	.0001	.0017	.0013	.0004
4.4593	-.01	1.97	.1070	.0240	.0148	.0000	.0001	.0019	.0012	.0003
5.5032	-.01	3.95	.1839	.0334	.0202	-.0002	.0001	.0025	.0011	.0003
5.5050	-.01	4.97	.2229	.0405	.0238	.0001	.0001	.0028	.0011	.0003
4.8543	-.01	7.96	.3332	.0686	.0338	-.0001	.0002	.0038	.0010	.0003
3.8074	-.02	11.95	.4660	.1224	.0462	-.0001	.0003	.0047	.0009	.0002
3.0232	-.03	16.02	.5965	.1973	.0581	.0001	.0005	.0063	.0010	.0003
2.4943	-.03	19.99	.7196	.2885	.0656	-.0001	.0002	.0082	.0009	.0003
1.5263	-.01	-.06	.0305	.0200	.0097	.0002	.0001	.0016	.0013	.0004

Table BIII. Continued

UPWT PROJECT 1532

RUN 13

MACH 1.80

BODY AXIS AXIAL FORCE CORRECTED FOR BASE AND CHAMBER PRESSURES

R/FT	BETA	ALPHA	CN	CA	CM	CLB	CNB	CY	CAC	CAB
1.998	-4.00	-.06	.0300	.0196	.0098	.0038	.0040	.0149	.0014	.0004
1.999	-2.01	-.07	.0294	.0197	.0096	.0021	.0021	.0076	.0014	.0004
1.999	-.00	-.06	.0300	.0199	.0095	.0003	.0001	.0016	.0013	.0004
2.000	2.01	-.07	.0290	.0199	.0094	-.0016	-.0020	-.0056	.0013	.0004
2.000	4.02	-.06	.0289	.0202	.0096	-.0033	-.0039	-.0122	.0013	.0004
2.000	6.01	-.05	.0315	.0204	.0099	-.0049	-.0057	-.0198	.0014	.0004
2.001	7.99	-.04	.0335	.0207	.0104	-.006	-.0078	-.0285	.0015	.0005

STABILITY AXIS DRAG CORRECTED FOR BASE AND CHAMBER PRESSURES

L/D	BETA	ALPHA	CL	CD	CM	CLS	CNS	CY	CDC	CDB
1.5339	-4.00	-.06	.0300	.0196	.0098	.0038	.0040	.0149	.0014	.0004
1.5003	-2.01	-.07	.0295	.0196	.0096	.0021	.0021	.0076	.0014	.0004
1.5067	-.00	-.06	.0300	.0199	.0095	.0003	.0001	.0016	.0013	.0004
1.4605	2.01	-.07	.0290	.0199	.0094	-.0016	-.0020	-.0056	.0013	.0004
1.4333	4.02	-.06	.0290	.0202	.0096	-.0033	-.0039	-.0122	.0013	.0004
1.5482	6.01	-.05	.0316	.0204	.0099	-.0049	-.0057	-.0198	.0014	.0004
1.6217	7.99	-.04	.0335	.0207	.0104	-.0063	-.0078	-.0285	.0015	.0005

Table BIII. Continued

UPWT PROJECT 1532

RUN 14

MACH 1.80

BODY AXIS AXIAL FORCE CORRECTED FOR BASE AND CHAMBER PRESSURES

R/FT	BETA	ALPHA	CN	CA	CM	CLB	CNB	CY	CAC	CAB
2.002	8.01	7.94	.3460	.0227	.0338	-.0129	-.0079	-.0327	.0011	.0003
2.003	6.00	7.95	.3457	.0224	.0340	-.0098	-.0057	-.0228	.0011	.0003
2.002	4.01	7.95	.3431	.0220	.0344	-.0068	-.0037	-.0139	.0010	.0003
2.002	2.00	7.94	.3419	.0218	.0344	-.0035	-.0015	-.0045	.0010	.0003
2.001	-.01	7.93	.3415	.0216	.0339	-.0001	.0002	.0046	.0010	.0003
2.001	-2.00	7.93	.3415	.0216	.0342	.0034	.0019	.0134	.0010	.0003
2.003	-4.03	7.94	.3431	.0216	.0341	.0067	.0039	.0225	.0010	.0003

STABILITY AXIS DRAG CORRECTED FOR BASE AND CHAMBER PRESSURES

L/D	BETA	ALPHA	CL	CD	CM	CLS	CNS	CY	CDC	CDB
4.7992	8.01	7.94	.3374	.0703	.0338	-.0138	-.0060	-.0327	.0011	.0003
4.8161	6.00	7.95	.3371	.0700	.0340	-.0105	-.0043	-.0228	.0011	.0003
4.8319	4.01	7.95	.3346	.0693	.0344	-.0072	-.0027	-.0139	.0010	.0003
4.8444	2.00	7.94	.3334	.0688	.0344	-.0037	-.0010	-.0045	.0010	.0003
4.8608	-.01	7.93	.3331	.0685	.0339	-.0001	.0002	.0046	.0010	.0003
4.8595	-2.00	7.93	.3330	.0685	.0342	.0036	.0014	.0134	.0010	.0003
4.8678	-4.03	7.94	.3347	.0687	.0341	.0072	.0029	.0225	.0010	.0003

Table BIII. Continued

UPWT PROJECT 1532

RUN 15

MACH 1.80

BODY AXIS AXIAL FORCE CORRECTED FOR BASE AND CHAMBER PRESSURES

R/FT	BETA	ALPHA	CN	CA	CM	CLB	CNB	CY	CAC	CAB
2.001	4.02	-4.02	-.1352	.0175	-.0015	.0005	-.0038	-.0140	.0015	.0004
2.001	4.02	-2.03	-.0540	.0190	.0034	-.0014	-.0039	-.0129	.0014	.0004
2.002	4.02	-1.00	-.0127	.0196	.0064	-.0025	-.0039	-.0126	.0014	.0004
2.001	4.01	-.04	.0265	.0201	.0096	-.0030	-.0039	-.0119	.0013	.0004
2.002	4.01	.95	.0660	.0203	.0121	-.0042	-.0039	-.0120	.0013	.0004
2.002	4.01	1.94	.1081	.0206	.0151	-.0048	-.0038	-.0121	.0012	.0004
2.002	4.01	3.97	.1905	.0209	.0206	-.0061	-.0037	-.0125	.0012	.0004
2.004	4.02	5.98	.2687	.0214	.0273	-.0068	-.0036	-.0130	.0011	.0004
2.005	4.02	7.98	.3426	.0220	.0342	-.0068	-.0036	-.0138	.0011	.0003
2.003	4.03	11.95	.4862	.0230	.0473	-.0074	-.0040	-.0166	.0010	.0003
2.003	4.05	16.00	.6303	.0243	.0589	-.0081	-.0046	-.0184	.0011	.0003
2.003	4.06	20.01	.7774	.0244	.0676	-.0091	-.0041	-.0218	.0011	.0003
2.004	4.01	-.04	.0301	.0202	.0098	-.0034	-.0039	-.0120	.0013	.0004

STABILITY AXIS DRAG CORRECTED FOR BASE AND CHAMBER PRESSURES

L/D	BETA	ALPHA	CL	CD	CM	CLS	CNS	CY	CDC	CDB
-4.9259	4.02	-4.02	-.1326	.0269	-.0015	.0007	-.0038	-.0140	.0015	.0004
-2.5234	4.02	-2.03	-.0528	.0209	.0034	-.0013	-.0040	-.0129	.0014	.0004
-.6083	4.02	-1.00	-.0121	.0198	.0064	-.0024	-.0040	-.0126	.0014	.0004
1.3206	4.01	-.04	.0265	.0201	.0096	-.0030	-.0039	-.0119	.0013	.0004
3.0526	4.01	.95	.0654	.0214	.0121	-.0042	-.0038	-.0120	.0013	.0004
4.4082	4.01	1.94	.1068	.0242	.0151	-.0049	-.0036	-.0121	.0012	.0004
5.5074	4.01	3.97	.1875	.0341	.0206	-.0064	-.0033	-.0125	.0012	.0004
5.3392	4.02	5.98	.2634	.0493	.0273	-.0071	-.0029	-.0130	.0011	.0003
4.8179	4.02	7.98	.3340	.0693	.0342	-.0073	-.0027	-.0138	.0010	.0003
3.7979	4.03	11.95	.4677	.1231	.0473	-.0081	-.0024	-.0166	.0010	.0003
3.0185	4.05	16.00	.5949	.1971	.0589	-.0091	-.0022	-.0184	.0011	.0003
2.4808	4.06	20.01	.7168	.2889	.0676	-.0099	-.0007	-.0218	.0011	.0003
1.4892	4.01	-.04	.0301	.0202	.0098	-.0034	-.0039	-.0120	.0013	.0004

Table BIII. Continued

UPWT PROJECT 1532

RUN 17

MACH 2.00

BODY AXIS AXIAL FORCE CORRECTED FOR BASE AND CHAMBER PRESSURES

R/FT	BETA	ALPHA	CN	CA	CM	CLB	CNB	CY	CAC	CAB
2.002	-.00	-3.98	-.1216	.0158	-.0010	.0004	.0000	.0005	.0012	.0003
2.002	-.00	-1.95	-.0422	.0173	.0029	.0003	.0001	.0011	.0012	.0004
2.002	-.01	-.91	-.0030	.0180	.0047	.0001	.0001	.0015	.0012	.0003
2.002	-.01	.11	.0369	.0187	.0074	.0003	.0002	.0020	.0011	.0003
2.002	-.01	1.11	.0738	.0190	.0097	.0002	.0002	.0021	.0010	.0003
2.002	-.01	2.12	.1113	.0194	.0122	.0002	.0002	.0025	.0010	.0003
2.002	-.01	4.10	.1844	.0199	.0169	.0001	.0002	.0028	.0009	.0003
2.001	-.01	6.10	.2556	.0206	.0230	.0001	.0002	.0036	.0008	.0003
2.001	-.02	8.10	.3242	.0212	.0295	.0002	.0003	.0046	.0008	.0002
2.001	-.02	12.09	.4594	.0227	.0452	.0001	.0004	.0049	.0008	.0002
2.001	-.03	16.09	.5950	.0244	.0579	.0001	.0005	.0065	.0010	.0003
2.000	-.03	20.13	.7359	.0251	.0671	-.0000	.0005	.0079	.0010	.0003
1.997	-.01	.14	.0389	.0187	.0079	.0002	.0001	.0019	.0011	.0003

STABILITY AXIS DRAG CORRECTED FOR BASE AND CHAMBER PRESSURES

L/D	BETA	ALPHA	CL	CD	CM	CLS	CNS	CY	CDC	CDB
-4.9295	-.00	-3.98	-.1192	.0242	-.0010	.0004	.0001	.0005	.0012	.0003
-2.1949	-.00	-1.95	-.0411	.0187	.0029	.0003	.0001	.0011	.0012	.0004
-.1387	-.01	-.91	-.0025	.0181	.0047	.0001	.0001	.0015	.0012	.0003
1.9655	-.01	.11	.0368	.0187	.0074	.0003	.0002	.0020	.0011	.0003
3.5848	-.01	1.11	.0731	.0204	.0097	.0002	.0002	.0021	.0010	.0003
4.6812	-.01	2.12	.1100	.0235	.0122	.0002	.0002	.0025	.0010	.0003
5.4910	-.01	4.10	.1814	.0330	.0169	.0001	.0002	.0028	.0009	.0003
5.2569	-.01	6.10	.2503	.0476	.0230	.0001	.0002	.0036	.0008	.0003
4.7343	-.02	8.10	.3157	.0667	.0295	.0002	.0002	.0046	.0007	.0002
3.7242	-.02	12.09	.4411	.1184	.0452	.0002	.0004	.0049	.0007	.0002
2.9754	-.03	16.09	.5605	.1884	.0579	.0003	.0004	.0065	.0009	.0003
2.4448	-.03	20.13	.6768	.2768	.0671	.0001	.0005	.0079	.0009	.0003
2.0679	-.01	.14	.0389	.0188	.0079	.0002	.0001	.0019	.0011	.0003

Table BIII. Continued

UPWT PROJECT 1532

RUN 20

MACH 2.16

BODY AXIS AXIAL FORCE CORRECTED FOR BASE AND CHAMBER PRESSURES

R/FT	BETA	ALPHA	CN	CA	CM	CLB	CNB	CY	CAC	CAB
2.002	-.00	-4.18	-.1218	.0154	-.0011	.0002	.0000	.0001	.0012	.0003
2.000	-.00	-2.17	-.0478	.0168	.0030	.0002	.0000	.0007	.0012	.0003
1.999	-.00	-1.15	-.0100	.0176	.0051	.0002	.0001	.0011	.0012	.0003
1.998	-.00	-.16	.0259	.0181	.0075	.0004	.0001	.0014	.0011	.0003
2.000	-.00	.83	.0621	.0187	.0096	.0002	.0001	.0015	.0010	.0003
1.999	-.01	1.79	.0970	.0192	.0115	.0002	.0001	.0019	.0009	.0003
1.999	-.01	3.82	.1700	.0201	.0162	.0002	.0002	.0025	.0009	.0003
2.000	-.01	5.85	.2395	.0210	.0222	.0001	.0002	.0030	.0008	.0002
2.001	-.01	7.79	.3025	.0217	.0286	.0002	.0003	.0035	.0007	.0002
2.000	-.02	11.78	.4330	.0232	.0428	.0001	.0005	.0043	.0008	.0002
1.998	-.03	15.84	.5680	.0248	.0586	.0001	.0006	.0054	.0009	.0002
2.000	-.03	19.82	.6981	.0263	.0703	.0002	.0006	.0066	.0010	.0003
2.000	-.00	-.22	.0260	.0183	.0076	.0003	.0001	.0015	.0011	.0003

STABILITY AXIS DRAG CORRECTED FOR BASE AND CHAMBER PRESSURES

L/D	BETA	ALPHA	CL	CD	CM	CLS	CNS	CY	CDC	CDB
-4.9181	-.00	-4.18	-.1193	.0243	-.0011	.0002	.0000	.0001	.0012	.0003
-2.5085	-.00	-2.17	-.0466	.0186	.0030	.0002	.0000	.0007	.0012	.0003
-.5272	-.00	-1.15	-.0094	.0178	.0051	.0002	.0001	.0011	.0012	.0003
1.4393	-.00	-.16	.0260	.0181	.0075	.0004	.0001	.0014	.0011	.0003
3.1461	-.00	.83	.0616	.0196	.0096	.0002	.0001	.0015	.0010	.0003
4.3211	-.01	1.79	.0959	.0222	.0115	.0002	.0001	.0019	.0009	.0003
5.3300	-.01	3.82	.1673	.0314	.0162	.0003	.0002	.0025	.0009	.0003
5.1826	-.01	5.85	.2346	.0453	.0222	.0001	.0001	.0030	.0008	.0002
4.7156	-.01	7.79	.2947	.0625	.0286	.0002	.0002	.0035	.0007	.0002
3.7431	-.02	11.78	.4160	.1111	.0428	.0002	.0004	.0043	.0008	.0002
2.9937	-.03	15.84	.5355	.1789	.0586	.0002	.0006	.0054	.0009	.0002
2.4582	-.03	19.82	.6427	.2614	.0703	.0003	.0005	.0066	.0010	.0003
1.4397	-.00	-.22	.0262	.0182	.0076	.0003	.0001	.0015	.0011	.0003

Table BIII. Continued

UPWT PROJECT 1532

RUN 21

MACH 2.16

BODY AXIS AXIAL FORCE CORRECTED FOR BASE AND CHAMBER PRESSURES

R/FT	BETA	ALPHA	CN	CA	CM	CLB	CNB	CY	CAC	CAB
2.001	-4.02	-.24	.0216	.0180	.0073	.0020	.0040	.0142	.0011	.0003
2.004	-1.99	-.23	.0233	.0181	.0073	.0011	.0020	.0079	.0011	.0003
2.003	-.00	-.23	.0237	.0182	.0073	.0003	.0001	.0016	.0011	.0003
2.002	2.00	-.23	.0248	.0186	.0072	-.0007	-.0019	-.0048	.0011	.0003
2.002	3.99	-.23	.0253	.0188	.0074	-.0014	-.0039	-.0119	.0011	.0003
2.002	6.00	-.22	.0258	.0190	.0079	-.0023	-.0058	-.0197	.0011	.0003
2.002	8.00	-.22	.0262	.0189	.0082	-.0030	-.0081	-.0282	.0012	.0003

STABILITY AXIS DRAG CORRECTED FOR BASE AND CHAMBER PRESSURES

L/D	BETA	ALPHA	CL	CD	CM	CLS	CNS	CY	CDC	CDB
1.2147	-4.02	-.24	.0218	.0179	.0073	.0019	.0040	.0142	.0011	.0003
1.3005	-1.99	-.23	.0235	.0180	.0073	.0011	.0020	.0079	.0011	.0003
1.3143	-.00	-.23	.0238	.0181	.0073	.0003	.0001	.0016	.0011	.0003
1.3526	2.00	-.23	.0250	.0185	.0072	-.0007	-.0019	-.0048	.0011	.0003
1.3608	3.99	-.23	.0254	.0187	.0074	-.0014	-.0039	-.0119	.0011	.0003
1.3709	6.00	-.22	.0259	.0189	.0079	-.0023	-.0059	-.0197	.0011	.0003
1.3955	8.00	-.22	.0263	.0188	.0082	-.0030	-.0081	-.0282	.0012	.0003

Table BIII. Continued

UPWT PROJECT 1532

RUN 22

MACH 2.16

BODY AXIS AXIAL FORCE CORRECTED FOR BASE AND CHAMBER PRESSURES

R/FT	BETA	ALPHA	CN	CA	CM	CLB	CNB	CY	CAC	CAB
2.001	8.05	7.81	.3031	.0221	.0300	-.0099	-.0091	-.0330	.0009	.0002
1.998	6.01	7.80	.3040	.0220	.0293	-.0079	-.0063	-.0227	.0008	.0002
1.998	4.02	7.81	.3039	.0220	.0289	-.0059	-.0040	-.0143	.0008	.0002
1.996	2.03	7.80	.3041	.0219	.0286	-.0030	-.0019	-.0053	.0008	.0002
1.999	-.01	7.80	.3030	.0216	.0286	.0001	.0002	.0029	.0007	.0002
1.999	-2.02	7.80	.3025	.0215	.0285	.0032	.0022	.0122	.0008	.0002
1.999	-3.99	7.80	.3033	.0213	.0287	.0057	.0043	.0212	.0008	.0002

STABILITY AXIS DRAG CORRECTED FOR BASE AND CHAMBER PRESSURES

L/D	BETA	ALPHA	CL	CD	CM	CLS	CNS	CY	CDC	CDB
4.6822	8.05	7.81	.2952	.0631	.0300	-.0111	-.0076	-.0330	.0009	.0002
4.6931	6.01	7.80	.2962	.0631	.0293	-.0087	-.0052	-.0227	.0008	.0002
4.6951	4.02	7.81	.2961	.0631	.0289	-.0063	-.0032	-.0143	.0008	.0002
4.7062	2.03	7.80	.2962	.0629	.0286	-.0032	-.0014	-.0053	.0007	.0002
4.7265	-.01	7.80	.2952	.0625	.0286	.0001	.0002	.0029	.0007	.0002
4.7298	-2.02	7.80	.2947	.0623	.0285	.0035	.0018	.0122	.0008	.0002
4.7481	-3.99	7.80	.2955	.0622	.0287	.0063	.0035	.0212	.0008	.0002

Table BIII. Continued

UPWT PROJECT 1532

RUN 23

MACH 2.16

BODY AXIS AXIAL FORCE CORRECTED FOR BASE AND CHAMBER PRESSURES

R/FT	BETA	ALPHA	CN	CA	CM	CLB	CNB	CY	CAC	CAB
2.001	4.02	-4.19	-.1235	.0158	-.0013	.0003	-.0039	-.0131	.0012	.0003
2.002	4.02	-2.18	-.0484	.0172	.0032	-.0004	-.0039	-.0123	.0012	.0003
2.002	4.02	-1.30	-.0176	.0180	.0047	-.0009	-.0039	-.0122	.0011	.0003
2.001	4.02	-.20	.0230	.0187	.0072	-.0014	-.0039	-.0119	.0011	.0003
2.001	4.01	.83	.0599	.0193	.0098	-.0021	-.0038	-.0119	.0011	.0003
2.001	4.02	1.88	.0980	.0198	.0122	-.0026	-.0039	-.0117	.0011	.0003
2.001	4.02	3.88	.1701	.0205	.0171	-.0040	-.0039	-.0127	.0009	.0003
2.002	4.02	5.76	.2320	.0210	.0227	-.0050	-.0039	-.0138	.0008	.0002
2.002	4.03	7.80	.2968	.0217	.0292	-.0058	-.0041	-.0150	.0008	.0002
2.002	4.05	11.85	.4323	.0231	.0437	-.0070	-.0049	-.0165	.0009	.0002
2.002	4.06	15.87	.5669	.0249	.0595	-.0078	-.0060	-.0171	.0011	.0003
2.003	4.07	19.86	.6968	.0267	.0714	-.0086	-.0054	-.0198	.0012	.0004
2.002	4.02	-.17	.0278	.0188	.0077	-.0016	-.0039	-.0119	.0011	.0003

STABILITY AXIS DRAG CORRECTED FOR BASE AND CHAMBER PRESSURES

L/D	BETA	ALPHA	CL	CD	CM	CLS	CNS	CY	CDC	CDB
-4.8738	4.02	-4.19	-.1209	.0248	-.0013	.0005	-.0039	-.0131	.0012	.0003
-2.4698	4.02	-2.18	-.0471	.0191	.0032	-.0003	-.0039	-.0123	.0012	.0003
-.9155	4.02	-1.30	-.0168	.0184	.0047	-.0008	-.0039	-.0122	.0011	.0003
1.2445	4.02	-.20	.0231	.0186	.0072	-.0014	-.0039	-.0119	.0011	.0003
2.9472	4.01	.83	.0593	.0201	.0098	-.0022	-.0038	-.0119	.0011	.0003
4.2134	4.02	1.88	.0968	.0230	.0122	-.0027	-.0038	-.0117	.0011	.0003
5.2324	4.02	3.88	.1673	.0320	.0171	-.0042	-.0036	-.0127	.0009	.0003
5.1401	4.02	5.76	.2272	.0442	.0227	-.0053	-.0034	-.0138	.0008	.0002
4.6812	4.03	7.80	.2891	.0618	.0292	-.0063	-.0033	-.0150	.0008	.0002
3.7266	4.05	11.85	.4152	.1114	.0437	-.0079	-.0034	-.0165	.0008	.0002
2.9860	4.06	15.87	.5344	.1790	.0595	-.0091	-.0036	-.0171	.0010	.0003
2.4491	4.07	19.86	.6411	.2618	.0714	-.0099	-.0021	-.0198	.0011	.0003
1.4872	4.02	-.17	.0279	.0188	.0077	-.0015	-.0039	-.0119	.0011	.0003

Table BIII. Continued

UPWT PROJECT 1532

RUN 25

MACH 1.60

BODY AXIS AXIAL FORCE CORRECTED FOR BASE AND CHAMBER PRESSURES

R/FT	BETA	ALPHA	CN	CA	CM	CLB	CNB	CY	CAC	CAB
2.004	.00	-4.01	-.1497	.0202	-.0009	.0001	-.0000	-.0001	.0018	.0005
2.000	-.00	-1.98	-.0620	.0216	.0058	.0002	-.0002	.0016	.0017	.0005
1.999	-.00	-.95	-.0172	.0221	.0098	.0002	-.0001	.0017	.0017	.0005
2.001	-.00	.05	.0238	.0223	.0129	.0001	-.0003	.0028	.0017	.0005
2.002	-.01	1.09	.0716	.0224	.0166	-.0000	-.0002	.0030	.0016	.0005
2.002	-.01	2.06	.1148	.0224	.0192	.0002	-.0003	.0038	.0016	.0005
2.001	-.01	4.06	.2036	.0226	.0253	-.0001	-.0003	.0047	.0015	.0004
2.002	-.01	6.02	.2878	.0228	.0306	-.0001	-.0002	.0054	.0014	.0004
2.003	-.02	8.01	.3716	.0232	.0359	.0001	-.0003	.0062	.0013	.0004
2.002	-.02	12.02	.5347	.0237	.0462	.0000	-.0006	.0089	.0011	.0003
2.002	-.03	16.04	.6895	.0217	.0556	-.0002	-.0001	.0094	.0013	.0004
2.003	-.04	20.07	.8534	.0204	.0657	-.0004	-.0006	.0136	.0013	.0004
2.004	-.00	.01	.0231	.0222	.0132	-.0001	-.0003	.0022	.0017	.0005

STABILITY AXIS DRAG CORRECTED FOR BASE AND CHAMBER PRESSURES

L/D	BETA	ALPHA	CL	CD	CM	CLS	CNS	CY	CDC	CDB
-4.7930	.00	-4.01	-.1467	.0306	-.0009	.0002	-.0000	-.0001	.0018	.0005
-2.5536	-.00	-1.98	-.0606	.0237	.0058	.0002	-.0002	.0016	.0017	.0005
-.7412	-.00	-.95	-.0166	.0224	.0098	.0002	-.0001	.0017	.0017	.0005
1.0655	-.00	.05	.0238	.0223	.0129	.0001	-.0003	.0028	.0017	.0005
2.9791	-.01	1.09	.0708	.0238	.0166	-.0000	-.0002	.0030	.0016	.0005
4.2740	-.01	2.06	.1133	.0265	.0192	.0002	-.0003	.0038	.0016	.0005
5.4194	-.01	4.06	.2003	.0370	.0253	-.0002	-.0003	.0047	.0015	.0004
5.3383	-.01	6.02	.2821	.0528	.0306	-.0001	-.0002	.0054	.0014	.0004
4.8487	-.02	8.01	.3624	.0747	.0359	.0001	-.0004	.0062	.0013	.0004
3.8243	-.02	12.02	.5144	.1345	.0462	-.0001	-.0005	.0089	.0011	.0003
3.0840	-.03	16.04	.6519	.2114	.0556	-.0002	-.0001	.0094	.0013	.0004
2.5276	-.04	20.07	.7887	.3121	.0657	-.0006	-.0004	.0136	.0012	.0004
1.0360	-.00	.01	.0231	.0223	.0132	-.0001	-.0003	.0022	.0017	.0005

Table BIII. Continued

UPWT PROJECT 1532

RUN 26

MACH 1.80

BODY AXIS AXIAL FORCE CORRECTED FOR BASE AND CHAMBER PRESSURES

R/FT	BETA	ALPHA	CN	CA	CM	CLB	CNB	CY	CAC	CAB
2.003	.00	-4.06	-.1385	.0195	-.0005	.0003	-.0002	.0000	.0015	.0004
2.003	-.00	-2.02	-.0548	.0210	.0047	.0003	-.0000	.0005	.0015	.0004
2.003	-.00	-1.06	-.0149	.0215	.0076	.0002	-.0001	.0009	.0014	.0004
2.003	-.00	-.07	.0234	.0219	.0104	.0001	-.0003	.0017	.0014	.0004
2.005	-.00	.99	.0663	.0221	.0134	.0000	-.0002	.0015	.0013	.0004
2.005	-.00	1.96	.1057	.0222	.0159	.0003	-.0002	.0019	.0012	.0004
2.006	-.00	3.99	.1882	.0225	.0218	.0001	-.0004	.0027	.0011	.0003
2.006	-.00	5.96	.2646	.0227	.0284	-.0000	-.0005	.0035	.0011	.0003
2.005	-.01	7.99	.3422	.0234	.0356	-.0000	-.0003	.0039	.0010	.0003
2.006	-.01	11.95	.4854	.0243	.0481	-.0000	-.0004	.0048	.0009	.0003
2.004	-.01	15.92	.6133	.0247	.0606	.0001	-.0001	.0050	.0011	.0003
2.003	-.02	19.99	.7771	.0242	.0680	.0001	-.0001	.0073	.0010	.0003
2.005	-.00	-.06	.0270	.0220	.0108	.0001	-.0001	.0012	.0014	.0004

STABILITY AXIS DRAG CORRECTED FOR BASE AND CHAMBER PRESSURES

L/D	BETA	ALPHA	CL	CD	CM	CLS	CNS	CY	CDC	CDB
-4.6383	.00	-4.06	-.1357	.0292	-.0005	.0003	-.0002	.0000	.0015	.0004
-2.3363	-.00	-2.02	-.0535	.0229	.0047	.0003	-.0000	.0005	.0015	.0004
-.6532	-.00	-1.06	-.0142	.0218	.0076	.0002	-.0001	.0009	.0014	.0004
1.0715	-.00	-.07	.0234	.0218	.0104	.0001	-.0003	.0017	.0014	.0004
2.8248	-.00	.99	.0656	.0232	.0134	.0000	-.0002	.0015	.0013	.0004
4.0468	-.00	1.96	.1043	.0258	.0159	.0003	-.0002	.0019	.0012	.0004
5.2120	-.00	3.99	.1851	.0355	.0218	.0000	-.0004	.0027	.0011	.0003
5.1747	-.00	5.96	.2591	.0501	.0284	-.0000	-.0005	.0035	.0010	.0003
4.7155	-.01	7.99	.3334	.0707	.0356	-.0001	-.0003	.0039	.0009	.0003
3.7540	-.01	11.95	.4666	.1243	.0481	-.0001	-.0004	.0048	.0009	.0002
3.0150	-.01	15.92	.5787	.1919	.0606	.0001	-.0001	.0050	.0011	.0003
2.4848	-.02	19.99	.7167	.2884	.0680	.0000	-.0002	.0073	.0009	.0003
1.2347	-.00	-.06	.0271	.0219	.0108	.0001	-.0001	.0012	.0014	.0004

Table BIII. Continued

UPWT PROJECT 1532

RUN 27

MACH 1.80

BODY AXIS AXIAL FORCE CORRECTED FOR BASE AND CHAMBER PRESSURES

R/FT	BETA	ALPHA	CN	CA	CM	CLB	CNB	CY	CAC	CAB
2.002	3.99	-4.08	-.1390	.0188	.0001	-.0034	.0141	-.0452	.0016	.0004
1.998	3.99	-2.09	-.0555	.0203	.0050	-.0053	.0134	-.0430	.0015	.0004
1.996	3.99	-1.09	-.0155	.0210	.0079	-.0061	.0131	-.0419	.0014	.0004
2.001	4.00	-.07	.0248	.0214	.0111	-.0069	.0129	-.0418	.0014	.0004
2.003	4.00	1.00	.0666	.0217	.0141	-.0076	.0125	-.0407	.0013	.0004
2.001	4.00	1.97	.1081	.0218	.0166	-.0083	.0124	-.0406	.0012	.0004
2.001	4.00	3.98	.1903	.0220	.0223	-.0096	.0125	-.0411	.0012	.0004
2.001	4.00	5.97	.2656	.0224	.0286	-.0100	.0126	-.0411	.0011	.0004
2.001	4.00	8.01	.3421	.0229	.0359	-.0105	.0124	-.0422	.0011	.0003
2.002	4.03	12.00	.4858	.0240	.0491	-.0111	.0104	-.0423	.0011	.0003
2.001	4.08	16.01	.6291	.0255	.0607	-.0112	.0065	-.0390	.0011	.0003
2.003	4.10	18.02	.7033	.0254	.0655	-.0112	.0042	-.0363	.0012	.0003
2.003	4.12	20.00	.7763	.0242	.0696	-.0111	.0028	-.0349	.0012	.0004
2.003	4.00	-.05	.0280	.0215	.0115	-.0069	.0126	-.0410	.0013	.0004

STABILITY AXIS DRAG CORRECTED FOR BASE AND CHAMBER PRESSURES

L/D	BETA	ALPHA	CL	CD	CM	CLS	CNS	CY	CDC	CDB
-4.7480	3.99	-4.08	-.1362	.0287	.0001	-.0044	.0138	-.0452	.0016	.0004
-2.4249	3.99	-2.09	-.0542	.0224	.0050	-.0058	.0132	-.0430	.0015	.0004
-.6965	3.99	-1.09	-.0148	.0213	.0079	-.0063	.0130	-.0419	.0014	.0004
1.1668	4.00	-.07	.0249	.0213	.0111	-.0069	.0128	-.0418	.0014	.0004
2.8907	4.00	1.00	.0659	.0228	.0141	-.0074	.0126	-.0407	.0013	.0004
4.1828	4.00	1.97	.1067	.0255	.0166	-.0078	.0127	-.0406	.0012	.0004
5.3187	4.00	3.98	.1872	.0352	.0223	-.0087	.0131	-.0411	.0012	.0004
5.2072	4.00	5.97	.2601	.0500	.0286	-.0086	.0135	-.0411	.0011	.0003
4.7390	4.00	8.01	.3334	.0704	.0359	-.0086	.0137	-.0422	.0011	.0003
3.7523	4.03	12.00	.4670	.1245	.0491	-.0087	.0125	-.0423	.0010	.0003
2.9961	4.08	16.01	.5933	.1980	.0607	-.0090	.0094	-.0390	.0011	.0003
2.7148	4.10	18.02	.6561	.2417	.0655	-.0093	.0075	-.0363	.0011	.0003
2.4834	4.12	20.00	.7158	.2882	.0696	-.0095	.0065	-.0349	.0011	.0003
1.3034	4.00	-.05	.0280	.0215	.0115	-.0069	.0126	-.0410	.0013	.0004

Table BIII. Continued

UPWT PROJECT 1532

RUN 28

MACH 1.80

BODY AXIS AXIAL FORCE CORRECTED FOR BASE AND CHAMBER PRESSURES

R/FT	BETA	ALPHA	CN	CA	CM	CLB	CNB	CY	CAC	CAB
2.003	-3.98	-.05	.0274	.0224	.0115	.0072	-.0123	.0417	.0014	.0004
2.004	-1.98	-.05	.0288	.0221	.0111	.0037	-.0062	.0214	.0014	.0004
2.004	-.00	-.06	.0275	.0219	.0107	.0001	-.0001	.0014	.0014	.0004
2.004	2.00	-.05	.0281	.0217	.0109	-.0035	.0064	-.0199	.0013	.0004
2.003	3.98	-.04	.0293	.0215	.0115	-.0068	.0128	-.0412	.0014	.0004
2.003	6.01	-.04	.0288	.0214	.0123	-.0100	.0186	-.0620	.0014	.0004
2.004	8.02	-.02	.0322	.0213	.0140	-.0133	.0243	-.0842	.0015	.0005

STABILITY AXIS DRAG CORRECTED FOR BASE AND CHAMBER PRESSURES

L/D	BETA	ALPHA	CL	CD	CM	CLS	CNS	CY	CDC	CDB
1.2224	-3.98	-.05	.0274	.0224	.0115	.0072	-.0123	.0417	.0014	.0004
1.3058	-1.98	-.05	.0289	.0221	.0111	.0037	-.0062	.0214	.0014	.0004
1.2569	-.00	-.06	.0275	.0219	.0107	.0001	-.0001	.0014	.0014	.0004
1.2986	2.00	-.05	.0281	.0216	.0109	-.0035	.0064	-.0199	.0013	.0004
1.3658	3.98	-.04	.0294	.0215	.0115	-.0068	.0128	-.0412	.0014	.0004
1.3492	6.01	-.04	.0288	.0214	.0123	-.0101	.0186	-.0620	.0014	.0004
1.5121	8.02	-.02	.0322	.0213	.0140	-.0133	.0243	-.0842	.0015	.0005

Table BIII. Continued

UPWT PROJECT 1532

RUN 29

MACH 1.80

BODY AXIS AXIAL FORCE CORRECTED FOR BASE AND CHAMBER PRESSURES

R/FT	BETA	ALPHA	CN	CA	CM	CLB	CNB	CY	CAC	CAB
1.999	8.02	7.98	.3432	.0223	.0365	-.0199	.0233	-.0867	.0012	.0004
2.000	6.01	7.99	.3446	.0228	.0359	-.0155	.0181	-.0631	.0011	.0003
2.000	3.98	7.99	.3420	.0229	.0361	-.0104	.0126	-.0418	.0011	.0003
2.000	2.00	7.96	.3379	.0230	.0356	-.0055	.0060	-.0190	.0011	.0003
2.000	-.01	7.97	.3403	.0231	.0354	-.0002	-.0004	.0043	.0010	.0003
2.001	-2.03	7.98	.3399	.0235	.0359	.0054	-.0064	.0269	.0010	.0003
2.001	-2.03	7.99	.3412	.0236	.0361	.0052	-.0066	.0271	.0010	.0003
2.001	-4.01	7.98	.3407	.0239	.0358	.0103	-.0127	.0498	.0011	.0003

STABILITY AXIS DRAG CORRECTED FOR BASE AND CHAMBER PRESSURES

L/D	BETA	ALPHA	CL	CD	CM	CLS	CNS	CY	CDC	CDB
4.7969	8.02	7.98	.3346	.0697	.0365	-.0164	.0259	-.0867	.0011	.0003
4.7652	6.01	7.99	.3359	.0705	.0359	-.0128	.0201	-.0631	.0011	.0003
4.7512	3.98	7.99	.3333	.0702	.0361	-.0086	.0139	-.0418	.0011	.0003
4.7334	2.00	7.96	.3293	.0696	.0356	-.0046	.0067	-.0190	.0011	.0003
4.7297	-.01	7.97	.3316	.0701	.0354	-.0002	-.0003	.0043	.0010	.0003
4.6981	-2.03	7.98	.3312	.0705	.0359	.0044	-.0071	.0269	.0010	.0003
4.6964	-2.03	7.99	.3325	.0708	.0361	.0043	-.0072	.0271	.0010	.0003
4.6773	-4.01	7.98	.3319	.0710	.0358	.0085	-.0140	.0498	.0011	.0003

Table BIII. Continued

UPWT PROJECT 1532

RUN 30

MACH 2.00

BODY AXIS AXIAL FORCE CORRECTED FOR BASE AND CHAMBER PRESSURES

R/FT	BETA	ALPHA	CN	CA	CM	CLB	CNB	CY	CAC	CAB
1.999	-.00	.08	.0389	.0205	.0086	.0002	-.0002	.0019	.0011	.0003
1.999	.00	-3.92	-.1198	.0179	.0007	.0002	-.0001	.0004	.0013	.0004
1.999	-.00	-1.91	-.0402	.0192	.0042	.0003	-.0001	.0009	.0013	.0004
1.999	-.00	-.93	-.0025	.0199	.0061	.0003	-.0000	.0012	.0012	.0004
1.999	-.00	.10	.0362	.0204	.0085	.0002	-.0002	.0019	.0012	.0004
1.999	-.00	1.09	.0732	.0207	.0107	-.0001	-.0002	.0021	.0011	.0003
2.000	-.00	2.10	.1110	.0211	.0134	.0003	-.0002	.0025	.0010	.0003
2.000	-.01	4.03	.1827	.0216	.0180	.0001	-.0002	.0031	.0009	.0003
2.000	-.01	6.09	.2556	.0222	.0243	.0000	-.0002	.0038	.0009	.0003
2.000	-.01	8.09	.3254	.0228	.0311	.0001	-.0003	.0047	.0008	.0002
2.000	-.01	12.10	.4620	.0243	.0469	.0002	-.0004	.0066	.0008	.0002
2.000	-.02	16.09	.5972	.0257	.0602	.0000	-.0002	.0075	.0010	.0003
2.000	-.03	20.09	.7350	.0260	.0692	-.0002	-.0001	.0089	.0010	.0003
2.000	-.00	.09	.0388	.0205	.0087	.0001	-.0002	.0020	.0012	.0003

STABILITY AXIS DRAG CORRECTED FOR BASE AND CHAMBER PRESSURES

L/D	BETA	ALPHA	CL	CD	CM	CLS	CNS	CY	CDC	CDB
1.8893	-.00	.08	.0389	.0206	.0086	.0002	-.0002	.0019	.0011	.0003
-4.5051	.00	-3.92	-.1172	.0260	.0007	.0002	-.0001	.0004	.0013	.0004
-1.8975	-.00	-1.91	-.0390	.0206	.0042	.0003	-.0001	.0009	.0013	.0004
-.0944	-.00	-.93	-.0019	.0199	.0061	.0003	-.0000	.0012	.0012	.0004
1.7619	-.00	.10	.0361	.0205	.0085	.0002	-.0002	.0019	.0012	.0004
3.2757	-.00	1.09	.0725	.0221	.0107	-.0001	-.0002	.0021	.0011	.0003
4.3607	-.00	2.10	.1096	.0251	.0134	.0003	-.0002	.0025	.0010	.0003
5.2298	-.01	4.03	.1796	.0343	.0180	.0001	-.0002	.0031	.0009	.0003
5.0900	-.01	6.09	.2502	.0491	.0243	-.0000	-.0002	.0038	.0009	.0003
4.6369	-.01	8.09	.3167	.0683	.0311	.0001	-.0003	.0047	.0008	.0002
3.6771	-.01	12.10	.4433	.1206	.0469	.0001	-.0004	.0066	.0008	.0002
2.9569	-.02	16.09	.5623	.1902	.0602	-.0001	-.0002	.0075	.0010	.0003
2.4414	-.03	20.09	.6759	.2769	.0692	-.0002	-.0001	.0089	.0010	.0003
1.8788	-.00	.09	.0387	.0206	.0087	.0001	-.0002	.0020	.0012	.0003

Table BIII. Continued

UPWT PROJECT 1532

RUN 31

MACH 2.16

BODY AXIS AXIAL FORCE CORRECTED FOR BASE AND CHAMBER PRESSURES

R/FT	BETA	ALPHA	CN	CA	CM	CLB	CNB	CY	CAC	CAB
1.997	-.00	-4.18	-.1249	.0172	.0010	.0003	.0001	.0001	.0012	.0003
1.999	.00	-2.23	-.0544	.0184	.0047	.0002	-.0001	.0006	.0012	.0003
1.999	-.00	-1.18	-.0158	.0192	.0067	.0003	.0000	.0008	.0012	.0003
1.999	-.00	-.18	.0204	.0197	.0086	.0003	.0000	.0010	.0011	.0003
1.999	-.00	.84	.0578	.0203	.0108	.0002	-.0000	.0015	.0010	.0003
1.999	-.00	1.81	.0937	.0208	.0128	.0002	-.0001	.0018	.0009	.0003
2.000	-.01	3.79	.1653	.0216	.0171	.0001	-.0001	.0026	.0009	.0003
2.000	-.01	5.81	.2332	.0223	.0230	.0001	-.0002	.0032	.0008	.0002
1.999	-.01	7.78	.2988	.0230	.0295	.0001	-.0001	.0037	.0007	.0002
2.000	-.01	11.83	.4315	.0245	.0440	.0001	-.0002	.0052	.0008	.0002
1.998	-.02	15.83	.5647	.0259	.0605	.0000	-.0002	.0063	.0009	.0003
2.000	-.02	19.86	.6978	.0271	.0715	-.0001	-.0006	.0086	.0010	.0003
2.001	-.00	-.19	.0232	.0199	.0092	.0003	-.0000	.0016	.0011	.0003

STABILITY AXIS DRAG CORRECTED FOR BASE AND CHAMBER PRESSURES

L/D	BETA	ALPHA	CL	CD	CM	CLS	CNS	CY	CDC	CDB
-4.6501	-.00	-4.18	-.1222	.0263	.0010	.0003	.0001	.0001	.0012	.0003
-2.5909	.00	-2.23	-.0531	.0205	.0047	.0003	-.0000	.0006	.0012	.0003
-.7747	-.00	-1.18	-.0151	.0195	.0067	.0003	.0000	.0008	.0012	.0003
1.0430	-.00	-.18	.0205	.0197	.0086	.0003	.0000	.0010	.0011	.0003
2.7055	-.00	.84	.0572	.0212	.0108	.0002	-.0000	.0015	.0010	.0003
3.9025	-.00	1.81	.0925	.0237	.0128	.0002	-.0001	.0018	.0009	.0003
5.0064	-.01	3.79	.1625	.0325	.0171	.0000	-.0001	.0026	.0009	.0003
4.9787	-.01	5.81	.2282	.0458	.0230	.0000	-.0002	.0032	.0008	.0002
4.6015	-.01	7.78	.2909	.0632	.0295	.0001	-.0001	.0037	.0007	.0002
3.6864	-.01	11.83	.4142	.1124	.0440	.0000	-.0002	.0052	.0008	.0002
2.9736	-.02	15.83	.5320	.1789	.0605	.0000	-.0002	.0063	.0009	.0002
2.4448	-.02	19.86	.6419	.2626	.0715	-.0002	-.0005	.0086	.0010	.0003
1.1777	-.00	-.19	.0233	.0198	.0092	.0003	-.0000	.0016	.0011	.0003

Table BIII. Continued

UPWT PROJECT 1532

RUN 32

MACH 2.16

BODY AXIS AXIAL FORCE CORRECTED FOR BASE AND CHAMBER PRESSURES

R/FT	BETA	ALPHA	CN	CA	CM	CLB	CNB	CY	CAC	CAB
2.000	4.02	-4.17	-.1228	.0170	.0016	-.0025	.0097	-.0368	.0013	.003
2.000	4.02	-2.17	-.0493	.0183	.0056	-.0033	.0097	-.0361	.0012	.003
2.000	4.02	-1.18	-.0137	.0190	.0075	-.0037	.0095	-.0355	.0011	.0003
2.001	4.02	-.21	.0210	.0197	.0096	-.0042	.0093	-.0351	.0011	.0003
2.000	4.02	.81	.0573	.0202	.0118	-.0048	.0092	-.0348	.0011	.0003
2.000	4.02	1.79	.0930	.0206	.0140	-.0052	.0091	-.0347	.0011	.0003
2.001	4.03	3.82	.1663	.0212	.0186	-.0067	.0090	-.0352	.0009	.0003
2.000	4.03	5.85	.2361	.0220	.0244	-.0080	.0089	-.0359	.0008	.0002
2.000	4.04	7.80	.2885	.0219	.0315	-.0087	.0087	-.0371	.0008	.0002
2.000	4.05	11.84	.4303	.0240	.0456	-.0099	.0080	-.0381	.0008	.0002
2.000	4.08	15.85	.5629	.0256	.0619	-.0106	.0050	-.0358	.0011	.0003
2.001	4.12	19.84	.6939	.0275	.0737	-.0104	.0016	-.0319	.0012	.0004
2.001	4.02	-.17	.0258	.0198	.0100	-.0043	.0093	-.0349	.0011	.0003

STABILITY AXIS DRAG CORRECTED FOR BASE AND CHAMBER PRESSURES

L/D	BETA	ALPHA	CL	CD	CM	CLS	CNS	CY	CDC	CDB
-4.6329	4.02	-4.17	-.1201	.0259	.0016	-.0032	.0095	-.0368	.0013	.0003
-2.3804	4.02	-2.17	-.0480	.0202	.0056	-.0036	.0096	-.0361	.0012	.0003
-.6718	4.02	-1.18	-.0130	.0193	.0075	-.0039	.0094	-.0355	.0011	.0003
1.0811	4.02	-.21	.0212	.0196	.0096	-.0042	.0093	-.0351	.0011	.0003
2.7017	4.02	.81	.0568	.0210	.0118	-.0047	.0093	-.0348	.0011	.0003
3.9092	4.02	1.79	.0918	.0235	.0140	-.0049	.0092	-.0347	.0011	.0003
5.0697	4.03	3.82	.1635	.0322	.0186	-.0061	.0094	-.0352	.0009	.0003
5.0264	4.03	5.85	.2311	.0460	.0244	-.0070	.0097	-.0359	.0008	.0002
4.6181	4.04	7.80	.2808	.0608	.0315	-.0075	.0098	-.0371	.0008	.0002
3.6976	4.05	11.84	.4131	.1117	.0456	-.0081	.0099	-.0381	.0008	.0002
2.9733	4.08	15.85	.5304	.1784	.0619	-.0088	.0077	-.0358	.0010	.0003
2.4423	4.12	19.84	.6382	.2613	.0737	-.0093	.0051	-.0319	.0011	.0004
1.3176	4.02	-.17	.0259	.0197	.0100	-.0043	.0093	-.0349	.0011	.0003

Table BIII. Continued

UPWT PROJECT 1532

RUN 33

MACH 2.16

BODY AXIS AXIAL FORCE CORRECTED FOR BASE AND CHAMBER PRESSURES

R/FT	BETA	ALPHA	CN	CA	CM	CLB	CNB	CY	CAC	CAB
2.000	-4.02	-.19	.0237	.0202	.0099	.0046	-.0094	.0363	.0011	.0003
2.000	-2.00	-.19	.0242	.0198	.0094	.0023	-.0049	.0186	.0012	.0003
2.000	-.00	-.18	.0252	.0197	.0093	.0002	-.0001	.0013	.0012	.0003
2.000	2.00	-.17	.0270	.0197	.0093	-.0020	.0050	-.0171	.0012	.0003
2.000	4.01	-.17	.0269	.0198	.0099	-.0043	.0092	-.0347	.0011	.0003
2.000	6.02	-.16	.0273	.0198	.0107	-.0063	.0135	-.0528	.0012	.0003
2.000	8.00	-.18	.0182	.0189	.0127	-.0083	.0176	-.0732	.0012	.0004

STABILITY AXIS DRAG CORRECTED FOR BASE AND CHAMBER PRESSURES

L/D	BETA	ALPHA	CL	CD	CM	CLS	CNS	CY	CDC	CDB
1.1855	-4.02	-.19	.0238	.0201	.0099	.0046	-.0094	.0363	.0011	.0003
1.2284	-2.00	-.19	.0243	.0198	.0094	.0024	-.0049	.0186	.0012	.0003
1.2878	-.00	-.18	.0253	.0197	.0093	.0002	-.0001	.0013	.0012	.0003
1.3803	2.00	-.17	.0271	.0196	.0093	-.0020	.0050	-.0171	.0012	.0003
1.3720	4.01	-.17	.0270	.0197	.0099	-.0044	.0092	-.0347	.0011	.0003
1.3916	6.02	-.16	.0274	.0197	.0107	-.0063	.0135	-.0528	.0012	.0003
.9741	8.00	-.18	.0183	.0188	.0127	-.0083	.0176	-.0732	.0012	.0004

Table BIII. Continued

UPWT PROJECT 1532

RUN 34

MACH 2.16

BODY AXIS AXIAL FORCE CORRECTED FOR BASE AND CHAMBER PRESSURES

R/FT	BETA	ALPHA	CN	CA	CM	CLB	CNB	CY	CAC	CAB
2.001	8.04	7.82	.2806	.0201	.0343	-.0150	.0146	-.0731	.0010	.0002
2.001	6.00	7.88	.3031	.0225	.0313	-.0123	.0122	-.0532	.0009	.0002
2.002	3.98	7.86	.3001	.0224	.0307	-.0087	.0086	-.0356	.0008	.0002
2.001	3.98	7.87	.3024	.0225	.0309	-.0087	.0085	-.0372	.0008	.0002
2.001	2.04	7.86	.3028	.0226	.0303	-.0049	.0048	-.0189	.0008	.0002
2.002	-.01	7.87	.3033	.0228	.0303	-.0001	-.0002	.0030	.0008	.0002
2.002	-1.99	7.87	.3019	.0230	.0302	.0046	-.0051	.0238	.0008	.0002
2.001	-4.04	7.87	.3019	.0231	.0308	.0087	-.0091	.0432	.0008	.0002

STABILITY AXIS DRAG CORRECTED FOR BASE AND CHAMBER PRESSURES

L/D	BETA	ALPHA	CL	CD	CM	CLS	CNS	CY	CDC	CDB
4.7008	8.04	7.82	.2733	.0581	.0343	-.0129	.0165	-.0731	.0009	.0002
4.6257	6.00	7.88	.2951	.0638	.0313	-.0105	.0137	-.0532	.0009	.0002
4.6226	3.98	7.86	.2922	.0632	.0307	-.0074	.0097	-.0356	.0008	.0002
4.6226	3.98	7.87	.2945	.0637	.0309	-.0075	.0097	-.0372	.0008	.0002
4.6180	2.04	7.86	.2948	.0638	.0303	-.0042	.0054	-.0189	.0008	.0002
4.6076	-.01	7.87	.2953	.0641	.0303	-.0001	-.0002	.0030	.0008	.0002
4.5833	-1.99	7.87	.2938	.0641	.0302	.0038	-.0057	.0238	.0008	.0002
4.5716	-4.04	7.87	.2938	.0643	.0308	.0073	-.0102	.0432	.0008	.0002

Table BIII. Continued

UPWT PROJECT 1532

RUN 45

MACH 1.60

BODY AXIS AXIAL FORCE CORRECTED FOR BASE AND CHAMBER PRESSURES

R/FT	BETA	ALPHA	CN	CA	CM	CLB	CNB	CY	CAC	CAB
2.001	.01	-3.97	-.1847	.0197	-.0083	-.0005	-.0002	-.0009	.0018	.0005
2.003	.00	-1.92	-.0758	.0200	.0009	-.0008	-.0001	.0001	.0017	.0005
2.003	.00	-1.00	-.0280	.0203	.0049	-.0008	-.0000	.0004	.0017	.0005
2.002	.00	.07	.0288	.0206	.0096	-.0005	.0000	.0008	.0016	.0005
2.002	-.00	1.16	.0888	.0212	.0147	-.0007	.0001	.0015	.0016	.0005
2.003	-.00	2.10	.1414	.0217	.0193	-.0006	.0001	.0016	.0015	.0005
2.003	-.01	4.13	.2456	.0230	.0290	-.0011	.0001	.0023	.0014	.0004
2.003	-.01	6.05	.3458	.0241	.0378	-.0010	.0003	.0031	.0014	.0004
2.004	-.01	8.13	.4482	.0248	.0456	-.0010	.0003	.0033	.0014	.0004
2.003	-.02	12.13	.6403	.0257	.0568	-.0010	.0005	.0043	.0014	.0004
2.002	-.03	16.19	.8330	.0265	.0647	-.0008	.0006	.0065	.0014	.0005
2.006	.00	.16	.0401	.0208	.0109	-.0008	.0000	.0008	.0016	.0005

STABILITY AXIS DRAG CORRECTED FOR BASE AND CHAMBER PRESSURES

L/D	BETA	ALPHA	CL	CD	CM	CLS	CNS	CY	CDC	CDB
-5.6055	.01	-3.97	-.1818	.0324	-.0083	-.0004	-.0002	-.0009	.0018	.0005
-3.3060	.00	-1.92	-.0745	.0225	.0009	-.0008	-.0001	.0001	.0017	.0005
-1.3155	.00	-1.00	-.0273	.0208	.0049	-.0008	-.0000	.0004	.0017	.0005
1.3936	.00	.07	.0288	.0207	.0096	-.0005	.0000	.0008	.0016	.0005
3.8369	-.00	1.16	.0880	.0229	.0147	-.0007	.0001	.0015	.0016	.0005
5.2040	-.00	2.10	.1399	.0269	.0193	-.0006	.0001	.0016	.0015	.0005
5.9580	-.01	4.13	.2421	.0406	.0290	-.0010	.0002	.0023	.0014	.0004
5.6231	-.01	6.05	.3396	.0604	.0378	-.0009	.0004	.0031	.0014	.0004
4.9833	-.01	8.13	.4380	.0879	.0456	-.0010	.0005	.0033	.0014	.0004
3.8661	-.02	12.13	.6173	.1597	.0568	-.0009	.0007	.0043	.0014	.0004
3.0578	-.03	16.19	.7881	.2577	.0647	-.0006	.0008	.0065	.0014	.0005
1.9157	.00	.16	.0400	.0209	.0109	-.0008	.0000	.0008	.0016	.0005

Table BIII. Continued

UPWT PROJECT 1532

RUN 48

MACH 1.80

BODY AXIS AXIAL FORCE CORRECTED FOR BASE AND CHAMBER PRESSURES

R/FT	BETA	ALPHA	CN	CA	CM	CLB	CNB	CY	CAC	CAB
2.003	.01	-4.11	-.1624	.0189	-.0064	-.0005	-.0000	-.0010	.0014	.0004
2.003	.00	-2.12	-.0720	.0195	.0010	-.0003	.0000	-.0003	.0013	.0004
2.000	.00	-.99	-.0220	.0198	.0051	-.0003	.0001	.0002	.0013	.0004
2.000	.00	-.05	.0204	.0201	.0084	-.0006	.0001	.0004	.0012	.0004
2.003	-.00	1.03	.0706	.0205	.0125	-.0005	.0001	.0010	.0012	.0004
2.004	-.00	1.90	.1123	.0208	.0156	-.0006	.0002	.0013	.0011	.0003
2.005	-.01	3.96	.2080	.0216	.0233	-.0005	.0002	.0021	.0010	.0003
2.004	-.01	5.93	.2976	.0225	.0308	-.0005	.0003	.0029	.0010	.0003
2.004	-.02	8.01	.3978	.0237	.0398	-.0010	.0004	.0035	.0010	.0003
2.002	-.02	11.98	.5792	.0256	.0517	-.0010	.0006	.0045	.0010	.0003
2.000	-.03	15.91	.7536	.0269	.0594	-.0012	.0006	.0064	.0011	.0004
2.002	-.05	19.92	.9278	.0284	.0681	-.0010	.0006	.0087	.0010	.0005
2.002	-.00	-.01	.0279	.0203	.0091	-.0005	.0001	.0006	.0012	.0004

STABILITY AXIS DRAG CORRECTED FOR BASE AND CHAMBER PRESSURES

L/D	BETA	ALPHA	CL	CD	CM	CLS	CNS	CY	CDC	CDB
-5.2280	.01	-4.11	-.1596	.0305	-.0064	-.0005	-.0000	-.0010	.0014	.0004
-3.1968	.00	-2.12	-.0707	.0221	.0010	-.0003	.0000	-.0003	.0013	.0004
-1.0601	.00	-.99	-.0214	.0202	.0051	-.0003	.0001	.0002	.0013	.0004
1.0153	.00	-.05	.0204	.0201	.0084	-.0006	.0001	.0004	.0012	.0004
3.2132	-.00	1.03	.0699	.0218	.0125	-.0005	.0001	.0010	.0012	.0004
4.5293	-.00	1.90	.1110	.0245	.0156	-.0006	.0002	.0013	.0011	.0003
5.7082	-.01	3.96	.2050	.0359	.0233	-.0005	.0003	.0021	.0010	.0003
5.5027	-.01	5.93	.2922	.0531	.0308	-.0005	.0003	.0029	.0010	.0003
4.9247	-.02	8.01	.3886	.0789	.0398	-.0009	.0005	.0035	.0010	.0003
3.8442	-.02	11.98	.5583	.1452	.0517	-.0009	.0008	.0045	.0010	.0003
3.0689	-.03	15.91	.7134	.2324	.0594	-.0010	.0010	.0064	.0011	.0004
2.5025	-.05	19.92	.8577	.3427	.0681	-.0007	.0010	.0087	.0010	.0004
1.3805	-.00	-.01	.0279	.0202	.0091	-.0005	.0001	.0006	.0012	.0004

Table BIII. Continued

UPWT PROJECT 1532

RUN 49

MACH 1.80

BODY AXIS AXIAL FORCE CORRECTED FOR BASE AND CHAMBER PRESSURES

R/FT	BETA	ALPHA	CN	CA	CM	CLB	CNB	CY	CAC	CAB
2.000	4.01	-4.05	-.1599	.0192	-.0062	-.0017	-.0025	-.0144	.0014	.0004
2.000	4.01	-2.03	-.0683	.0198	.0012	-.0018	-.0026	-.0132	.0014	.0004
1.999	4.01	-1.07	-.0246	.0202	.0048	-.0020	-.0026	-.0127	.0013	.0004
1.999	4.01	.02	.0245	.0205	.0087	-.0020	-.0026	-.0124	.0012	.0004
1.998	4.00	1.02	.0716	.0209	.0125	-.0021	-.0026	-.0119	.0012	.0004
2.000	4.01	1.94	.1134	.0212	.0158	-.0020	-.0026	-.0122	.0011	.0004
2.001	4.00	4.03	.2108	.0220	.0235	-.0025	-.0025	-.0116	.0011	.0003
2.000	4.00	6.01	.3031	.0229	.0314	-.0030	-.0025	-.0116	.0011	.0003
1.999	4.00	7.95	.3931	.0239	.0395	-.0037	-.0024	-.0123	.0012	.0003
2.000	4.01	12.01	.5770	.0257	.0530	-.0052	-.0018	-.0147	.0012	.0004
2.000	4.02	14.04	.6674	.0262	.0581	-.0059	-.0019	-.0163	.0012	.0004
2.001	4.03	16.07	.7566	.0270	.0624	-.0062	-.0025	-.0158	.0012	.0004
2.001	4.04	20.11	.9320	.0284	.0702	-.0064	-.0031	-.0153	.0012	.0005
2.001	4.01	-.06	.0248	.0206	.0088	-.0020	-.0026	-.0123	.0012	.0004

STABILITY AXIS DRAG CORRECTED FOR BASE AND CHAMBER PRESSURES

L/D	BETA	ALPHA	CL	CD	CM	CLS	CNS	CY	CDC	CDB
-5.1600	4.01	-4.05	-.1571	.0304	-.0062	-.0015	-.0027	-.0144	.0014	.0004
-3.0196	4.01	-2.03	-.0670	.0222	.0012	-.0017	-.0027	-.0132	.0014	.0004
-1.1606	4.01	-1.07	-.0240	.0207	.0048	-.0019	-.0027	-.0127	.0013	.0004
1.1941	4.01	.02	.0245	.0205	.0087	-.0020	-.0026	-.0124	.0012	.0004
3.2087	4.00	1.02	.0710	.0221	.0125	-.0021	-.0026	-.0119	.0012	.0004
4.4866	4.01	1.94	.1121	.0250	.0158	-.0021	-.0025	-.0122	.0011	.0004
5.6533	4.00	4.03	.2077	.0367	.0235	-.0027	-.0023	-.0116	.0011	.0003
5.4576	4.00	6.01	.2975	.0545	.0314	-.0032	-.0021	-.0116	.0011	.0003
4.9172	4.00	7.95	.3840	.0781	.0395	-.0040	-.0019	-.0123	.0012	.0003
3.8308	4.01	12.01	.5560	.1451	.0530	-.0055	-.0007	-.0147	.0012	.0003
3.4027	4.02	14.04	.6376	.1874	.0581	-.0062	-.0004	-.0163	.0012	.0004
3.0414	4.03	16.07	.7156	.2353	.0624	-.0067	-.0007	-.0158	.0012	.0004
2.4786	4.04	20.11	.8604	.3471	.0702	-.0071	-.0007	-.0153	.0012	.0005
1.2105	4.01	-.06	.0249	.0206	.0088	-.0020	-.0027	-.0123	.0012	.0004

Table BIII. Continued

UPWT PROJECT 1532

RUN 51

MACH 1.80

BODY AXIS AXIAL FORCE CORRECTED FOR BASE AND CHAMBER PRESSURES

R/FT	BETA	ALPHA	CN	CA	CM	CLB	CNB	CY	CAC	CAB
2.003	-4.01	-.07	.0261	.0199	.0090	.0011	.0028	.0130	.0013	.0004
2.000	-2.03	-.07	.0254	.0200	.0089	.0001	.0015	.0068	.0012	.0004
1.999	-1.03	-.06	.0265	.0201	.0088	-.0002	.0008	.0038	.0012	.0004
1.998	.02	-.06	.0273	.0202	.0089	-.0007	.0001	.0006	.0012	.0004
2.000	2.01	-.06	.0259	.0204	.0088	-.0015	-.0013	-.0054	.0012	.0004
2.000	3.99	-.06	.0261	.0205	.0087	-.0020	-.0026	-.0120	.0012	.0004
2.002	6.04	-.06	.0272	.0207	.0092	-.0026	-.0039	-.0197	.0013	.0004
2.004	8.04	-.05	.0289	.0209	.0094	-.0034	-.0053	-.0277	.0014	.0005

STABILITY AXIS DRAG CORRECTED FOR BASE AND CHAMBER PRESSURES

L/D	BETA	ALPHA	CL	CD	CM	CLS	CNS	CY	CDC	CDB
1.3120	-4.01	-.07	.0261	.0199	.0090	.0011	.0028	.0130	.0013	.0004
1.2736	-2.03	-.07	.0255	.0200	.0089	.0001	.0015	.0068	.0012	.0004
1.3205	-1.03	-.06	.0266	.0201	.0088	-.0002	.0008	.0038	.0012	.0004
1.3556	.02	-.06	.0273	.0202	.0089	-.0007	.0001	.0006	.0012	.0004
1.2765	2.01	-.06	.0260	.0204	.0088	-.0015	-.0013	-.0054	.0012	.0004
1.2751	3.99	-.06	.0261	.0205	.0087	-.0020	-.0026	-.0120	.0012	.0004
1.3135	6.04	-.06	.0272	.0207	.0092	-.0026	-.0039	-.0197	.0013	.0004
1.3894	8.04	-.05	.0290	.0208	.0094	-.0034	-.0053	-.0277	.0014	.0005

Table BIII. Continued

UPWT PROJECT 1532

RUN 52

MACH 1.80

BODY AXIS AXIAL FORCE CORRECTED FOR BASE AND CHAMBER PRESSURES

R/FT	BETA	ALPHA	CN	CA	CM	CLB	CNB	CY	CAC	CAB
2.004	8.05	8.00	.3935	.0244	.0406	-.0062	-.0053	-.0304	.0012	.0004
2.004	5.96	8.01	.3958	.0242	.0400	-.0046	-.0036	-.0195	.0011	.0003
2.003	4.03	8.00	.3925	.0235	.0408	-.0032	-.0025	-.0133	.0012	.0003
2.003	1.99	8.01	.3943	.0235	.0403	-.0020	-.0011	-.0036	.0011	.0003
2.002	-.04	8.02	.3966	.0236	.0398	-.0009	.0004	.0041	.0011	.0003
2.003	-2.00	8.02	.3974	.0235	.0398	.0007	.0018	.0111	.0010	.0003
2.003	-4.04	8.01	.3967	.0235	.0395	.0021	.0031	.0192	.0010	.0003

STABILITY AXIS DRAG CORRECTED FOR BASE AND CHAMBER PRESSURES

L/D	BETA	ALPHA	CL	CD	CM	CLS	CNS	CY	CDC	CDB
4.8694	8.05	8.00	.3843	.0789	.0406	-.0069	-.0044	-.0304	.0012	.0003
4.8822	5.96	8.01	.3865	.0792	.0400	-.0050	-.0030	-.0195	.0011	.0003
4.9175	4.03	8.00	.3834	.0780	.0408	-.0035	-.0020	-.0133	.0012	.0003
4.9220	1.99	8.01	.3851	.0782	.0403	-.0021	-.0008	-.0036	.0011	.0003
4.9277	-.04	8.02	.3875	.0786	.0398	-.0008	.0005	.0041	.0010	.0003
4.9341	-2.00	8.02	.3882	.0787	.0398	.0010	.0017	.0111	.0010	.0003
4.9332	-4.04	8.01	.3876	.0786	.0395	.0026	.0027	.0192	.0010	.0003

Table BIII. Continued

UPWT PROJECT 1532

RUN 53

MACH 2.00

BODY AXIS AXIAL FORCE CORRECTED FOR BASE AND CHAMBER PRESSURES

R/FT	BETA	ALPHA	CN	CA	CM	CLB	CNB	CY	CAC	CAB
2.002	.00	-3.91	-.1373	.0170	-.0036	-.0002	.0000	-.0013	.0012	.0003
2.002	-.00	-1.89	-.0555	.0179	.0025	-.0003	.0000	-.0002	.0011	.0003
2.003	-.00	-.91	-.0137	.0185	.0050	-.0002	.0001	.0000	.0011	.0003
2.003	-.00	.10	.0259	.0190	.0080	-.0005	.0001	.0003	.0010	.0003
2.002	-.01	1.16	.0688	.0193	.0119	-.0004	.0002	.0008	.0009	.0003
2.002	-.01	2.12	.1082	.0198	.0148	-.0005	.0002	.0011	.0009	.0003
2.002	-.01	4.15	.1911	.0206	.0215	-.0008	.0002	.0014	.0008	.0003
2.002	-.01	6.13	.2710	.0214	.0280	-.0007	.0003	.0022	.0008	.0002
2.003	-.02	8.11	.3567	.0222	.0336	-.0007	.0004	.0029	.0008	.0002
2.001	-.02	12.17	.5306	.0241	.0472	-.0007	.0005	.0039	.0009	.0003
1.998	-.03	16.16	.7028	.0263	.0582	-.0009	.0007	.0053	.0009	.0003
2.000	-.04	20.14	.8693	.0284	.0674	-.0008	.0006	.0067	.0007	.0004
1.998	-.01	.17	.0325	.0191	.0090	-.0006	.0001	.0008	.0010	.0003

STABILITY AXIS DRAG CORRECTED FOR BASE AND CHAMBER PRESSURES

L/D	BETA	ALPHA	CL	CD	CM	CLS	CNS	CY	CDC	CDB
-5.1171	.00	-3.91	-.1348	.0263	-.0036	-.0002	.0000	-.0013	.0012	.0003
-2.7605	-.00	-1.89	-.0544	.0197	.0025	-.0003	-.0000	-.0002	.0011	.0003
-.7040	-.00	-.91	-.0132	.0187	.0050	-.0002	.0001	.0000	.0011	.0003
1.3609	-.00	.10	.0259	.0190	.0080	-.0005	.0001	.0003	.0010	.0003
3.2863	-.01	1.16	.0681	.0207	.0119	-.0004	.0002	.0008	.0009	.0003
4.4869	-.01	2.12	.1069	.0238	.0148	-.0005	.0002	.0011	.0009	.0003
5.4686	-.01	4.15	.1880	.0344	.0215	-.0007	.0003	.0014	.0008	.0003
5.2931	-.01	6.13	.2656	.0502	.0280	-.0007	.0004	.0022	.0008	.0002
4.8086	-.02	8.11	.3479	.0724	.0336	-.0006	.0005	.0029	.0008	.0002
3.7685	-.02	12.17	.5105	.1355	.0472	-.0006	.0007	.0039	.0008	.0003
3.0042	-.03	16.16	.6636	.2209	.0582	-.0007	.0009	.0053	.0008	.0003
2.4585	-.04	20.14	.8013	.3259	.0674	-.0006	.0009	.0067	.0006	.0004
1.6863	-.01	.17	.0324	.0192	.0090	-.0006	.0001	.0008	.0010	.0003

Table BIII. Continued

UPWT PROJECT 1532

RUN 56

MACH 2.16

BODY AXIS AXIAL FORCE CORRECTED FOR BASE AND CHAMBER PRESSURES

R/FT	BETA	ALPHA	CN	CA	CM	CLB	CNB	CY	CAC	CAB
2.001	.00	-4.23	-.1382	.0169	-.0057	-.0004	-.0000	-.0012	.0011	.0003
2.000	.00	-2.15	-.0596	.0177	.0011	-.0002	.0001	-.0005	.0011	.0003
2.000	-.00	-1.18	-.0244	.0182	.0044	-.0001	.0001	-.0002	.0011	.0003
2.000	-.00	-.16	.0140	.0187	.0076	-.0001	.0001	.0002	.0010	.0003
2.001	-.01	.90	.0530	.0192	.0111	-.0003	.0001	.0007	.0009	.0003
2.001	-.01	1.88	.0911	.0197	.0143	-.0002	.0002	.0008	.0008	.0003
2.001	-.01	3.93	.1706	.0207	.0207	-.0002	.0003	.0019	.0008	.0002
2.002	-.01	5.80	.2381	.0213	.0274	-.0002	.0003	.0023	.0007	.0002
2.001	-.02	7.80	.3173	.0222	.0327	-.0007	.0004	.0030	.0007	.0002
2.002	-.02	11.88	.4815	.0237	.0447	-.0007	.0004	.0042	.0008	.0002
2.000	-.03	15.83	.6509	.0259	.0571	-.0009	.0006	.0055	.0008	.0003
2.002	-.05	19.93	.8200	.0282	.0676	-.0008	.0006	.0082	.0004	.0004
2.002	-.00	-.16	.0177	.0189	.0080	-.0000	.0001	.0008	.0010	.0003

STABILITY AXIS DRAG CORRECTED FOR BASE AND CHAMBER PRESSURES

L/D	BETA	ALPHA	CL	CD	CM	CLS	CNS	CY	CDC	CDB
-5.0215	.00	-4.23	-.1356	.0270	-.0057	-.0004	-.0001	-.0012	.0011	.0003
-2.9259	.00	-2.15	-.0583	.0199	.0011	-.0002	.0000	-.0005	.0011	.0003
-1.2723	-.00	-1.18	-.0238	.0187	.0044	-.0001	.0001	-.0002	.0011	.0003
.7539	-.00	-.16	.0141	.0187	.0076	-.0001	.0001	.0002	.0010	.0003
2.6160	-.01	.90	.0525	.0201	.0111	-.0003	.0001	.0007	.0009	.0003
3.9603	-.01	1.88	.0899	.0227	.0143	-.0002	.0002	.0008	.0008	.0003
5.1858	-.01	3.93	.1679	.0324	.0207	-.0001	.0003	.0019	.0008	.0002
5.1597	-.01	5.80	.2333	.0452	.0274	-.0002	.0003	.0023	.0007	.0002
4.7597	-.02	7.80	.3095	.0650	.0327	-.0006	.0005	.0030	.0007	.0002
3.7895	-.02	11.88	.4634	.1223	.0447	-.0006	.0006	.0042	.0008	.0002
3.0397	-.03	15.83	.6153	.2024	.0571	-.0007	.0008	.0055	.0007	.0003
2.4720	-.05	19.93	.7565	.3060	.0676	-.0006	.0009	.0082	.0004	.0004
.9451	-.00	-.16	.0178	.0188	.0080	-.0000	.0001	.0008	.0010	.0003

Table BIII. Continued

UPWT PROJECT 1532

RUN 57

MACH 2.16

BODY AXIS AXIAL FORCE CORRECTED FOR BASE AND CHAMBER PRESSURES

R/FT	BETA	ALPHA	CN	CA	CM	CLB	CNB	CY	CAC	CAB
2.002	4.00	-4.10	-.1341	.0174	-.0050	-.0010	-.0026	-.0134	.0011	.0003
2.002	3.99	-2.25	-.0643	.0182	.0007	-.0013	-.0025	-.0125	.0011	.0003
2.001	3.99	-1.15	-.0228	.0187	.0044	-.0014	-.0025	-.0126	.0010	.0003
2.001	3.99	-.13	.0139	.0192	.0075	-.0015	-.0026	-.0122	.0010	.0003
2.003	3.99	.87	.0529	.0197	.0108	-.0016	-.0025	-.0121	.0010	.0003
2.002	3.99	1.88	.0910	.0202	.0140	-.0018	-.0026	-.0120	.0009	.0003
2.002	3.99	3.90	.1697	.0211	.0204	-.0021	-.0027	-.0116	.0008	.0003
2.004	4.00	5.90	.2460	.0218	.0263	-.0023	-.0027	-.0124	.0008	.0002
2.004	4.00	7.82	.3206	.0225	.0322	-.0026	-.0027	-.0135	.0008	.0002
2.004	4.01	11.84	.4824	.0239	.0446	-.0032	-.0028	-.0153	.0009	.0002
2.003	4.03	15.87	.6511	.0262	.0575	-.0042	-.0034	-.0168	.0009	.0003
2.002	4.04	19.81	.8124	.0282	.0681	-.0059	-.0034	-.0191	.0008	.0004
2.001	3.99	-.18	.0178	.0194	.0077	-.0016	-.0026	-.0125	.0010	.0003

STABILITY AXIS DRAG CORRECTED FOR BASE AND CHAMBER PRESSURES

L/D	BETA	ALPHA	CL	CD	CM	CLS	CNS	CY	CDC	CDB
-4.8807	4.00	-4.10	-.1316	.0270	-.0050	-.0008	-.0027	-.0134	.0011	.0003
-3.0412	3.99	-2.25	-.0630	.0207	.0007	-.0012	-.0026	-.0125	.0011	.0003
-1.1566	3.99	-1.15	-.0221	.0191	.0044	-.0013	-.0026	-.0126	.0010	.0003
.7313	3.99	-.13	.0140	.0191	.0075	-.0015	-.0026	-.0122	.0010	.0003
2.5471	3.99	.87	.0523	.0206	.0108	-.0016	-.0025	-.0121	.0010	.0003
3.8814	3.99	1.88	.0898	.0231	.0140	-.0019	-.0025	-.0120	.0009	.0003
5.1267	3.99	3.90	.1669	.0326	.0204	-.0022	-.0025	-.0116	.0008	.0003
5.1290	4.00	5.90	.2410	.0470	.0263	-.0026	-.0025	-.0124	.0008	.0002
4.7447	4.00	7.82	.3126	.0659	.0322	-.0029	-.0024	-.0135	.0008	.0002
3.7927	4.01	11.84	.4643	.1224	.0446	-.0037	-.0020	-.0153	.0008	.0002
3.0270	4.03	15.87	.6152	.2033	.0575	-.0050	-.0021	-.0168	.0009	.0003
2.4849	4.04	19.81	.7500	.3018	.0681	-.0067	-.0012	-.0191	.0007	.0004
.9256	3.99	-.18	.0179	.0193	.0077	-.0016	-.0026	-.0125	.0010	.0003

Table BIII. Continued

UPWT PROJECT 1532

RUN 58

MACH 2.16

BODY AXIS AXIAL FORCE CORRECTED FOR BASE AND CHAMBER PRESSURES

R/FT	BETA	ALPHA	CN	CA	CM	CLB	CNB	CY	CAC	CAB
2.003	-4.03	-.20	.0155	.0186	.0077	.0012	.0027	.0120	.0010	.0003
2.002	-2.03	-.20	.0157	.0186	.0079	.0006	.0014	.0058	.0010	.0003
2.002	-.01	-.20	.0138	.0185	.0087	-.0002	.0000	.0002	.0010	.0003
2.001	1.99	-.18	.0189	.0191	.0078	-.0009	-.0012	-.0057	.0010	.0003
2.002	3.97	-.17	.0199	.0193	.0078	-.0015	-.0026	-.0122	.0010	.0003
2.002	5.99	-.18	.0202	.0193	.0078	-.0021	-.0039	-.0200	.0010	.0003
2.001	8.02	-.17	.0211	.0192	.0077	-.0028	-.0056	-.0281	.0011	.0003

STABILITY AXIS DRAG CORRECTED FOR BASE AND CHAMBER PRESSURES

L/D	BETA	ALPHA	CL	CD	CM	CLS	CNS	CY	CDC	CDB
.8424	-4.03	-.20	.0156	.0185	.0077	.0012	.0027	.0120	.0010	.0003
.8518	-2.03	-.20	.0158	.0185	.0079	.0006	.0014	.0058	.0010	.0003
.7552	-.01	-.20	.0139	.0184	.0087	-.0002	.0000	.0002	.0010	.0003
.9958	1.99	-.18	.0190	.0191	.0078	-.0009	-.0012	-.0057	.0010	.0003
1.0386	3.97	-.17	.0200	.0193	.0078	-.0015	-.0026	-.0122	.0010	.0003
1.0536	5.99	-.18	.0203	.0193	.0078	-.0021	-.0039	-.0200	.0010	.0003
1.1094	8.02	-.17	.0212	.0191	.0077	-.0028	-.0056	-.0281	.0011	.0003

Table BIII. Continued

UPWT PROJECT 1532

RUN 59

MACH 2.16

BODY AXIS AXIAL FORCE CORRECTED FOR BASE AND CHAMBER PRESSURES

R/FT	BETA	ALPHA	CN	CA	CM	CLB	CNB	CY	CAC	CAB
2.001	8.05	7.91	.3282	.0225	.0335	-.0046	-.0060	-.0316	.0009	.0003
1.998	5.98	7.90	.3269	.0225	.0333	-.0035	-.0042	-.0216	.0009	.0002
1.997	4.02	7.90	.3256	.0225	.0328	-.0027	-.0028	-.0129	.0008	.0002
1.999	2.01	7.89	.3240	.0222	.0330	-.0017	-.0014	-.0049	.0008	.0002
2.000	-.01	7.89	.3239	.0222	.0327	-.0006	.0003	.0026	.0007	.0002
2.000	-2.01	7.89	.3244	.0220	.0327	.0004	.0019	.0097	.0007	.0002
1.999	-4.04	7.89	.3247	.0218	.0327	.0014	.0033	.0179	.0008	.0003
2.000	-.01	7.88	.3228	.0222	.0327	-.0008	.0003	.0024	.0007	.0002
2.002	-.14	-.28	-.0348	.0187	-.0028	-.0015	.0051	.0591	.0010	.0003
2.001	-4.14	-.30	-.0363	.0206	-.0034	-.0067	.0110	.2090	.0008	.0003
2.002	-8.21	-.31	-.0378	.0222	-.0038	-.0122	.0169	.3655	.0008	.0002

STABILITY AXIS DRAG CORRECTED FOR BASE AND CHAMBER PRESSURES

L/D	BETA	ALPHA	CL	CD	CM	CLS	CNS	CY	CDC	CDB
4.7450	8.05	7.91	.3201	.0675	.0335	-.0054	-.0053	-.0316	.0009	.0003
4.7432	5.98	7.90	.3188	.0672	.0333	-.0040	-.0037	-.0216	.0009	.0002
4.7391	4.02	7.90	.3175	.0670	.0328	-.0030	-.0024	-.0129	.0008	.0002
4.7516	2.01	7.89	.3160	.0665	.0330	-.0019	-.0011	-.0049	.0008	.0002
4.7518	-.01	7.89	.3159	.0665	.0327	-.0006	.0004	.0026	.0007	.0002
4.7673	-2.01	7.89	.3164	.0664	.0327	.0006	.0018	.0097	.0007	.0002
4.7829	-4.04	7.89	.3167	.0662	.0327	.0018	.0031	.0179	.0008	.0003
4.7515	-.01	7.88	.3148	.0663	.0327	-.0007	.0004	.0024	.0007	.0002
-1.8335	-.14	-.28	-.0346	.0189	-.0028	-.0016	.0050	.0591	.0010	.0003
-1.7420	-4.14	-.30	-.0362	.0208	-.0034	-.0067	.0110	.2090	.0008	.0003
-1.6740	-8.21	-.31	-.0376	.0224	-.0038	-.0123	.0169	.3655	.0008	.0002

Table BIII. Continued

UPWT PROJECT 1532

RUN 35

MACH 1.60

BODY AXIS AXIAL FORCE CORRECTED FOR BASE AND CHAMBER PRESSURES

R/FT	BETA	ALPHA	CN	CA	CM	CLB	CNB	CY	CAC	CAB
1.999	.00	-3.92	-.1843	.0221	-.0058	-.0008	.0001	-.0008	.0017	.0005
2.000	.00	-1.96	-.0801	.0226	.0026	-.0009	-.0002	.0007	.0017	.0005
2.035	-.00	-.92	-.0257	.0228	.0071	-.0008	-.0001	.0010	.0016	.0005
2.000	-.00	-.88	-.0230	.0227	.0074	-.0003	-.0001	.0012	.0016	.0005
2.013	-.00	.16	.0326	.0230	.0121	-.0005	.0001	.0009	.0016	.0005
2.009	-.01	1.06	.0837	.0234	.0164	-.0007	.0000	.0019	.0016	.0005
2.005	-.01	2.12	.1391	.0239	.0214	-.0009	-.0002	.0027	.0015	.0004
2.001	-.01	4.28	.2522	.0251	.0321	-.0010	-.0000	.0033	.0014	.0004
2.001	-.02	6.10	.3463	.0260	.0400	-.0009	-.0000	.0044	.0014	.0004
1.995	-.02	8.10	.4451	.0267	.0475	-.0009	-.0001	.0057	.0014	.0004
1.995	-.02	12.13	.6378	.0272	.0599	-.0013	-.0002	.0068	.0014	.0004
1.994	-.04	16.09	.8268	.0276	.0690	-.0009	.0001	.0086	.0015	.0005

STABILITY AXIS DRAG CORRECTED FOR BASE AND CHAMBER PRESSURES

L/D	BETA	ALPHA	CL	CD	CM	CLS	CNS	CY	CDC	CDB
-5.2368	.00	-3.92	-.1813	.0346	-.0058	-.0008	.0001	-.0008	.0017	.0005
-3.1099	.00	-1.96	-.0788	.0253	.0026	-.0009	-.0002	.0007	.0017	.0005
-1.0815	-.00	-.92	-.0251	.0232	.0071	-.0008	-.0001	.0010	.0016	.0005
-.9700	-.00	-.88	-.0224	.0231	.0074	-.0003	-.0001	.0012	.0016	.0005
1.4096	-.00	.16	.0325	.0231	.0121	-.0005	.0001	.0009	.0016	.0005
3.3307	-.01	1.06	.0829	.0249	.0164	-.0007	.0000	.0019	.0016	.0005
4.7387	-.01	2.12	.1375	.0290	.0214	-.0009	-.0002	.0027	.0015	.0004
5.6621	-.01	4.28	.2485	.0439	.0321	-.0010	.0001	.0033	.0014	.0004
5.4224	-.02	6.10	.3399	.0627	.0400	-.0009	.0001	.0044	.0014	.0004
4.8792	-.02	8.10	.4347	.0891	.0475	-.0009	.0000	.0057	.0014	.0004
3.8277	-.02	12.13	.6146	.1606	.0599	-.0013	.0001	.0068	.0014	.0004
3.0603	-.04	16.09	.7824	.2557	.0690	-.0008	.0004	.0086	.0014	.0005

Table BIII. Continued

UPWT PROJECT 1532

RUN 36

MACH 1.80

BODY AXIS AXIAL FORCE CORRECTED FOR BASE AND CHAMBER PRESSURES

R/FT	BETA	ALPHA	CN	CA	CM	CLB	CNB	CY	CAC	CAB
2.000	.00	-4.04	-.1613	.0211	-.0042	-.0009	.0001	-.0009	.0014	.0004
2.000	-.00	-2.05	-.0721	.0216	.0031	-.0005	.0002	-.0003	.0014	.0004
2.001	-.00	-1.05	-.0269	.0219	.0068	-.0005	.0000	.0005	.0013	.0004
2.001	-.00	-.06	.0188	.0222	.0103	-.0006	-.0001	.0011	.0012	.0004
2.000	-.00	.95	.0636	.0225	.0141	-.0006	-.0001	.0016	.0012	.0004
2.000	-.01	1.97	.1140	.0229	.0179	-.0005	-.0001	.0022	.0011	.0003
2.001	-.01	3.94	.2053	.0235	.0253	-.0008	.0000	.0026	.0010	.0003
2.000	-.01	6.01	.3011	.0244	.0335	-.0007	-.0000	.0036	.0010	.0003
2.000	-.02	7.98	.3941	.0254	.0417	-.0012	.0000	.0043	.0011	.0003
2.000	-.02	11.98	.5759	.0269	.0552	-.0009	.0000	.0060	.0011	.0003
1.999	-.04	15.99	.7527	.0278	.0641	-.0010	.0004	.0070	.0011	.0004
2.001	-.04	19.97	.9271	.0289	.0719	-.0010	.0000	.0095	.0010	.0004
2.000	-.00	-.05	.0184	.0222	.0104	-.0008	-.0001	.0015	.0012	.0004

STABILITY AXIS DRAG CORRECTED FOR BASE AND CHAMBER PRESSURES

L/D	BETA	ALPHA	CL	CD	CM	CLS	CNS	CY	CDC	CDB
-4.8889	.00	-4.04	-.1584	.0324	-.0042	-.0009	.0001	-.0009	.0014	.0004
-2.9309	-.00	-2.05	-.0708	.0242	.0031	-.0005	.0002	-.0003	.0014	.0004
-1.1703	-.00	-1.05	-.0263	.0224	.0068	-.0005	.0000	.0005	.0013	.0004
.8508	-.00	-.06	.0188	.0222	.0103	-.0006	-.0001	.0011	.0012	.0004
2.6727	-.00	.95	.0630	.0236	.0141	-.0006	-.0001	.0016	.0012	.0004
4.2055	-.01	1.97	.1127	.0268	.0179	-.0005	-.0000	.0022	.0011	.0003
5.3757	-.01	3.94	.2022	.0376	.0253	-.0008	.0001	.0026	.0010	.0003
5.2979	-.01	6.01	.2954	.0558	.0335	-.0007	.0001	.0036	.0010	.0003
4.8185	-.02	7.98	.3848	.0799	.0417	-.0012	.0002	.0043	.0011	.0003
3.8023	-.02	11.98	.5547	.1459	.0552	-.0009	.0002	.0060	.0010	.0003
3.0404	-.04	15.99	.7119	.2341	.0641	-.0008	.0007	.0070	.0011	.0004
2.4909	-.04	19.97	.8565	.3438	.0719	-.0010	.0004	.0095	.0010	.0004
.8309	-.00	-.05	.0185	.0222	.0104	-.0008	-.0001	.0015	.0012	.0004

Table BIII. Continued

UPWT PROJECT 1532

RUN 37

MACH 1.80

BODY AXIS AXIAL FORCE CORRECTED FOR BASE AND CHAMBER PRESSURES

R/FT	BETA	ALPHA	CN	CA	CM	CLB	CNB	CY	CAC	CAB
2.000	4.01	-4.02	-.1617	.0206	-.0035	-.0052	.0151	-.0434	.0015	.0004
1.999	4.01	-4.00	-.1577	.0207	-.0031	-.0056	.0153	-.0438	.0015	.0004
2.000	4.01	-2.02	-.0694	.0212	.0040	-.0051	.0150	-.0422	.0014	.0004
2.000	4.01	-1.05	-.0264	.0215	.0074	-.0053	.0147	-.0414	.0013	.0004
2.000	4.01	-.04	.0188	.0218	.0110	-.0054	.0143	-.0404	.0012	.0004
1.998	4.02	.99	.0674	.0222	.0148	-.0054	.0139	-.0398	.0012	.0004
1.997	4.02	1.99	.1150	.0226	.0186	-.0053	.0134	-.0383	.0011	.0004
1.998	4.02	3.98	.2063	.0233	.0259	-.0055	.0126	-.0363	.0011	.0003
1.998	4.03	6.03	.3028	.0241	.0340	-.0058	.0118	-.0353	.0012	.0003
1.999	4.04	7.98	.3881	.0243	.0438	-.0061	.0112	-.0344	.0012	.0003
1.999	4.07	11.96	.5553	.0252	.0606	-.0075	.0091	-.0342	.0013	.0003
1.998	4.09	16.03	.7516	.0276	.0667	-.0086	.0074	-.0327	.0013	.0004
1.999	4.11	19.96	.9227	.0286	.0738	-.0087	.0067	-.0330	.0012	.0005
2.000	4.01	-.05	.0210	.0219	.0113	-.0054	.0145	-.0409	.0012	.0004

STABILITY AXIS DRAG CORRECTED FOR BASE AND CHAMBER PRESSURES

L/D	BETA	ALPHA	CL	CD	CM	CLS	CNS	CY	CDC	CDB
-4.9812	4.01	-4.02	-.1589	.0319	-.0035	-.0063	.0147	-.0434	.0015	.0004
-4.8975	4.01	-4.00	-.1549	.0316	-.0031	-.0066	.0149	-.0438	.0014	.0004
-2.8887	4.01	-2.02	-.0681	.0236	.0040	-.0057	.0148	-.0422	.0014	.0004
-1.1712	4.01	-1.05	-.0258	.0220	.0074	-.0056	.0146	-.0414	.0013	.0004
.8644	4.01	-.04	.0188	.0218	.0110	-.0054	.0143	-.0404	.0012	.0004
2.8614	4.02	.99	.0667	.0233	.0148	-.0052	.0140	-.0398	.0012	.0004
4.2776	4.02	1.99	.1137	.0266	.0186	-.0048	.0136	-.0383	.0011	.0004
5.4170	4.02	3.98	.2032	.0375	.0259	-.0046	.0129	-.0363	.0011	.0003
5.3219	4.03	6.03	.2970	.0558	.0340	-.0046	.0124	-.0353	.0011	.0003
4.8619	4.04	7.98	.3789	.0779	.0438	-.0045	.0119	-.0344	.0012	.0003
3.8276	4.07	11.96	.5350	.1398	.0606	-.0055	.0105	-.0342	.0012	.0003
3.0375	4.09	16.03	.7108	.2340	.0667	-.0063	.0095	-.0327	.0012	.0004
2.4938	4.11	19.96	.8526	.3419	.0738	-.0059	.0092	-.0330	.0012	.0004
.9592	4.01	-.05	.0210	.0219	.0113	-.0054	.0145	-.0409	.0012	.0004

Table BIII. Continued

UPWT PROJECT 1532

RUN 38

MACH 1.80

BODY AXIS AXIAL FORCE CORRECTED FOR BASE AND CHAMBER PRESSURES

R/FT	BETA	ALPHA	CN	CA	CM	CLB	CNB	CY	CAC	CAB
2.000	-4.02	-.02	.0225	.0227	.0116	.0039	-.0137	.0407	.0013	.0004
1.999	-2.02	-.02	.0219	.0222	.0114	.0018	-.0067	.0203	.0013	.0004
2.000	-.00	-.01	.0235	.0222	.0108	-.0006	.0000	.0011	.0012	.0004
2.000	2.00	-.02	.0229	.0220	.0108	-.0031	.0071	-.0194	.0012	.0004
2.001	3.99	-.00	.0246	.0219	.0114	-.0053	.0140	-.0397	.0012	.0004
2.001	5.99	-.01	.0222	.0216	.0127	-.0073	.0206	-.0605	.0013	.0004
2.002	8.02	.03	.0272	.0216	.0141	-.0094	.0263	-.0804	.0014	.0005

STABILITY AXIS DRAG CORRECTED FOR BASE AND CHAMBER PRESSURES

L/D	BETA	ALPHA	CL	CD	CM	CLS	CNS	CY	CDC	CDB
.9929	-4.02	-.02	.0225	.0226	.0116	.0039	-.0137	.0407	.0013	.0004
.9859	-2.02	-.02	.0219	.0222	.0114	.0018	-.0067	.0203	.0013	.0004
1.0598	-.00	-.01	.0235	.0222	.0108	-.0006	.0000	.0011	.0012	.0004
1.0431	2.00	-.02	.0229	.0220	.0108	-.0031	.0071	-.0194	.0012	.0004
1.1236	3.99	-.00	.0246	.0219	.0114	-.0053	.0140	-.0397	.0012	.0004
1.0249	5.99	-.01	.0222	.0216	.0127	-.0074	.0206	-.0605	.0013	.0004
1.2591	8.02	.03	.0272	.0216	.0141	-.0094	.0264	-.0804	.0014	.0005

Table BIII. Continued

UPWT PROJECT 1532

RUN 39

MACH 1.80

BODY AXIS AXIAL FORCE CORRECTED FOR BASE AND CHAMBER PRESSURES

R/FT	BETA	ALPHA	CN	CA	CM	CLB	CNB	CY	CAC	CAB
2.000	8.07	7.99	.3921	.0245	.0443	-.0116	.0212	-.0747	.0012	.0004
1.998	6.02	8.01	.3940	.0247	.0428	-.0089	.0159	-.0536	.0012	.0003
2.000	4.03	8.01	.3939	.0250	.0420	-.0064	.0110	-.0337	.0012	.0003
1.998	-.02	8.01	.3947	.0253	.0419	-.0010	-.0001	.0048	.0011	.0003
2.000	-2.04	8.02	.3963	.0257	.0420	.0020	-.0055	.0234	.0010	.0003
1.999	-4.05	8.01	.3949	.0259	.0419	.0048	-.0107	.0420	.0011	.0003
2.000	-.02	8.01	.3944	.0253	.0420	-.0008	.0000	.0044	.0011	.0003

STABILITY AXIS DRAG CORRECTED FOR BASE AND CHAMBER PRESSURES

L/D	BETA	ALPHA	CL	CD	CM	CLS	CNS	CY	CDC	CDB
4.8586	8.07	7.99	.3828	.0788	.0443	-.0086	.0227	-.0747	.0012	.0004
4.8476	6.02	8.01	.3847	.0794	.0428	-.0066	.0170	-.0536	.0012	.0003
4.8300	4.03	8.01	.3846	.0796	.0420	-.0048	.0118	-.0337	.0012	.0003
4.8093	-.02	8.01	.3853	.0801	.0419	-.0010	.0001	.0048	.0011	.0003
4.7909	-2.04	8.02	.3868	.0807	.0420	.0013	-.0058	.0234	.0010	.0003
4.7768	-4.05	8.01	.3854	.0807	.0419	.0033	-.0112	.0420	.0010	.0003
4.8140	-.02	8.01	.3850	.0800	.0420	-.0008	.0002	.0044	.0011	.0003

Table BIII. Continued

UPWT PROJECT 1532

RUN 40

MACH 2.00

BODY AXIS AXIAL FORCE CORRECTED FOR BASE AND CHAMBER PRESSURES

R/FT	BETA	ALPHA	CN	CA	CM	CLB	CNB	CY	CAC	CAB
2.000	.00	-3.85	-.1303	.0193	-.0024	-.0003	.0002	-.0005	.0012	.0003
2.000	-.00	-1.87	-.0526	.0200	.0039	-.0003	.0001	.0004	.0012	.0003
2.002	-.00	-.85	-.0125	.0204	.0069	-.0004	.0001	.0009	.0011	.0003
2.000	-.00	.17	.0283	.0208	.0101	-.0004	.0001	.0011	.0011	.0003
2.000	-.01	1.14	.0679	.0212	.0134	-.0005	-.0000	.0016	.0009	.0003
2.001	-.01	2.12	.1082	.0216	.0168	-.0005	.0000	.0019	.0009	.0003
2.001	-.01	4.16	.1916	.0224	.0234	-.0007	.0000	.0025	.0008	.0003
2.002	-.01	6.16	.2744	.0232	.0298	-.0006	.0001	.0033	.0008	.0002
2.001	-.02	8.15	.3579	.0240	.0362	-.0008	.0001	.0040	.0008	.0002
2.002	-.02	12.17	.5316	.0257	.0506	-.0009	.0001	.0054	.0009	.0003
2.002	-.03	14.19	.6186	.0266	.0569	-.0009	.0002	.0056	.0009	.0003
2.002	-.03	16.14	.7030	.0273	.0619	-.0010	.0000	.0071	.0009	.0004
2.003	-.04	20.15	.8692	.0289	.0705	-.0010	.0002	.0086	.0006	.0004
2.002	-.00	.16	.0320	.0209	.0106	-.0007	-.0000	.0015	.0010	.0003

STABILITY AXIS DRAG CORRECTED FOR BASE AND CHAMBER PRESSURES

L/D	BETA	ALPHA	CL	CD	CM	CLS	CNS	CY	CDC	CDB
-4.5545	.00	-3.85	-.1277	.0280	-.0024	-.0003	.0001	-.0005	.0012	.0003
-2.3689	-.00	-1.87	-.0515	.0217	.0039	-.0003	.0001	.0004	.0012	.0003
-.5803	-.00	-.85	-.0120	.0206	.0069	-.0004	.0001	.0009	.0011	.0003
1.3497	-.00	.17	.0282	.0209	.0101	-.0004	.0001	.0011	.0011	.0003
2.9781	-.01	1.14	.0672	.0226	.0134	-.0005	.0000	.0016	.0009	.0003
4.1654	-.01	2.12	.1068	.0256	.0168	-.0005	.0001	.0019	.0009	.0003
5.1927	-.01	4.16	.1884	.0363	.0234	-.0007	.0001	.0025	.0008	.0003
5.1162	-.01	6.16	.2687	.0525	.0298	-.0006	.0002	.0033	.0008	.0002
4.6789	-.02	8.15	.3488	.0745	.0362	-.0008	.0002	.0040	.0008	.0002
3.7267	-.02	12.17	.5111	.1372	.0506	-.0009	.0003	.0054	.0009	.0003
3.3240	-.03	14.19	.5896	.1774	.0569	-.0008	.0004	.0056	.0009	.0003
2.9926	-.03	16.14	.6636	.2218	.0619	-.0010	.0003	.0071	.0008	.0003
2.4525	-.04	20.15	.8009	.3266	.0705	-.0009	.0005	.0086	.0006	.0004
1.5165	-.00	.16	.0319	.0210	.0106	-.0007	-.0000	.0015	.0010	.0003

Table BIII. Continued

UPWT PROJECT 1532

RUN 41

MACH 2.16

BODY AXIS AXIAL FORCE CORRECTED FOR BASE AND CHAMBER PRESSURES

R/FT	BETA	ALPHA	CN	CA	CM	CLB	CNB	CY	CAC	CAB
2.003	.00	-4.17	-.1373	.0188	-.0032	-.0003	.0001	-.0005	.0011	.0003
2.002	-.00	-2.22	-.0647	.0195	.0030	-.0003	.0000	.0002	.0011	.0003
2.002	-.00	-1.23	-.0288	.0199	.0061	-.0004	-.0000	.0007	.0011	.0003
1.999	-.00	-.11	.0129	.0204	.0097	-.0002	.0000	.0010	.0010	.0003
2.001	-.00	.84	.0485	.0209	.0128	-.0003	-.0000	.0016	.0009	.0003
2.000	-.01	1.85	.0868	.0214	.0160	-.0003	.0001	.0017	.0008	.0003
2.002	-.01	3.84	.1628	.0223	.0222	-.0003	.0001	.0025	.0008	.0002
2.002	-.02	7.88	.3194	.0240	.0347	-.0005	.0002	.0040	.0007	.0002
2.001	-.02	11.86	.4814	.0254	.0465	-.0006	.0002	.0053	.0008	.0002
2.001	-.03	15.87	.6522	.0270	.0594	-.0009	.0002	.0066	.0007	.0003
2.000	-.04	19.87	.8162	.0286	.0698	-.0008	.0001	.0083	.0004	.0004
2.001	-.00	-.11	.0185	.0206	.0101	-.0003	.0000	.0013	.0010	.0003

STABILITY AXIS DRAG CORRECTED FOR BASE AND CHAMBER PRESSURES

L/D	BETA	ALPHA	CL	CD	CM	CLS	CNS	CY	CDC	CDB
-4.6827	.00	-4.17	-.1346	.0287	-.0032	-.0004	.0001	-.0005	.0011	.0003
-2.8862	-.00	-2.22	-.0633	.0219	.0030	-.0003	.0000	.0002	.0011	.0003
-1.3703	-.00	-1.23	-.0281	.0205	.0061	-.0004	-.0000	.0007	.0011	.0003
.6365	-.00	-.11	.0130	.0204	.0097	-.0002	.0000	.0010	.0010	.0003
2.2157	-.00	.84	.0480	.0216	.0128	-.0003	-.0000	.0016	.0009	.0003
3.5353	-.01	1.85	.0856	.0242	.0160	-.0003	.0001	.0017	.0008	.0003
4.8266	-.01	3.84	.1601	.0332	.0222	-.0003	.0001	.0025	.0008	.0002
4.6064	-.02	7.88	.3112	.0675	.0347	-.0005	.0002	.0040	.0007	.0002
3.7396	-.02	11.86	.4630	.1238	.0465	-.0005	.0003	.0053	.0008	.0002
3.0160	-.03	15.87	.6161	.2043	.0594	-.0008	.0004	.0066	.0007	.0003
2.4750	-.04	19.87	.7531	.3043	.0698	-.0008	.0003	.0083	.0004	.0004
.9008	-.00	-.11	.0186	.0206	.0101	-.0003	.0000	.0013	.0010	.0003

Table BIII. Continued

UPWT PROJECT 1532

RUN 42

MACH 2.16

BODY AXIS AXIAL FORCE CORRECTED FOR BASE AND CHAMBER PRESSURES

R/FT	BETA	ALPHA	CN	CA	CM	CLB	CNB	CY	CAC	CAB
2.002	3.98	-4.17	-.1379	.0187	-.0023	-.0035	.0102	-.0342	.0012	.0003
1.998	3.97	-2.18	-.0643	.0194	.0036	-.0037	.0108	-.0343	.0011	.0003
1.998	3.97	-1.19	-.0273	.0199	.0068	-.0038	.0108	-.0341	.0010	.0003
1.997	3.97	-.12	.0128	.0204	.0102	-.0040	.0110	-.0343	.0010	.0003
1.998	3.97	.82	.0473	.0209	.0130	-.0042	.0111	-.0344	.0010	.0003
1.998	3.97	1.79	.0857	.0213	.0160	-.0043	.0111	-.0341	.0010	.0003
1.998	3.97	3.91	.1677	.0222	.0226	-.0047	.0112	-.0342	.0008	.0002
1.997	3.97	5.88	.2432	.0228	.0284	-.0050	.0105	-.0331	.0008	.0002
1.997	3.98	7.87	.3209	.0235	.0347	-.0051	.0096	-.0320	.0008	.0002
1.998	4.01	11.90	.4838	.0250	.0475	-.0054	.0071	-.0303	.0009	.0002
1.998	4.04	15.90	.6493	.0269	.0610	-.0061	.0047	-.0291	.0009	.0003
1.998	4.05	19.89	.8132	.0287	.0708	-.0075	.0043	-.0289	.0008	.0004
1.998	3.97	-.11	.0161	.0206	.0104	-.0040	.0110	-.0340	.0010	.0003

STABILITY AXIS DRAG CORRECTED FOR BASE AND CHAMBER PRESSURES

L/D	BETA	ALPHA	CL	CD	CM	CLS	CNS	CY	CDC	CDB
-4.7158	3.98	-4.17	-.1352	.0287	-.0023	-.0042	.0100	-.0342	.0012	.0003
-2.8802	3.97	-2.18	-.0630	.0219	.0036	-.0042	.0106	-.0343	.0011	.0003
-1.2996	3.97	-1.19	-.0266	.0204	.0068	-.0040	.0107	-.0341	.0010	.0003
.6318	3.97	-.12	.0129	.0204	.0102	-.0040	.0110	-.0343	.0010	.0003
2.1680	3.97	.82	.0468	.0216	.0130	-.0040	.0112	-.0344	.0010	.0003
3.5276	3.97	1.79	.0845	.0240	.0160	-.0040	.0112	-.0341	.0010	.0003
4.9152	3.97	3.91	.1648	.0335	.0226	-.0039	.0115	-.0342	.0008	.0002
5.0044	3.97	5.88	.2381	.0476	.0284	-.0039	.0110	-.0331	.0008	.0002
4.6551	3.98	7.87	.3128	.0672	.0347	-.0038	.0102	-.0320	.0008	.0002
3.7460	4.01	11.90	.4653	.1242	.0475	-.0038	.0080	-.0303	.0008	.0002
3.0109	4.04	15.90	.6133	.2037	.0610	-.0046	.0062	-.0291	.0009	.0003
2.4701	4.05	19.89	.7501	.3037	.0708	-.0056	.0066	-.0289	.0007	.0004
.7872	3.97	-.11	.0162	.0206	.0104	-.0040	.0110	-.0340	.0010	.0003

Table BIII. Continued

UPWT PROJECT 1532

RUN 43

MACH 2.16

BODY AXIS AXIAL FORCE CORRECTED FOR BASE AND CHAMBER PRESSURES

R/FT	BETA	ALPHA	CN	CA	CM	CLB	CNB	CY	CAC	CAB
1.999	-3.97	-.18	.0128	.0208	.0106	.0035	-.0107	.0349	.0010	.0003
1.998	-2.01	-.18	.0134	.0205	.0103	.0016	-.0057	.0182	.0011	.0003
1.999	-.00	-.18	.0138	.0203	.0101	-.0003	.0000	.0010	.0011	.0003
2.000	1.99	-.17	.0150	.0204	.0100	-.0022	.0059	-.0170	.0010	.0003
2.001	3.99	-.17	.0158	.0205	.0105	-.0040	.0111	-.0345	.0010	.0003
1.999	6.00	-.17	.0155	.0202	.0112	-.0058	.0159	-.0525	.0011	.0003
2.001	8.04	-.16	.0165	.0199	.0117	-.0075	.0206	-.0712	.0011	.0003

STABILITY AXIS DRAG CORRECTED FOR BASE AND CHAMBER PRESSURES

L/D	BETA	ALPHA	CL	CD	CM	CLS	CNS	CY	CDC	CDB
.6237	-3.97	-.18	.0129	.0207	.0106	.0035	-.0106	.0349	.0010	.0003
.6589	-2.01	-.18	.0135	.0205	.0103	.0016	-.0057	.0182	.0011	.0003
.6838	-.00	-.18	.0139	.0203	.0101	-.0003	.0000	.0010	.0011	.0003
.7421	1.99	-.17	.0151	.0204	.0100	-.0022	.0059	-.0170	.0010	.0003
.7787	3.99	-.17	.0159	.0204	.0105	-.0040	.0111	-.0345	.0010	.0003
.7761	6.00	-.17	.0156	.0201	.0112	-.0059	.0159	-.0525	.0011	.0003
.8359	8.04	-.16	.0166	.0199	.0117	-.0076	.0205	-.0712	.0011	.0003

Table BIII. Concluded

UPWT PROJECT 1532

RUN 44

MACH 2.16

BODY AXIS AXIAL FORCE CORRECTED FOR BASE AND CHAMBER PRESSURES

R/FT	BETA	ALPHA	CN	CA	CM	CLB	CNB	CY	CAC	CAB
2.001	8.05	7.90	.3200	.0228	.0371	-.0091	.0159	-.0671	.0009	.0002
2.001	5.99	7.81	.2863	.0205	.0434	-.0065	.0130	-.0504	.0009	.0002
2.001	3.98	7.91	.3227	.0236	.0348	-.0051	.0094	-.0320	.0008	.0002
1.998	1.89	7.90	.3208	.0238	.0348	-.0029	.0050	-.0137	.0008	.0002
2.000	-.01	7.89	.3201	.0240	.0346	-.0007	.0003	.0036	.0007	.0002
2.000	-2.00	7.90	.3201	.0240	.0346	.0017	-.0049	.0218	.0008	.0002
2.000	-4.01	7.90	.3216	.0240	.0347	.0040	-.0088	.0389	.0008	.0002

STABILITY AXIS DRAG CORRECTED FOR BASE AND CHAMBER PRESSURES

L/D	BETA	ALPHA	CL	CD	CM	CLS	CNS	CY	CDC	CDB
4.6872	8.05	7.90	.3120	.0666	.0371	-.0068	.0170	-.0671	.0009	.0002
4.7084	5.99	7.81	.2790	.0593	.0434	-.0047	.0138	-.0504	.0009	.0002
4.6435	3.98	7.91	.3144	.0677	.0348	-.0037	.0100	-.0320	.0008	.0002
4.6208	1.89	7.90	.3126	.0676	.0348	-.0022	.0054	-.0137	.0008	.0002
4.6038	-.01	7.89	.3119	.0677	.0346	-.0007	.0004	.0036	.0007	.0002
4.6009	-2.00	7.90	.3119	.0678	.0346	.0010	-.0051	.0218	.0008	.0002
4.6098	-4.01	7.90	.3133	.0680	.0347	.0028	-.0093	.0389	.0008	.0002

References

1. Rolfe, Douglas; Dawydoff, Alexis; Winter, William; Byshyn, William; and Clark, Hank: *Airplanes of the World—1490 to 1969*, Third rev. ed. Simon & Schuster, 1969.
2. Houbolt, John C.: Why Twin-Fuselage Aircraft? *Astronaut. & Aeronaut.*, vol. 20, no. 4, Apr. 1982, pp. 26–35.
3. Maglieri, Domenic J.; and Dollyhigh, Samuel M.: We Have Just Begun To Create Efficient Transport Aircraft. *Astronaut. & Aeronaut.*, vol. 20, no. 1, Feb. 1982, pp. 26–38.
4. Ferri, Antonio; Clarke, Joseph H.; and Ting, Lu: Favorable Interference in Lifting Systems in Supersonic Flow. *J. Aeronaut. Sci.*, vol. 24, no. 11, Nov. 1957, pp. 791–804.
5. Friedman, Morris D.; and Cohen, Doris: *Arrangement of Fusiform Bodies To Reduce the Wave Drag at Supersonic Speeds*. NACA Rep. 1236, 1955. (Supersedes NACA RM A51120 by Friedman and TN 3345 by Friedman and Cohen.)
6. Ferri, Antonio; and Clarke, Joseph H.: On the Use of Interfering Flow Fields for the Reduction of Drag at Supersonic Speeds. *J. Aeronaut. Sci.*, vol. 24, no. 1, Jan. 1957, pp. 1–18.
7. Jones, Robert T.: *Minimum Wave Drag for Arbitrary Arrangements of Wings and Bodies*. NACA Rep. 1335, 1957. (Supersedes NACA TN 3530.)
8. Wood, Richard M.; Miller, David S.; and Brentner, Kenneth S.: *Theoretical and Experimental Investigation of Supersonic Aerodynamic Characteristics of a Twin-Fuselage Concept*. NASA TP-2184, 1983.
9. Wood, Richard M.; Rose, O. J.; and McMillin, S. Naomi: *Effects of Body Cross-Sectional Shape on the Supersonic Aerodynamics of Multibody Configurations*. NASA TP-2587, 1986.
10. Wood, Richard M.; and Miller, David S.: *Wing Planform Effects at Supersonic Speeds for an Advanced Fighter Configuration*. NASA TP-2269, 1984.
11. Wood, Richard M.; Miller, David S.; Hahne, David E.; Niedling, Larry G.; and Klein, John R.: Status Review of a Supersonically-Biased Fighter Wing-Design Study. AIAA-83-1857, July 1983.
12. Jackson, Charlie M., Jr.; Corlett, William A.; and Monta, William J.: *Description and Calibration of the Langley Unitary Plan Wind Tunnel*. NASA TP-1905, 1981.
13. Braslow, Albert L.; Hicks, Raymond M.; and Harris, Roy V., Jr.: Use of Grit-Type Boundary-Layer-Transition Trips. *Conference on Aircraft Aerodynamics*, NASA SP-124, 1966, pp. 19–36.
14. Wood, Richard M.; and Miller, David S.: Fundamental Aerodynamic Characteristics of Delta Wings With Leading-Edge Vortex Flows. *J. Aircr.*, vol. 22, no. 6, June 1985, pp. 479–485.
15. Miller, David S.; and Wood, Richard M.: *Lee-Side Flow Over Delta Wings at Supersonic Speeds*. NASA TP-2430, 1985.
16. Murman, Earl M.; Powell, Kenneth G.; Miller, David S.; and Wood, Richard M.: Comparison of Computations and Experimental Data for Leading Edge Vortices—Effects of Yaw and Vortex Flaps. AIAA-86-0439, Jan. 1986.
17. Craidon, Charlotte B.: *User's Guide for a Computer Program for Calculating the Zero-Lift Wave Drag of Complex Aircraft Configurations*. NASA TM-85670, 1983.
18. Middleton, W. D.; Lundry, J. L.; and Coleman, R. G.: *A System for Aerodynamic Design and Analysis of Supersonic Aircraft. Part 2—User's Manual*. NASA CR-3352, 1980.
19. Sorrells, Russell B.; and Miller, David S.: *Numerical Method for Design of Minimum-Drag Supersonic Wing Camber With Constraints on Pitching Moment and Surface Deformation*. NASA TN D-7097, 1972.
20. Sommer, Simon C.; and Short, Barbara J.: *Free-Flight Measurements of Turbulent-Boundary-Layer Skin Friction in the Presence of Severe Aerodynamic Heating at Mach Numbers From 2.8 to 7.0*. NACA TN 3391, 1955.
21. Ames Research Staff: *Equations, Tables, and Charts for Compressible Flow*. NACA Rep. 1135, 1953. (Supersedes NACA TN 1428.)



Report Documentation Page

1. Report No. NASA TP-2762		2. Government Accession No.		3. Recipient's Catalog No.	
4. Title and Subtitle Planform Effects on the Supersonic Aerodynamics of Multibody Configurations				5. Report Date December 1987	
				6. Performing Organization Code	
7. Author(s) S. Naomi McMillin and Richard M. Wood				8. Performing Organization Report No. L-16312	
9. Performing Organization Name and Address NASA Langley Research Center Hampton, VA 23665-5225				10. Work Unit No. 505-61-71-01	
				11. Contract or Grant No.	
12. Sponsoring Agency Name and Address National Aeronautics and Space Administration Washington, DC 20546-0001				13. Type of Report and Period Covered Technical Paper	
				14. Sponsoring Agency Code	
15. Supplementary Notes					
16. Abstract <p>An experimental and theoretical investigation of the effects of planform on the supersonic aerodynamics of three low-fineness-ratio multibody configurations has been conducted. Longitudinal and lateral-directional aerodynamic and flow visualization data were obtained. The data indicate that planform has a small effect on the zero-lift drag of a multibody configuration. The longitudinal data obtained at lifting conditions show a sensitivity to planform shape. Lateral-directional data obtained for all configurations do not uncover any unusual stability traits for this class of configuration. A comparison was also made between the planform effects observed on single-body and multibody configurations. Results indicate that the multibody concept appears to offer a mechanism for employing a low-sweep wing with no significant increase in zero-lift drag while retaining high-performance characteristics at high-lift conditions. Evaluation of the linear-theory prediction methods revealed a general inability of the methods to predict the characteristics of low-fineness-ratio geometries.</p>					
17. Key Words (Suggested by Authors(s)) Supersonic Aerodynamics Multiple fuselage Zero-lift drag Planform shaping Fighter aircraft Linear theory Longitudinal aerodynamics Lateral-directional aerodynamics				18. Distribution Statement Unclassified—Unlimited Subject Category 02	
19. Security Classif.(of this report) Unclassified		20. Security Classif.(of this page) Unclassified		21. No. of Pages 135	
				22. Price A07	